MICROTURBULENCE AND ABUNDANCE ANOMALIES IN CLUSTER METALLIC LINE A STARS

by

Myron Arthur Smith

A Dissertation Submitted to the Faculty of the

DEPARTMENT OF ASTRONOMY

In Partial Fulfillment of the Requirements
For the Degree of

DOCTOR OF PHILOSOPHY

In the Graduate College

THE UNIVERSITY OF ARIZONA

1 9 7 1

THE UNIVERSITY OF ARIZONA

GRADUATE COLLEGE

I hereby recommend that this dissertation prepared under my direction by Myron Arthur Smith

entitled Microturbulence and Abundance Anomalies in Cluster Metallic Line A Stars

be accepted as fulfilling the dissertation requirement of the degree of Doctor of Philosophy

Helmut A. Abt — 11/2/70

Dissertation Director — Date

After inspection of the final copy of the dissertation, the following members of the Final Examination Committee concur in its approval and recommend its acceptance:*

T. L. Swihart	10/20/70
Karl J. Wegmann	10/30/70
W. T. Cochran	10/26/70
W. S. Fitch	10/26/70

*This approval and acceptance is contingent on the candidate's adequate performance and defense of this dissertation at the final oral examination. The inclusion of this sheet bound into the library copy of the dissertation is evidence of satisfactory performance at the final examination.

STATEMENT BY AUTHOR

This dissertation has been submitted in partial fulfillment of requirements for an advanced degree at The University of Arizona and is deposited in the University Library to be made available to borrowers under rules of the Library.

Brief quotations from this dissertation are allowable without special permission, provided that accurate acknowledgment of source is made. Requests for permission for extended quotation from or reproduction of this manuscript in whole or in part may be granted by the head of the major department or the Dean of the Graduate College when in his judgment the proposed use of the material is in the interests of scholarship. In all other instances, however, permission must be obtained from the author.

SIGNED: Myron Arthur Smith

To Anne

and

To Helmut

ACKNOWLEDGMENTS

The author wishes to acknowledge the following individuals for their help and advice in the completion of this dissertation:

Dr. A. A. Hoag and the staff of the Stellar Division of the Kitt Peak National Observatory for providing ample 84-inch telescope time for the acquisition of the data. I also wish to thank the night assistants, principally Mr. Saul Levy, who do most of the real work at the telescope;

Dr. S. Lovell and his computing department staff for their aid in the running of the computing programs;

Mr. Robert Kurucz for his adapting of the ATLAS3 and WIDTH4 programs to use on the Kitt Peak 6400 C.D.C. computer; these programs were essential to the execution of this project and his instruction and advice in the use of them is gratefully acknowledged;

Drs. Stephen Strom and Ray Weymann for their many helpful discussions, comments, and suggestions relating to several portions of this work;

Drs. C. R. Cowley, R. P. Kraft, G. Wallerstein, A. Slettebak, W. D. Watson, R. K. Ulrich, A. Young, and D. Barry for their correspondences and their helpful comments. I am especially indebted to Dr. Peter S. Conti for his constructive suggestions and correspondences;

Mr. Edwin Howell and Mr. John Daniels of the Steward Observatory Photographic Department for their aid in the preparation of the figures;

Dr. Bart J. Bok for his always enthusiastic interest and support of my endeavors;

Dr. Thomas L. Swihart for serving faithfully as my departmental adviser under adverse conditions;

Finally, I can only thank the director of this dissertation, Dr. Helmut A. Abt, sufficiently for the many things he has done by pledging to follow his example toward others in the future.

TABLE OF CONTENTS

TABLE OF CONTENTS--Continued

LIST OF ILLUSTRATIONS

LIST OF ILLUSTRATIONS--Continued

LIST OF TABLES

ABSTRACT

In this study high dispersion spectra were obtained for sixteen metallic line (Am) stars in three galactic clusters and for four normal standards. Three spectra of each star were obtained in the blue at 8.9 A/mm dispersion, and two in the yellow at 17.8 A/mm. A detailed model atmospheres curve of growth analysis was made of the equivalent width data of each star in order to obtain microturbulent parameters and abundances.

Examination of the ionization equilibrium of iron for these stars confirms the recent studies in which spectroscopic gravities of Am stars have been found to be dwarf-like.

Analysis of our program star data confirms the conclusion of previous authors that microturbulence is the same for both Am and normal A stars in a given temperature range. Microturbulence may even be a unique function of temperature along the main sequence. The indicated rise in this parameter among the late A stars coincides precisely with the intersection of the main sequence with the instability strip. This finding offers interesting speculation for the physical nature of microturbulence itself.

The abundance of iron is found to be enhanced in Am stars by a variable factor of up to five or more. The iron enhancement factor is correlated positively with effective temperature and inversely with apparent rotational velocity.

Inspection of the run of abundances in Am stars suggests that the observed peculiarities do not arise through nucleosynthetic processes. When plotted relative to iron, the abundances of the elements examined behave similarly to those of their neighbors in the periodic table. Also, the scatter in the relative abundances is surprisingly small except among the deficient elements. The scatter in these latter elements may be accounted for by their correlation with effective temperature and apparent rotation.

The impression that degrees of metallicism exist is tested by synthesizing an index composed of various anomalies. This index is found to be strongly anti-correlated with apparent rotation. Recent photoelectric K-line data also show that as Am stars evolve off the main sequence at least some anomalies become more moderate. It thus appears that metallicism involves a stability problem, and that the mechanism responsible for it is subject to rotational or convective disruption.

It is also concluded that in marginal cases, such as with HR 906, it may be difficult at times to decide whether a star is metallic lined or "normal."

No evidence for subgrouping in Am properties is found. However, various anomalies vary with effective temperature in various ways and this may account for differences between "hot" and "classical" Am stars.

A model is proposed in which metallicism is explained in terms of a subsurface diffusion process. A "quiescent zone" located between the convection zones due to H I, He I and He II ionization is postulated to be the seat of the element separation. Selective radiation pressure probably accounts for the enhanced elemental abundances, whereas gravitational settling and thermal diffusion processes are the likely cause of deficiencies of a few light elements. The types of anomalies found in Am stars, the location of the Am domain in the H-R diagram, and several other boundary conditions placed on metallicism all appear to be reasonably explained in terms of this model.

CHAPTER I

INTRODUCTION

A Review of the Gross Properties of Metallic Line Stars

The group of A-type stars known as metallic line (Am) stars comprises fifteen per cent or more of all the A stars near the main sequence. It follows that whatever is responsible for producing the spectral anomalies for which these stars are named should not be thought of as peculiar or uncommon. That we comprehend so little about the Am phenomenon points out a glaring deficiency in our current knowledge of main sequence stars. For this reason, these stars constitute an especially important group for study.

The existence of these stars was first noted accidentally by Maury (1897). She noticed several sharp-lined A stars which showed spectral peculiarities, and often designated them as having composite spectra. Cannon classified many of these same stars as "A2" in the Henry Draper Catalogue on the basis of their weak Ca II K-lines. In a subsequent study on the Ca II K/(Ca II H + Hε) ratios and equivalent colors of A and F stars, Hertzsprung (1911) found that the stars now known as the Am stars 63 Tauri and 68 Tauri do not fall on the sequence defined by these parameters for most other stars.

It was not until the Titus and Morgan (1940) study of the classification of A stars in the Hyades that metallic line stars were first recognized as a distinct group of stars with their own spectral "peculiarities." The principal spectral characteristic these authors noted is the weak K-lines of these stars compared to those of "normal" A stars with the same hydrogen line strengths. They also noticed that the metallic lines are generally enhanced, as in F stars. They decided that these objects should be thought of as A stars, since only the early A-type K-lines would be visible in fainter Am stars discovered thereafter.

From the Stebbins-Whitford photoelectric colors of two Am stars, Morgan and Bidelman (1946) concluded that the colors of these stars agree more with the (late) metallic line types of these stars than with the K-line types. They felt that the K-line is the most abnormal spectral feature, and that therefore metallic line stars are actually F stars.

In a classic study in 1948, Roman, Morgan, and Eggen first defined these stars as a class by listing thirteen Am spectral standards. They defined these stars by contrasting their early (A1 to A6) K-line types with their late (A5 to F6) metallic line types. The hydrogen line types were found to be intermediate (A5 to F2). In their description, they stated that the spectra could not be confused with composite spectra, shell spectra, or "peculiar A" spectra. On the basis of the Am stars' colors, their absolute magnitudes,

their metallic line types, and their low apparent rotational velocities, these authors, too, classified these stars as F stars. This conclusion influenced several other authors for years to come, and, as will be demonstrated in Chapter II, has been shown more recently to be incorrect.

The Roman, Morgan, Eggen (hereinafter referred to as "RME") definition of Am stars in terms of their substantially different K-line and metallic line spectral types has lasted very well for over twenty years. However, even in the Morgan, Keenan, and Kellman Spectral Atlas (1943) it was noted that the K-line behaves "erratically" in the eight Am stars described there. Several authors have noted, on the basis of curve of growth abundance analyses (Hack 1956c, Jaschek and Jaschek 1960) and K-line photoelectric photometry (Henry 1969), that some Am stars have normal or nearly normal apparent calcium abundances. For this reason, Conti (1970) has proposed that the definition of Am stars be modified to include a scandium or a calcium spectral defect, since lines of the former are also generally weak in Am stars (Hack 1956a, 1956b, 1965, Conti 1965a). Conti stressed, however, the importance of a phenomenological rather than a spectroscopic definition. Therefore, we too shall define the Am phenomenon as that process which produces apparent calcium and/or scandium deficiencies and also apparent heavy element enhancements in the spectrum of an A (or F) type star. This phenomenon will often be referred to

herein as "metallicism." It is to be distinguished from "metallicity," which is usually taken to mean that the abundances of all the metals, including calcium and scandium, rise (or fall) with the iron peak and the heavier metals. Finally, in this dissertation we shall avoid discussion of peculiar A (Ap) stars except where necessary.

The foregoing early studies and additional early lists of metallic line stars (e.g., Slettebak 1949, Weaver 1952) defined their region of occurrence by the hydrogen line spectral types A4 to F2.[1] Conti (1965b) has pointed out, however, that if metallic line stars do exist with early A hydrogen line types, they would be difficult to distinguish as Am stars for two reasons. First, it would be difficult to assign accurate hydrogen line types, and hence to determine what the normal K-line strengths should be, because the hydrogen line strengths peak in this spectral range. Second, such early stars would have K-lines that are so weak that they would lie upon the flat region of the curve of growth; therefore, the apparent abundance of calcium would be difficult to estimate. An example of such a star (Conti 1965b) would be 68 Tauri, which, as already mentioned, Hertzsprung had originally noted as "peculiar."

---

1. Metallic line stars occurring in this domain will hereinafter be referred to as "classical" Am stars.

The hottest Am stars presently known[1] are α Gem A (Conti 1965b) and Sirius, which has been found to be a metallic line star by several authors who used curve of growth analyses (Boyarchuk 1963, Wallerstein and Hunziker 1964, Kohl 1964, Warner 1966, Strom, Gingerich, and Strom 1966). The existence of Sirius defines the known hot boundary for the occurrence of Am stars at about 10,000°K (Strom, Gingerich, and Strom 1968). It should be noted, however, that if hotter Am stars do exist, it would be very difficult to classify them as such because of the faintness of the K-line, Sc II lines, and metallic line features in such early-type stars. In this connection, Olson (1969) has remarked that 66 Eridani may be a metallic line star; this star has a hydrogen line type of B9.5 (Cowley et al. 1969).

The cool boundary for the occurrence of Am stars is somewhat easier to define because of the increasing strength and numbers of the many metallic lines. Greenstein (1948) pointed out that τ Ursa Majoris is a convenient, bright prototype of the cool Am stars. Recently, however, Harlan (1969) has discovered a very cool Am star, HD 103877. The (b - y) and Hβ photoelectric indices for this star are,

---

1. As with normal A stars, effective temperatures for Am stars can be taken from their hydrogen line types, a conclusion to be justified in Chapter II.

respectively, 0.236 and 2.731,[1] which indicate a temperature (see Chapter III) of 7200°K, or a spectral type of about F2 (Barry 1970). The metallic line type of this star is GO (Morgan, 1970). This star defines the known cool boundary for the occurrence of Am stars. Abt and Bidelman (1969), on the basis of classification of spectroscopic binaries, have determined the boundary for Am stars to be at F1.

To complete the picture of where Am stars occur in the H-R diagram, it should be noted that there are no known Am stars which are actually located up in the giant region, even though several have moderate Stromgren Δc_1 indices (see Chapter III, Figure 1b). Of such stars, two have been analyzed by curve of growth techniques, and both of these have been found to have dwarf-like gravities ($\log g \cong 4.0$). One of these was studied by Praderie (1967); the other is θ Cep from the present study (see Chapter IV). In both cases these gravities agree with those deduced from the stars' trigonometric parallaxes, which are 0".025 and 0".032, respectively (Hoffleit 1964). The apparent positions of these stars above the main sequence in the H-R diagram will be discussed in the next chapter.

The detection of metallic line stars has usually been accomplished by accidental discovery during the course

---

1. We wish to express our gratitude to Mrs. J. V. Barnes and Mr. J. C. Golson of the Kitt Peak National Observatory who made two photoelectric observations of this star in both the uvby and Hβ photometric systems.

of spectral classification programs of larger groups of stars. Nevertheless, it is possible to devise techniques that will facilitate their discovery in larger numbers. A potentially valuable, though limited, technique is that of obtaining objective prism spectra. Brunck (1963) has used Case objective prism plates to detect these stars by using their weak K-line criterion. Honeycutt and McCuskey (1966) re-examined this technique with both Brunck's and their own material. They found that the length of exposure time is critical in determining the strength of stellar absorption features. The exposure time is difficult to control over an objective prism field containing stars of different apparent brightnesses. Moreover, they found that bad atmospheric seeing or bad guiding can often give rise to spurious features. They concluded that objective prism techniques make possible the detection of the more pronounced Am members, but that otherwise the classification of Am candidates can be a very subjective enterprise. Nonetheless, Bidelman and Victor (1966) and Bond (1970) have had considerable success in discovering new Am stars with four and ten degree objective prism plates.

Conti (1965b) and Smith (1970) have defined spectral line ratios involving certain Sc II, Sr II, and Y II lines. Such ratios are doubly sensitive to the Am trait, since scandium lines are weakened and strontium and yttrium lines are enhanced compared to normal A stars. These ratios are

also virtually independent of effective temperature and surface gravity. They are particularly convenient in the case of early A stars, where it becomes difficult to determine whether the K-line is weak, for the reasons listed above.

A final method of detecting Am stars involves photoelectric indices which are primarily sensitive to metallicity. Stromgren (1956) and Golay (1964) have demonstrated that such indices can separate Am stars from the normal A star sequence. The more commonly used index currently is the m_1 metallicity index introduced by Stromgren (1963). Stromgren noted that a star's having a negative Δm_1 index is not a sufficient condition for it to be metallic lined. Many normal A stars are slightly metal enriched, and therefore have negative Δm_1 indices. Conversely, many Am stars are located on the "metal poor" side of the m_1 envelope. Nevertheless, Stromgren (1966) has pointed out that all stars with Δm_1 indices more negative than -0.035 (i.e., large m_1 values) have been found to be Am from the spectroscopic criterion. Milton and Conti (1968) concluded that all A stars having $m_1 > 0.230$ are metallic lined.

There have been several attempts to estimate the incidence of Am stars relative to the total population of A-type main sequence stars. Such estimates depend sensitively on how the sample of stars is chosen and how conservatively the definition of metallic line stars is

applied. In the first such study, Slettebak (1949) was unsure of the true spectral type of these stars. He estimated their incidence to be 15%, if Am stars are late A and F stars, or 10% if they are early A stars. Based on cluster statistics, Weaver (1950) estimated the incidence to be as high as 35%. However, his sample included the Hyades, Praesepe, and Coma clusters, which happen to have large numbers of Am stars in them. Therefore this number can be regarded as an upper limit. The Jascheks (Jaschek and Jaschek 1962) have estimated an incidence of 10%, based on relatively large statistics of field stars. In her review paper on Am stars, Hack (1965) took the incidence to be 15%. Most recently, in a homogeneous classification study of all the bright A stars (Cowley et al. 1969), the authors found that 11% of the total A-type population in the solar neighborhood are metallic line stars. This is a lower limit, however, since many early type Am stars, such as Sirius, α Gem A, and 68 Tau, are classified as normal stars. Abt and Smith have under way a study which will investigate this incidence. They will examine high dispersion spectra of stars in a narrow color interval in order to determine which exhibit weak K-lines or scandium lines. At the outset of this study, of seventy-six A stars chosen, seventeen, or 22%, have been classified by others as Am.

That Am stars occur frequently in clusters was immediately apparent from the Titus and Morgan study,

which included Am stars in the Hyades cluster. Weaver (1946, 1950) conducted the first surveys for the detection of these stars in galactic clusters. He found a high incidence in the Hyades, Praesepe, and Coma Berenices clusters. In a review of the incidence of Am stars in clusters, the Jaschek s (Jaschek and Jaschek 1962) concluded that the number of these stars tends to increase with cluster age and to reach a maximum in clusters 6 to 10×10^8 years old. This finding was to form the basis of an evolutionary interpretation of Am stars later, despite the kinematic evidence (Jaschek and Jaschek 1967) that Am stars are not evolved stars. The Jaschek s 1962 conclusion was based largely on the lack of Am stars in young clusters such as the Pleiades and α Persei. However, Conti and Strom (1968a) have found four early-type Am stars in the Pleiades. In addition, Conti and van den Heuvel (1970) have concluded that the statistics of the original cluster search by the Jaschek s was inadequate. They have found two Am stars in the young cluster Messier 7. Finally, Garrison (1967) and Glaspey (in prep.) have each found an Am star in the Scorpio-Centaurus association; both of these stars have very large m_1 indices (Glaspey in prep.). It therefore appears that Am stars can be present in young clusters. On the other hand, the question is presently open as to whether Am stars can occur in extremely young clusters in which the A stars have not yet contracted onto the main sequence.

Further insight into the question of non-existence of "classical" Am stars in the Pleiades or the α Persei cluster comes from another consideration. Shortly, it will be shown that Am stars characteristically exhibit low rotational velocities and a high binary frequency. Abt and Hunter (1962) have concluded that the mean rotational velocity of stars in a cluster tends to be inversely correlated with the cluster's binary frequency. This correlation has been corroborated by several studies (Abt et al. 1965, Abt and Snowden 1964, Abt and Chaffee 1967, Kraft 1965, Heard and Petrie 1966). Anderson, Stoeckley, and Kraft (1965) and Kraft (1967) have shown that the Pleiades and α Persei clusters have high rotational velocities and very low duplicities. From these results a very natural explanation for the lack of Am stars in these two clusters follows: A-type stars do not exist in these particular clusters with the characteristics allowing metallicism to develop. According to this interpretation, the young ages of the Pleiades and α Persei clusters simply would not be relevant.

It should be mentioned that metallic line stars may also be found in old galactic clusters. Pesch (1967) has found two in Messier 67. Sargent (1968) has argued that several of the blue members of this cluster, including the two Am stars discovered by Pesch, constitute a "Population I horizontal branch." However, Deutsch (1969) has pointed out

that Feige 81 is a spectroscopic binary, so that it is doubtful that these stars are returnees from the red giant branch. There appears to be little evidence, therefore, for metallicism occurring in any post-main sequence evolutionary phase.

The low apparent rotational velocities of Am stars was apparent from their sharp-line spectral appearance as early as in the RME study in 1948. This discovery was confirmed in later studies (Slettebak 1954, 1955, Jaschek-Corvalon and Jaschek 1957). Typical values for the mean apparent rotational velocity of these stars as a group, $\overline{V \sin i}$, were found to be 40 to 50 km/sec. Abt (1961) found that the observed $M \sin^3 i$ distribution among double-line Am spectroscopic binaries was consistent with the hypothesis of a random orientation of orbital axes. If their orbital and rotational axes are parallel as a result of tidal interactions, as is usually assumed for close binaries, this implies that the rotational axes of these stars are also oriented randomly in space. Abt concluded that the observed sharp-lined appearance of spectral lines in Am stars is not an inclination effect. One may draw similar conclusions from the existence of eclipsing Am systems such as RR Lyncis, WW Aurigae, and δ Capricorni (Abt 1961).

The difference in characteristic rotational velocities between normal A stars and Am stars is sufficiently pronounced that one may say that a dichotomy exists

in the rotational velocity distribution of these stars (Abt 1965). Van den Heuvel (1968a) has demonstrated that if Am stars are included in with normal A stars, then a bimodal rotational velocity distribution occurs along the main sequence from B5 to F2. This fact implies that Am stars are part of a continuous sequence of slowly rotating stars. Deutsch (1967) has argued, on the basis of analysis of the rotational velocity distribution of A stars, that slow rotation ($V \sin i < 100$ km/sec) is a necessary and sufficient condition for an A star to be metallic lined. A few words of caution should be interjected about such an important conclusion, however. First, Deutsch's sample of stars did not include some of the fastest rotating Am stars known. There are several Am stars noted in the literature with measured apparent rotational velocities greater than 100 km/sec, such as HD 110500, which has $V \sin i = \sim 125$ km/sec (Slettebak 1970). Second, both normal A and Am stars occur as primaries in ultra-short period ($P < 2\text{-}1/2$ days) binary systems (Abt and Bidelman 1969). Since stars in such systems apparently rotate synchronously (Abt 1965), one concludes that both Am and normal A stars can co-exist at the same rotational velocity. One may use a similar argument for eclipsing systems since Olson (1969) has pointed out examples of systems having either type of star and having similar periods. However, while there may be a slight overlap in rotational velocities between these two

groups of stars, the growing consensus (Stromgren 1963, Abt 1967, Conti 1970) appears to be that rotation is the single most important factor in determining the onset of metallicism in an A star. Moreover, the Jascheks (Jaschek and Jaschek 1959) have found evidence that the slowest rotating Am stars tend to be the most pronounced cases.

As already mentioned, Am stars appear to have a very high binary frequency. This was first noted by RME. The Jascheks (Jaschek and Jaschek 1959) have confirmed this high incidence. They felt, however, that a selection effect could create an artificially high duplicity rate, since it is easier to detect radial velocity variations in sharp-lined stars. They found, in fact, that the binary frequency was equally high among normal A stars having V sin i $\leq$ 75 km/sec.

In an important study, Abt (1961) found that twenty-two out of twenty-five Am stars investigated exhibit radial velocity variations. Out of such a sample, he estimated that one should expect to find four nearly pole-on rotators with no detectable radial velocity variations. He concluded that the results of his study were consistent with the hypothesis that all Am stars are spectroscopic binaries. This study was followed by another on the frequency of binaries in a sample of fifty-five A stars (Abt 1965). In this investigation, Abt found that the fraction of long period (P > 100 days) binaries is similar among normal A and

Am stars. More importantly, he discovered that all A stars that occur in short period binaries are metallic lined.

Batten (1967a) has pointed out that the Abt results are very significant and so should be subjected to further scrutiny. In his criticism, he pointed out that five Am stars in the 1961 Abt study may not show real velocity variations because of the small velocity amplitudes or long periods Abt determined for them. In addition, he has found short period systems in his Sixth Catalogue of the Orbital Elements of Spectroscopic Binary Systems (Batten 1967b) with primaries in the A4 to F2 range which have been classified as normal A stars. Most of these stars, however, have not been classified according to any homogeneous classification scheme. Therefore, doubts may arise to the normality of the stars to which Batten alluded. As a result, Abt and Bidelman (1969) re-investigated the spectral range and the orbital period range in which Am stars occur in spectroscopic binaries. They found that the original Abt results should be modified slightly to read that all A4 to F1 primaries in binaries with periods between 2-1/2 and 100 days are metallic line stars.

Conti (1967) has noted that there are three short period binary systems in which the primaries are normal sharp-lined A1 to A3 stars. One possible interpretation of this discovery is that the "early type" (A1 to A3) may differ somehow from the slightly cooler "classical" Am

stars (Conti 1970). An alternative interpretation lies in the Stromgren c_1 indices of these three stars being so large (such that $\Delta c_1 = 0^m.2$) as to indicate that they are already semi-evolved and therefore that they have deeper convection zones than main sequence A stars. Since other evidence (see Conti 1970 and Figure 15 of Chapter V) already suggests that pronounced metallicism does not occur in stars having deep convection zones, the existence of these normal A stars in binaries would thus not be surprising. They would be understood to be Am antecedents rather than counterexamples to Abt and Bidelman's conclusions for this spectral range.

If the binary frequency among Am stars is indeed 100%, then metallicism may be linked directly to their binary nature. Various authors (Conti 1965b, Renson 1967, van den Heuvel 1968b) have argued that Am stars occur in close binaries as a result of mass overflowing the Lagrangian lobe of the primary component onto the surface of the secondary. If this happened sufficiently late in the primary's history, then nuclear processed material from the core could conceivably be convected to the surface and transferred to the surface of the secondary component, giving rise to the observed Am spectral features. According to this picture, the erstwhile secondary would become the presently observed Am primary, and the erstwhile primary would evolve to the (unobservable) white dwarf stage. A

corollary of this theory is that double-lined Am systems would be expected to have identical compositions.

The primary basis for such an evolutionary picture was the Jascheks' (Jaschek and Jaschek 1962) conclusion that the frequency of occurrence of Am stars is correlated with cluster age and the apparent lack of them in young clusters. Further evidence for this idea came from the observation (Conti 1965b) that binaries with two A-type components are invariably both Am. Finally, the example of Sirius with its white dwarf companion implies that some Am systems have gone through an evolutionary history.

However, other evidence does not support this evolutionary picture. It has already been pointed out that Am stars have recently been found in young clusters. In addition, the Jaschek's age correlation results have been challenged by Conti and van den Heuvel (1970). There is also increasing evidence that the apparent compositions of components of double-lined Am systems are not always identical. Conti (1969b) has found that η Virginis is a double-lined system in which one component may actually be a normal star. The components of the double-lined eclipsing systems BV 357 (Young 1970) and WW Aurigae (Abt et al. n.d.) also exhibit dissimilar apparent compositions. Finally, that the fraction of short period binaries is constant from spectral types B to G argues strongly against an evolutionary interpretation (Conti 1970).

Since the observed data do not appear consistent with evolutionary interpretation of Am stars, it is difficult to maintain the view that duplicity is a direct cause of metallicism. This difficulty is especially apparent in the long period, widely separated systems in which any interactions must be very weak (Abt 1961). A more plausible interpretation (Abt 1965, 1967) may be simply that duplicity is effective in slowing down an A star's rotation through synchronism. Certainly the 1961 Abt result appears consistent with two statements: first, that slow rotation helps induce metallicism, and, second, that the few Am stars which are single, or which are in long period binaries where tidal interactions do not occur, may simply lie on the low velocity "tail" of the rotational velocity distribution of normal A stars.

A final physical characteristic of Am stars which should be mentioned is the possible variability in brightness of them. Breger (1969) has found that the pulsational instability strip intersects the main sequence at types A4 and F2. Since most of the Am stars occur in this region near the main sequence, it might be expected that at least a few of them exhibit variability. However, Breger (1970b) has determined that out of nineteen Am stars observed, none has been found to be variable by as much as 0.01 magnitudes. In the same sample of A stars containing these nineteen Am stars, thirty-one out of ninety-three normal stars were

shown to exhibit variability on at least this scale. Breger concluded that these numbers are statistically significant, so that Am stars probably do not pulsate.

Considerable attention has been paid in this review to the rotational and binary aspects of Am stars. If the Abt and Hunter hypothesis is correct, then the number of Am stars in a galactic cluster depends on how angular momentum of the A stars in that cluster is divided between binaries and rotational velocity in single stars. This leaves unanswered, however, the question as to whether Am stars in different clusters are different in their apparent compositions. One aim of this dissertation is to investigate this question by employing detailed curve of growth analyses of several Am stars in different clusters.

There are three other general goals of this study:

1. We wish to determine from the spectroscopic analysis whether the derived surface gravities and microturbulent parameters in Am stars are different from those in normal A dwarf stars. From these studies, we would hope to make inferences on the nature of microturbulence in A stars.
2. We shall derive the apparent abundances of the Am stars on a homogeneous system. These data, and the data from four "standard" stars, should permit a clearer definition of the anomalies which exist in Am stars.

3. From the data on apparent abundances, we wish to investigate the possibility of subgroups occurring among the Am stars; this information will tend to confirm or refute the negative results found by the Jascheks (Jaschek and Jaschek 1960) on this question. Possible correlations in abundance among the elements will be sought. Finally, and most importantly, we wish to infer boundary conditions on the mechanism responsible for metallicism from the observed pattern of anomalies.

In this Introduction, the more prominent gross characteristics of Am stars have been outlined. We have not yet discussed the determination of effective temperatures or surface gravities of these stars. Such characteristics will be investigated in Chapter II, which concerns itself with the physical state of the atmospheres of metallic line stars. In that chapter, it will be demonstrated that their atmospheres are not significantly different from those of normal main sequence stars. This will constitute a justification for the use of conventional dwarf model atmospheres used in the curve of growth analysis described in Chapter III. In Chapter III, we discuss pertinent aspects of the selection of the stars observed, the reduction of the data, and the model atmosphere and equivalent width programs used for the abundance and microturbulence

determinations. In Chapter IV, the microturbulence and abundance results will be presented and discussed in the context of the goals outlined above. In Chapter V, we shall suggest an interpretation of the metallicism phenomenon.

CHAPTER II

THE PHYSICAL STRUCTURE OF THE ATMOSPHERES OF Am STARS

No statements can be made regarding the origin of spectral peculiarities without some knowledge of the physical state of the stellar atmosphere. Only when this state is specified, and the correct curve of growth problem formulated, can the reality of "apparent" abundance anomalies be established.

Early Studies

Soon after the metallic line stars were discovered and isolated as a separate group, a feeling arose among many authors that the spectral peculiarities in Am stars are not due to real composition differences. Even before they were discovered, Morgan (1935) offered the following opinion on the spectral peculiarities in Ap stars: "It seems safe to conclude that there is some physical factor other than temperature and surface gravity concerned in the production of the spectra of A stars." Struve and Swings (1942) noted that a few authors had attempted to interpret spectral characteristics of these stars in terms of composition differences. However, they stated: "It is almost certain that these escapist ideas have done more harm than good." Aller (1967) has explained that during this period the accepted belief was that all stars have the same chemical

composition as the sun, and that spectral differences could be interpreted in terms of special excitation or ionization conditions. In the case of Am stars, we shall see that this reluctance to appeal to composition anomalies prevailed for over two decades. This view was not without scientific merit, since some of the earliest discovered Am stars are members of the Hyades cluster; even today, it is thought that unevolved stars in a cluster have nearly identical compositions because of their common origin.

The first curve of growth analysis of an Am star was carried out by Greenstein (1948). In this analysis he compared τ Ursa Majoris to several F stars. He justified the use of a conventional analysis by first showing that no combination of composite spectra can explain either the strong metallic lines or the weak K-line observed in these stars. The formal results of his analysis indicated apparent abundance deficiencies of magnesium, scandium, calcium, and zirconium, as well as enhancements of nickel, zinc, and europium. The fact that the neutral calcium lines are found to be weakened along with the K-line in this star indicates that any possible peculiar ionization effects are not confined to a single ionization stage.

The 1948 Greenstein paper was followed by a more extensive study (Greenstein 1949) in which the anomalies he had found for τ Ursa Majoris were scrutinized. He found that a good correlation does not exist between the derived

anomalies of elements and their atomic numbers. He concluded that an explanation of metallicism in terms of nucleosynthesis could be ruled out. However, he pointed out that the ions responsible for the determinations of certain elemental deficiencies have ionization potentials in the range of ten to sixteen electron volts. This range is centered close to the 13.54 ev. ionization potential of hydrogen. This observation led him to venture two explanations for the observed anomalies, both of which entail a shift in the ionization equilibrium of atoms to an (unobserved) high state of ionization. One alternative entails a charge transfer process between protons and metallic atoms having nearly the same ionization potential as hydrogen. The other involves a postulated excess emission in the ultraviolet Lyman lines or Lyman continuum. However, he concluded that if the latter were true, then the resulting coupling between atomic levels in hydrogen atoms would cause the Balmer lines to become shallower, or even to appear in emission. No such effect has in fact been observed. It has also been pointed out (Conti 1965a) that any Lyβ emission would produce an (unobserved) fluorescence in the λ8446 line of neutral oxygen. More recent abundance analyses of Am stars have indicated enhancements of strontium and yttrium, the second ionization stage of which have ionization potentials near, and between (respectively), the ionization potentials of scandium and calcium (which are deficient).

This fact has been taken (van't Veer-Menneret 1963) as additional evidence against any interpretation involving excess ionization.

An interesting aspect of the Greenstein analysis of τ Ursa Majoris is his discovery of a low spectroscopic gravity (log g = 1.6) and high microturbulent velocity (4 km/sec) in this star. Large values for the microturbulent velocity and low spectroscopic gravities were also found by Hack (1955a, 1955b, 1955c, 1956a, 1956b, 1956c). On the basis of high microturbulence in the Am stars 8 Comae and 15 Vulpeculae, Miczaika et al. (1956) concluded that microturbulence is related to metallicism in stars. This conclusion supported a suggestion by Greenstein (1949) that the Am anomalies arise in a very distended, unstable atmosphere, since it had also been shown (Struve and Elvey 1934, Wright 1955) that microturbulent velocities are large in the atmospheres of supergiant stars. In a number of subsequent curve of growth studies of Am stars, microturbulent velocities were found to be large compared to those derived for "normal standards." Conti and Strom (1968a) found them to be as large as 10 km/sec, which is slightly supersonic in these atmospheres. High microturbulence became such an expected secondary characteristic of Am stars that when a hotter candidate eventually was found to have Am-like abundance anomalies but also to have low

microturbulence, the metallicism of the star was questioned (Conti and Strom 1968b).

In an important paper, Baschek and Reimers (1969) found that when the microturbulent velocities of normal dwarf A and Am stars is plotted against their effective temperatures that a general rise in microturbulence is revealed for both groups of stars in the late-A spectral range. The authors could not explain this rise in terms of elementary mixing-length theory. It was noted, however, that the increased microturbulence occurs where the instability strip intersects the main sequence, and that this consideration might explain the observed peak. The Baschek and Reimers result may be subject to the criticism that the heterogeneity of the data they used from the literature may have somehow introduced a spurious effect. Nevertheless, Chaffee's (1970) study of microturbulence among A and F dwarfs, based on homogeneous data, does show a rise from 2 to 4 km/sec in the late-A region, which is in qualitative agreement with the Baschek and Reimers finding. In Chapter IV we shall present results confirming a general rise among all late-A dwarf stars.

The importance of the Baschek and Reimers result lies in its implication that microturbulence is actually no higher in the atmospheres of Am stars than in those of normal A dwarf stars of the same effective temperature, thereby disassociating microturbulence considerations from

metallicism. Baschek and Reimers attempted to reconcile their result with previous "high" determinations of microturbulence in Am stars by remarking that there are very few normal A stars with sharp-lined spectra that would lend themselves to curve of growth analysis. There is in fact considerable justification for this claim. First, many authors in early analyses compared Am stars with early F standards; low microturbulence may be a natural attribute of these F stars. Second, a survey of the literature shows that there had been no reliable curve of growth analyses of normal late-A dwarfs prior to the Conti and Strom (1968a, 1968b) studies.

Metallic Line Blanketing

The results of several photometric studies (Eggen 1955, 1957, 1959, Jaschek and Jaschek 1959) have shown that Am stars lie 0.5 to 1.0 magnitudes above the main sequence in color-magnitude diagrams of galactic clusters. It has also been demonstrated (Bidelman 1956, Abt 1961) that these stars lie in the same region of the two-color diagram occupied by giant stars. The Jaschek s (Jaschek and Jaschek 1959) have found that the distance of Am stars above the main sequence in the color-magnitude diagram is correlated with the star's "metallicity," which they define in terms of the difference in metallic line and hydrogen line spectral types. One interpretation of these observations is that

this photometric evidence agrees with the spectroscopic studies in demonstrating the distended nature of the atmospheres of Am stars. An alternative interpretation, advanced by Abt in 1961, is that the colors of Am stars may be due to excess line blanketing in the blue and ultraviolet photometric filter bandpasses. This suggestion was expanded by Varsovsky (1962), who argued that line-blanketed colors of a "superdwarf" sequence would produce an apparent shift of Am stars from the main sequence which is proportional to their degree of metal richness. Kopylov, Belyakina, and Vitrichenko (1963) pointed out that one could explain an observed increased departure of Am stars from the main sequence with decreasing temperature in terms of the rapid onset of many lines of neutral elements.

The line blanketing explanation has in fact been shown recently to be correct, however even during the early nineteen sixties the matter was not well understood. Confusion arose because the (U - B) color is a measure of <u>both</u> metallicity and surface gravity effects. However, the blanketing interpretation was soon bolstered with the advent of a new generation of photometric systems that offer "metallicity" indices independent of luminosity or surface gravity considerations, e.g., those of Stromgren (1963) and Golay (1964). Such indices have been shown (Kraft 1965, Golay 1964) to be correlated with the graduated "Metallic Line" spectral types of Weaver (1952). Both Stromgren and

Golay, however, were uncertain that their indices actually measure a metallicity content, since other effects such as increased microturbulence or a low continuous opacity can also produce stronger lines. Without accurate knowledge of the correct effective temperatures and surface gravities for Am stars, it was not possible to determine reliable absolute abundances in them and, therefore, to confirm or refute the idea of general metallic enhancements. Thus the interpretation of line strengths and of photometric colors of Am stars seemed very much of a circular problem.

The dilemma of interpreting the physical parameters of the atmospheres of Am stars was only resolved after several studies of hydrogen line strengths and profiles (Jaschek-Corvalon and Jaschek 1957, Jaschek and Jaschek 1959, Bohm-Vitense 1960, Slettebak, Bahner, and Stock 1961, van't Veer-Menneret 1963, Conti 1965a). These studies showed that hydrogen line types in these stars are well correlated with (B - V) photometric colors[1] and, by implication, effective temperature. Baschek and Oke (1965) compared photoelectric scanner observations of Hγ profiles of several normal A and Am stars. They concluded that, when corrected for the low resolution of their scanning instrument, Hγ lines in Am stars are identical to those in normal stars. Therefore,

---

1. However, their colors are slightly systematically redder than normal main sequence stars of the same temperatures or hydrogen line strengths.

this spectral feature may be taken as a reliable indicator of effective temperature in Am stars. The authors also found that the (B - V) colors of five Am stars they observed are too red for their effective temperatures, based on their Hγ profiles. They took this excess reddening to be due to excess metallic line blanketing in Am stars and deduced "corrected" (B - V) colors. The inferred de-blanketing slopes in the two-color diagram for two of these stars, 63 Tauri and τ Ursa Majoris, were found to be parallel. This slope was assumed to be universal among Am stars and was applied to the observed colors of those Am stars in the Hyades cluster. The result was that their positions in the color-magnitude diagrams were moved back near, or even beyond the main sequence. Thus while Baschek and Oke did not prove the hypothesis of increased line blanketing explicitly, by measuring aggregate line strengths, they were able to demonstrate the self-consistency of their approach. Strittmatter and Sargent (1966) have carried out a similar study on the blanketing of Am stars in the Coma and Praesepe clusters, with similar conclusions emerging.

More recently, Ferrar, Jaschek, and Jaschek (1970) have used (blanketing-free) infrared colors to establish temperatures of Am stars in order to investigate more fully the effects of blanketing in the blue and violet spectral regions. They confirmed the tentative conclusion of Baschek and Oke that the blanketing trajectory in the two-color

diagram has the same slope for Am stars as for normal A stars. They also determined that the amount of blanketing is proportional to the Jaschek's "degree of metallicity," even to the extent that those Am stars showing only marginal reddening have a metallicity of zero. This result strongly suggests that the photometric colors of Am stars can be fully explained in terms of a higher general abundance of the metals in their atmospheres.

Effective Temperatures of Am Stars

The inability of investigators to determine unambiguous effective temperatures for Am stars has in the past been a major barrier in the interpretation of these stars. It has already been mentioned that hydrogen lines provide a very good measure of effective temperature. In addition, Praderie (1968) has demonstrated that temperatures inferred from (V - R) and (V - I) infrared colors agree very well with the hydrogen line determinations. The temperatures derived from these studies indicate clearly that Am stars are A stars and that they occupy the spectral domain mentioned in the Introduction.

The above conclusion is amplified by the spectral classification work of Barry (1967). He found that the metallic line types of the thirteen Am "standards" in the RME study tend to be three subclasses later than their Stromgren (b - y) colors indicate. Evidently, this

discrepancy arises because of the mimicking of several Am spectral characteristics with low luminosity or cool temperature effects, according to the MK classification system. When these stars are reclassified according to the more purely temperature-dependent ultraviolet spectral criteria suggested by Barry, it is found that their new metallic line types are in excellent agreement with their colors (Barry 1967).

There was, however, also early spectrophotometric evidence that appeared to confirm the RME conclusion that Am stars are F stars. Berger and Fringant (1951) and Berger, Fringant, and Menneret (1956) found that both the blue gradient and the "break" in the gradient at λ4800 in several Am stars were characteristic of late F stars. However, in 1962 Rozis-Saulgeot showed that the "λ4800 break" was due to the inadequate resolution of partially blended spectral lines in the earlier investigations. Van't Veer-Menneret (1963) has also shown that the observed blue gradient can be corrected to that of a normal A7 or A8 dwarf in the case of the pronounced Am star 63 Tauri, when proper account is taken of the same line blending problem. It should also be mentioned that inspection reveals that most of the Am stars examined in the early Berger et al. studies tend to be among the cooler members of the Am class, so that it is not surprising that F spectral types were derived for them. Therefore, one can conclude once again that when proper

allowance is made for the increased spectral line strengths that the spectrophotometric features of Am stars are virtually identical to those of normal A dwarfs.

Surface Gravities, Abnormal Atmospheric Structures of Am Stars

With the effective temperatures and the blanketed colors of Am stars apparently well explained, it remains to be determined what the true surface gravities of these stars are. An even more basic question is whether a single effective gravity applies to the entire atmosphere of an Am star.

It has long been recognized that the wings of hydrogen lines in Am stars are strong; this is a dwarf-like characteristic. Aller (1947) concluded that there are as many hydrogen atoms excited to the second atomic level in the atmospheres of Am stars as in the case of dwarf A stars. The Inglis-Teller (1939) visibility criterion for high level Balmer lines also implies that the effective gravities of the hydrogen line formation regions of Am atmospheres are dwarf-like (Jaschek and Jaschek 1959, Komarov 1965). The sizes of the Balmer jump have been found to be indicative of A dwarfs, both spectrophotometrically (van't Veer-Menneret 1963) and photometrically (Stromgren 1963).

The conflicting surface gravities indicated from spectroscopic studies on one hand and Balmer line or Balmer jump criteria on the other has led some authors to

speculate that the continua and hydrogen lines in Am stars are formed in a normal, dwarf-like atmosphere (log g = 4.0), while the metallic lines are formed in an outer, somehow distended, region of the atmosphere. This hypothesis was investigated in some detail by Bohm-Vitense (1960). She showed that even if the observed microburbulence is a real turbulent motion, it is not sufficient to produce an appreciable reduction in the effective gravities of the atmospheres of these stars. She suggested, however, that since it has been observed (Babcock 1958) that small magnetic fields exist in some Am stars, that these might serve to distend the atmospheres through their "magnetic pressure." This effect would require a field of the order of several kilogauss.

It is very instructive to consider the arguments used by Bohm-Vitense to demonstrate the abnormality of the atmospheres in Am stars. First, it should be noted that she explicitly stated that she was disposed to accept the reality of abundance anomalies as explanation for the observed spectral peculiarities only after the hypothesis of atmospheric abnormality could be discarded. She then presented evidence which she interpreted as supporting this latter hypothesis. Profiles of the K-lines of the Am stars 63 Tau and 16 Ori were compared to those of γ Vir N and γ Vir S, chosen as standards. The Am K-lines were shown to have much less developed wings, and so are the weaker lines.

Their cores, however, are considerably deeper. Since the line absorption coefficient is very large in the core, the core of the line is formed near the top of the stellar atmosphere. Therefore, Bohm-Vitense interpreted the deep K-line cores as evidence that the atmospheric boundary temperature in Am stars is lower than in normal A stars.

A simpler explanation for the deeper K-line cores in the Am stars is that the K-line cores of the standard stars Bohm-Vitense used are in fact rotationally broadened. One of her standards, γ Vir N, is also used as a standard in this present study (see Chapter III). According to the broadening of its metallic lines, it exhibits V sin i = 27 km/sec (Uesugi and Fukuda 1969); the residual intensity at the K-line center is 15%. On the other hand, another standard used herein is the extremely sharp-lined normal star HR 114. Its K-line center has a residual intensity of only 3%, which is in precise agreement with those found in 63 Tau, 16 Ori, and several other sharp-lined Am stars. We conclude that rotational broadening of the K-line cores of normal stars is the most likely explanation for the effect noted by Bohm-Vitense.

According to Stark line-broadening theory, the strength of line wings increases with the square root of the product of the electron density times the number of atoms producing the absorption. Bohm-Vitense chose to interpret the weak K-line wings as evidence of a reduced

electron pressure in those layers of the atmosphere responsible for the K-line formation. Because of the lack of independent evidence to support this interpretation, however, more recent authors (e.g., van't Veer-Menneret 1963, Praderie 1967) have taken the weak K-line wings to be due to an actual calcium deficiency. Additional support for the latter alternative comes from a study on Am stars in the Hyades by Conti (1965a). He showed that the indicated Ca/Fe abundance ratio remains almost constant when semi-empirical model atmospheres are used, in which the electron pressure is permitted to be artificially reduced outwards by arbitrary amounts. The Ca/Fe ratio also remains constant for several models having arbitrarily chosen boundary temperatures. The physical reason for this constancy is that the "contribution functions" (measures of where an absorption line is formed through the atmosphere) of iron and calcium lines used in abundance analyses are remarkably similar. It is therefore difficult to change the derived Ca/Fe ratio by modifying the atmospheric structure, although derived individual elemental abundances may be altered substantially. It should also be mentioned in this connection that several authors have computed contribution functions for particular lines in a given model atmosphere and plotted them as a function of log (τ continuum) (hereinafter "τ_C"). They take the peak of this function to be representative of a single level near which the line

is substantially formed. A more meaningful quantity is the "mean depth of formation," $\overline{\tau}_c$, which can be obtained by locating the centroid of the contribution function weighted by τ line, when plotted against τ_c, as abcissa. When this is done, it is found that lines with contribution functions peaking at $\tau_c = 0.1$ typically have $\overline{\tau}_c = 0.5$ to 0.7, or even larger. Therefore, these weaker lines which are sensitive to abundance, i.e., those on the linear portion of the curve of growth, are actually formed quite deep in the atmosphere. Accordingly, it is difficult to reconcile the observed metallic line strengths to the picture of a distended atmosphere. Such an atmosphere would presumably also produce (unobserved) very modified continuum features, such as an increased Balmer jump.

Bohm-Vitense (1960) has also pointed out that the ratio of measured aggregate line blocking in 63 Tau and 16 Ori, as compared to γ Vir N and S, increases toward the ultraviolet. Because of the relative way in which this is measured, it cannot be an abundance effect. She suggested that this wavelength dependency may arise from the decreased strength of the nearly gray, H^- continuum opacity source relative to that of the wavelength-dependent hydrogen opacity source. Since the H^- opacity is directly proportional to the electron pressure, she interpreted this effect as confirmatory evidence that the electron pressure is low in Am atmospheres. This conclusion rests, however,

upon the assumption that the effective temperatures of 63 Tau and 16 Ori are similar to those of γ Vir N and S. In Chapter III, we shall find that these two Am stars are several hundred degrees hotter than γ Vir N. In Chapter IV we shall show that their gravities are very similar. It is therefore likely that at least a large portion of the relative wavelength dependence of line strengths in Am stars is due to a temperature rather than a surface gravity effect.

Finally, it should be noted that the original Babcock evidence that magnetic fields exist in Am stars was at best marginal, since those few in which he found them typically showed longitudinal field components of about 300 gauss. Conti (1969a) has recently shown, however, that 16 Ori, Babcock's best case, and 15 Vul must have longitudinal fields less than 50 and 100 gauss, respectively. Conti concluded that Babcock's estimated internal errors may have been chosen too small and that Am stars probably do not have substantive magnetic fields. Recent polarimetry of Sirius with the McMath Solar Telescope at Kitt Peak does not exhibit a detectable longitudinal or transverse magnetic field component (Livingston and M. Smith 1970). In conclusion, it appears that magnetic fields strong enough to produce an atmospheric distension almost certainly do not exist in the atmospheres of Am stars.

At the present time there does not appear to be any compelling evidence that there is any structural abnormality

in the atmosphere of Am stars. It has been concluded by several authors (van't Veer-Menneret 1963, Sargent 1964, Hack 1965, Conti 1970) that the choice of excessively low ionization temperatures in Am stars, resulting from the belief that they were actually F stars, led the earlier investigators to derive low electron pressures and to infer low effective gravities in their curve of growth analyses. A survey of the recent literature since Conti's 1965 paper shows that there have been nineteen separate investigations (e.g., Conti and Strom 1968a, 1968b, Olson 1969) of surface gravities of nineteen different Am stars. These studies have utilized such independent techniques as curve of growth analyses, Balmer jump sizes, hydrogen and K-line profiles, and eclipsing binary solutions. The surface gravities of all these determinations are all very close to $10^{4.0}$ cm/sec^2, which is also that usually found for dwarf A stars (see Conti and Strom 1968a). Therefore, the more recent work on Am stars indicates that there no longer appears to be any discrepancy in surface gravities derived by different methods.

Miscellaneous Atmospheric Effects

This review would not be complete without mentioning a few additional explanations which have been suggested for the metallicism phenomenon. One of these has been the suggestion that the helium content of Am stars is high.

This idea was advanced by Struve (1950) to account for the apparent positions of these stars above the main sequence. Bidelman (1960) suggested that these stars might be returnees from the red giant branch and that their atmospheres might be expected to have an enriched helium content. It has also been pointed out (Conti 1965a) that since enhanced helium means deficient hydrogen, a high derived [Fe/H] could be interpreted as a hydrogen deficiency rather than as a real iron enrichment. However, Conti investigated this possibility by repeating his curve of growth analyses of Hyades Am stars with helium-rich model atmospheres. He found, first, that such atmospheres would produce incorrect Hγ profiles and, second, that, as before, helium abundance changes do not affect the Ca/Fe ratio. Boyarchuk (1963) and Kohl (1964) have found a slight absolute overabundance of helium in Sirius by curve of growth analyses of a few He I lines. We have re-analyzed Kohl's data by means of the model atmosphere curve of growth analysis described in the next chapter. We find that if an effective temperature of 10,000°K (Strom et al. 1968) is assumed for Sirius, then log (He/H) = -0.92, which is normal. However, because of the difficulties in assigning accurate temperatures to stars in this spectral domain, it is most advisable to rely on differential analyses. Kohl found in his analysis that the relative helium abundance in Sirius, as compared with that of Vega, is normal. Thus from the

present data, there appears to be no evidence for abnormal helium abundance in Am stars.

In 1950 Rudkjøbing suggested that whereas F stars have a deep surface convection zone, Am stars may be F stars whose surface regions are in radiative equilibrium. Such stars might exist (ironically) if their surface gravities are high, or their helium content low (Pecker-Wimel 1953); either condition would tend to suppress convection. According to this proposal, the change in the temperature gradient between atmosphere models in adiabatic and radiative equilibrium would serve to alter the K-line strength. This argument can be criticized today on several grounds. First, as Conti showed, one cannot explain the low Ca/Fe ratios observed in Am stars by structural changes in the atmospheres. Prbzylski (1954) showed that even if convection were as important as it is in F stars, it could not explain as much as a 10% change in the K-line strength. Finally, it has been noted that Am stars are principally A stars, in which surface convection does not play an appreciable role in energy transport.

A few astronomers have suggested (Underhill 1969) that the spectral anomalies observed in Am stars may be due to non-LTE line formation processes, however no specific calculations have been published to account for the observed line strengths in detail. As noted in Figure 8 of Chapter IV, the mean depths of formation of the weak lines,

from which one infers abundances, are in the range $\bar{\tau}_c = 0.5$ to 0.9. At these depths in dwarf star atmospheres, one does not usually expect departures from LTE to be significant, since the electron pressures are so high (Unsold 1955). There is some evidence (Athay and Skumanich 1968) that if the lines located on the flat region of the curve of growth are formed by non-coherent scattering processes, and if they are fit to a conventional (LTE) curve of growth, that the microturbulence derived will be excessively high. However, since there does not appear to be any substantial structural differences between the atmospheres of Am and normal A dwarfs, it is difficult to see how non-LTE processes could occur in the one group of stars and not the other. It should also be noted that Greenstein (1949) found that for iron atoms, the ratio of the populations of those normal levels at least two electron volts above the ground state, and of those of metastable levels, is the same for τ Ursa Majoris as for normal F stars. His interpretation of this observation was that the line source functions do not suffer noticeable dilutions below their LTE values in the atmospheres of Am stars. In view of the present evidence, therefore, there does not appear any basis for interpreting the Am spectral anomalies as non-LTE effects.

We have concluded that there does not appear to be substantive evidence that the structure of atmospheres of Am stars are dissimilar to those of normal dwarf stars of

the same effective temperature. Any possible non-LTE effects do not appear to be unique attributes of Am stars. In addition, there is evidence that microturbulence is "normal" in Am stars. We conclude that the atmospheres of Am stars are not "abnormal" in any manner discussed above,[1] and that, by implication, the observed abundance anomalies in these atmospheres are real. We interpret the "metallic line" nature of these stars' spectra as being due to a general enhancement of the metals in these atmospheres. Therefore, the analysis of equivalent width data may be carried out by use of conventional LTE, dwarf model atmospheres, such as those discussed in the next chapter.

---

1. We neglect for the present such secondary considerations as differential backwarming in these atmospheres due to the increased line blanketing.

CHAPTER III

THE ACQUISITION AND REDUCTION OF THE DATA

Selection of the Program Stars

Recent determinations of age and metallicity differences between galactic clusters have opened the question as to whether metallic line stars in one cluster may differ in composition from those in another. In order to test for this, we have chosen several Am stars in the Hyades and Coma Berenices clusters and the Ursa Major Stream. Of these nearby aggregates, the Hyades and Coma groups are presently thought to be well-defined clusters whose members were formed from chemically homogeneous interstellar clouds at common times. Stars in the Ursa Major Stream are defined by their common space velocities (Roman 1949, Eggen 1958).

It has been noted by several investigators that stars in the Hyades have particularly enhanced metallic lines. Among the A stars they exhibit m_1 indices about $0^m.01$ larger than those in a field sample of the solar neighborhood (Barry 1970). One may infer that these effects are due to actual metal enrichment becuase of the slight overabundances found for the Hyades G2 star HD 28344 (Wallerstein and Helfer 1960) and from the observation that other Hyades stars have the same composition as HD 28344

(Conti, Wallerstein, and Wing 1965). Alexander (1967) and Nissen (1970) have also concluded that the Hyades stars are metal rich by a factor of two. On the other hand, the Coma and Ursa Major A stars have m_1 indices about $0^m.01$ smaller than the Hyades stars (Crawford and Barnes 1969a), so that their metallicity is virtually "normal." Although the metallicity differences between the Hyades and other clusters and field stars are only about a factor of two, some attention has been called to the particularly pronounced character of the Hyades Am stars. One wishes to determine whether this effect may be due to primordial composition differences.

Based on recent evolutionary models and temperature calibrations, van den Heuvel (1969) has found ages of 9 and 6.5×10^8 years for the Hyades and Coma clusters, respectively. These ages are about twice the older values (Allen 1963). The age of the Ursa Major Stream is in the same general range since its color-magnitude diagram also exhibits a main sequence turn-off at A0 (Roman 1949, Eggen 1958). The range in these ages is negligible compared to the total range in ages of clusters in which Am stars are known to exist. There is therefore little possibility of using these particular clusters to determine whether age is correlated with the Am spectral peculiarities.

There are two conditions that determined the choice of Am stars in these clusters for the present study. The

first is that their spectra be single-lined so that line misidentification and dilution problems might be minimized. Second, we have adopted Chaffee's (1968) empirical rotation velocity limit of program stars having V sin i $\lesssim$ 40 km/sec; otherwise the weak lines become lost in the continuum noise while the stronger lines blend into one another. In order to investigate the effects of mild rotation on abundances, however, this last condition was relaxed to include the broad-lined Am stars, ξ U Ma B and θ Cep.

These criteria resulted in the selection of sixteen Am stars for this study, seven in the Hyades, five in Coma, and four in Ursa Major.[1] Of these, a few merit specific remarks. 22 Comae was classified by Weaver (1952) as a "weak" Am star, however more recently other investigators (Kraft 1965, Cowley et al. 1969) have classified it as normal. In a recently compiled spectral atlas Abt et al. (1968) have used this star as an A3 V standard. The Ursa Major star θ Cep has also been classified normal (Cowley et al. 1969), however we shall show that several anomalies exist. As noted earlier, 68 Tau is an excellent example of Conti's "early Am" stars; this star is in fact located well above the Hyades turn-off point. The star 88 Tau has been found by Abt (1961) to be double-lined. We have taken six high dispersion, blue plates of this star at such

---

1. One star, ξ U Ma B, is actually in the Ursa Major Cluster.

intervals, according to Abt's radial velocity curve, as to resolve the double line components. No double components or variations in line profiles were observed, however. We conclude tentatively that 88 Tau has single lines, with dilution effects probably present, and that it exhibits V sin i ~ 30 km/sec. Finally, RR Lyn is an eclipsing binary system whose secondary may be inferred (Linnell 1966) to be early F. The only secondary lines observed were the sodium D lines on one yellow plate taken 24 hours after eclipse. The spectral lines in the blue suffer about 8% dilution compared to two blue spectra taken during eclipse.

In Figures 1 and 2 we compare Am stars and those in the field in histograms of the Stromgren parameters Δm_1 and Δc_1, respectively. The latter were selected from the Stromgren-Perry Catalogue (Stromgren and Perry 1965). Those Am stars in the Hyades are also represented in Figure 1. From these histograms one infers that even if, for an unspecified reason, the program stars have not been randomly selected, that their distributions in Δm_1 and Δc_1 are representative of those of the larger field example. We take this as prima facie evidence that the program stars are generally representative of the class of Am stars.

Four standard stars were chosen with temperatures close to those of the Am stars under study. Two of them, η Lep and ζ Vir N, are F0 V stars used in the Chaffee (1968) Thesis. The third star, 28 And, is a very sharp-lined star

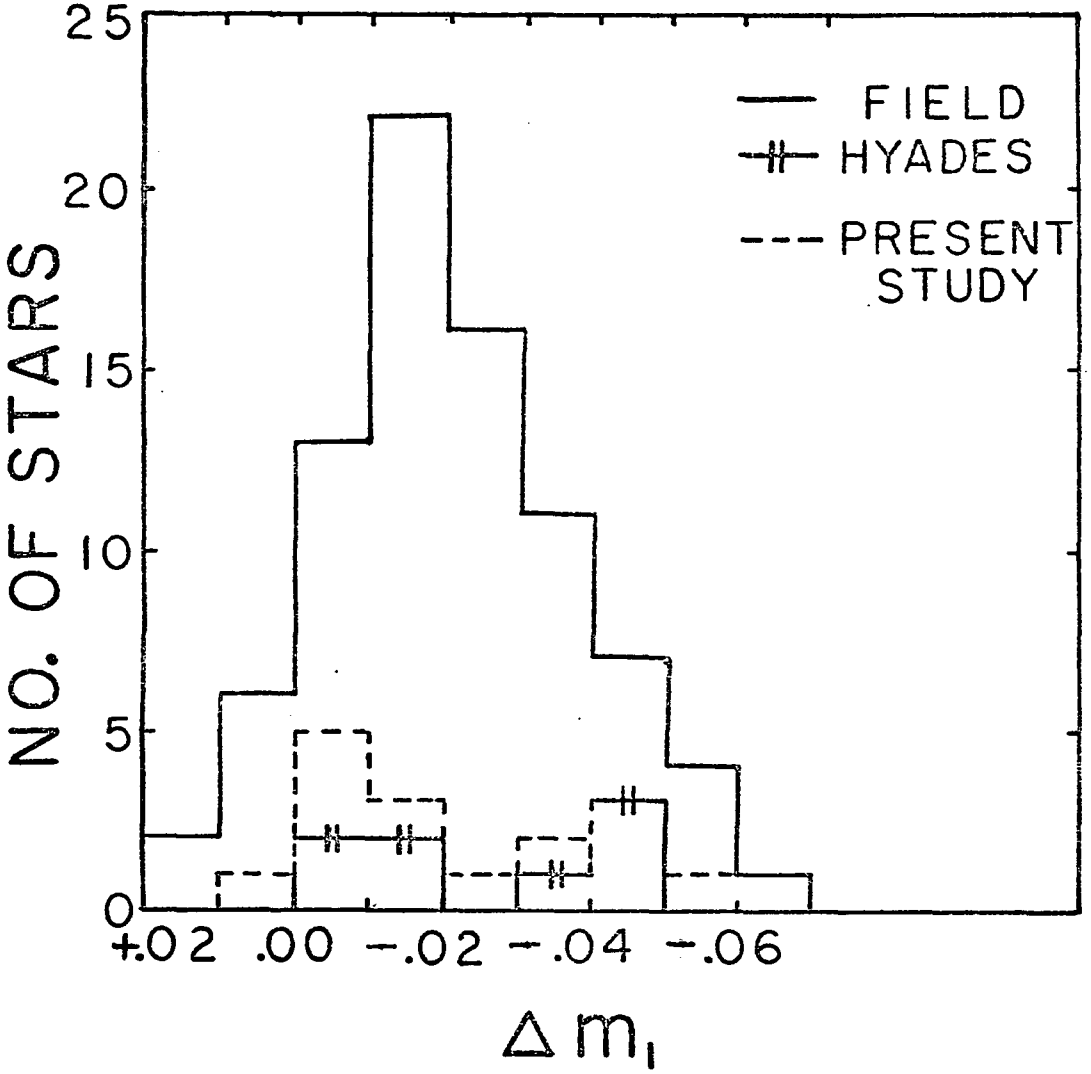

Figure 1. Frequency distribution of Am stars with Δm_1

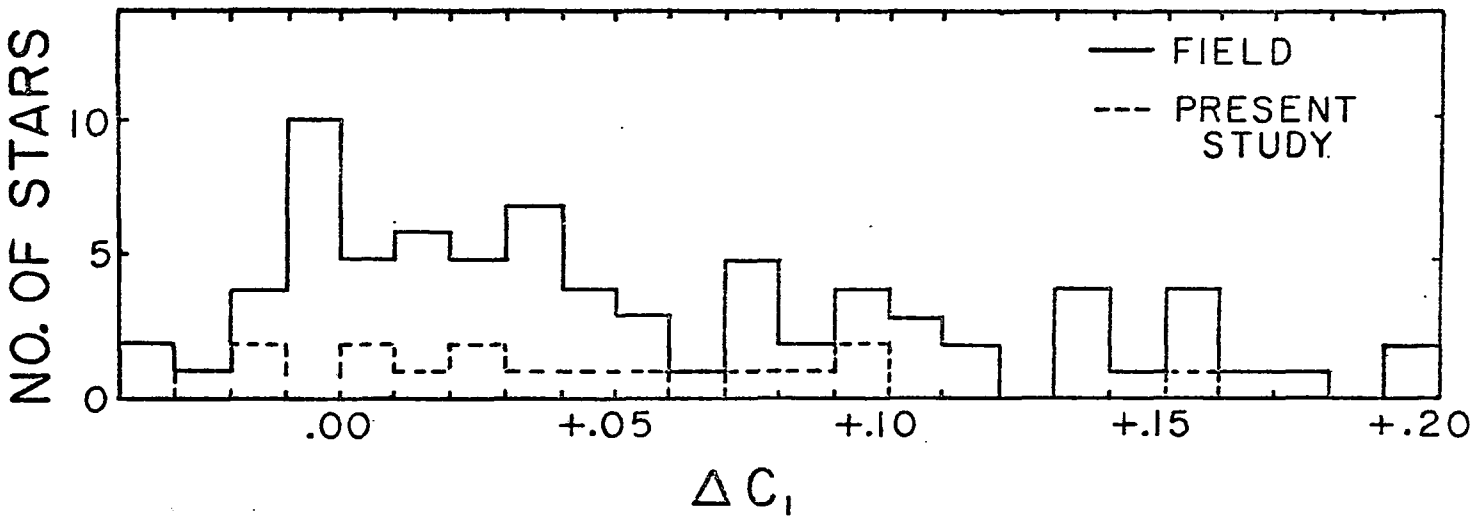

Figure 2. Frequency distribution of Am stars with Δc_1

whose spectral type we estimate to be A9. This star is a δ Scuti star with a small light amplitude of $0^{m}.035$ (Breger 1969). The final standard, HR 906, is in the Ursa Major Stream. It has been classified Am (Hoffleit 1964), however Cowley et al. (1969) classified it as A7 III-IV. In Chapter IV it will be demonstrated that this star is in many respects normal. A total of four standards were chosen in order to obtain reliable average abundances for normal stars and to estimate the apparent dispersion in abundances among them.

In Table 1 the names, Harvard Revised Numbers, colors, and apparent rotational velocities for the twenty stars of this study are listed. The Stromgren four-color data and (V - R) colors are those of the Stromgren-Perry Catalogue (Stromgren and Perry 1965) and Johnson et al. (1966). The Hβ measures are taken from Crawford et al. (1966). All observed colors are to be considered as intrinsic since none of the three clusters suffers measurable reddening (Crawford and Stromgren 1966, Crawford and Barnes 1969a). In the final column, V sin i estimates are shown. They are taken from Uesugi and Fukuda (unpublished), or are personal estimates (asterisks).

The Temperature Calibration

In Chapter II it was remarked that infrared colors and hydrogen line measures form reliable effective

Table 1. Colors and Rotational Velocities of Program Stars

Name	HR (HD)	b - y	V - R	Hβ	Adopted T_{eff}	V sin i (km/sec)
(Coma)						
8 Com	4685	.081	.13	2.868	8625°K	< 12, < 10*
	(108486)	.095	--	2.851	8500	30
	4750	.097	.15	2.846	8400	< 12
	4751	.121	.15	2.843	8350	< 12
22 Com	4780	.058	.09	2.878	8850	8
(Hyades)						
60 Tau	1368	.204	.31	2.757	7550	15, 25*
63 Tau	1376	.180	.27	2.783	7700	< 12, < 10*
68 Tau	1389	.081	.09	2.889	9100	16, < 10*
81 Tau	1428	.140	.24	2.809	8050	23
88 Tau	1458	.095	.19	2.834	8350	27
	1519	.084	.18	2.844	8400	64, 40*
16 Ori	1672	.138	.20	2.820	8125	30, < 10*
(U Ma)						
RR Lyn	2291	.137	.22	2.826	8125	< 10
ζ U Ma B	5055	.079	--	2.755	8800:	59
θ Cep	7850	.106	.17	2.834	8350	59
32 Aqr	8410	.124	.18	2.817	8225	51, < 10*
(Standards)						
28 And	114	.169	--	2.755	7700	22, < 10*
	906	.075:	.13	2.874	8625	15*

Table 1.--Continued

η Lep	2085	.218	.33	2.726	7400	0, ~ 10*
γ Vir N	4825	.245	.29	2.694	7100	27

*Personal estimate.

temperature indicators. For the assignment of temperatures to the program stars, the photometric (V - R) colors and Hβ indices noted in Table 1 have been utilized. Both colors are very insensitive to metallic line blanketing in A or early F stars. Powell (1969) has recently used the Hβ index to calibrate temperatures for F stars.

We have also used a third color index, Stromgren (b - y), for the temperature calibration. This color is analogous to the (B - V) color of Johnson, however it tends to be much freer of blanketing. It has been shown from the work of Baschek and Oke and others that (B - V) is substantially affected by the presence of metal lines. This sensitivity reflects the fact that the B filter peaks at λ4400 and still retains nearly 90% of its peak transmission at λ4000 (Johnson and Mitchell 1962), where the blanketing effect is already strong. The V filter, however, peaks in the yellow at λ5500 and suffers virtually no compensatory blanketing. On the other hand, the b filter of the Stromgren system peaks at λ4670. Even at λ4550, where there is very little blanketing, its transmission is negligible (Crawford 1966). The insensitivity of (b - y) has been quantified by Crawford and Barnes (1969b) for A and F stars. They found that the calibration of the zero-age, normal composition color $(b - y)_o$ necessitates a correction of 0.1 Δm_1 for metallicity differences. According to this correction if $\Delta m_1 = -0^m.05$, as for a rather pronounced cool

Am star, then the (b - y) color suffers a blanketing correction of only $0^{m}.005$. One may also convince himself that (b - y) is practically insensitive to blanketing by plotting the Hβ indices against the (b - y) colors of all the Am stars in the Stromgren-Perry Catalogue. If this is done, it is found that only the coolest, most pronounced cases, such as τ U Ma, deviate redward of the mean relation for normal A stars. We conclude that (b - y) forms a reliable temperature index for Am stars.

One now seeks a basic calibration of stellar effective temperatures with which to compare the observed colors. Most of these calibrations are given in terms of the (B - V) color so that it becomes necessary to convert to the above colors by means of standard color relations given in the literature. There are several recent calibrations. Oke and Conti (1966) derived temperatures for stars cooler than AO by comparing photoelectric continuum scans of Hyades stars with hydrogen line blanketed model atmospheres. These scans were extended from the near ultraviolet to the near infrared and were corrected for metallic line blanketing. Morton and Adams (1968) have established a temperature scale for O to G2 stars. This scale is also based on hydrogen line blanketed models. Wolff, Kuhi, and Hayes (1968) have calibrated the temperatures of B and A stars from scans of their Balmer discontinuities and continua. This work is based upon a revised absolute spectrophotometric calibration

by Hayes (1970). Matsushima (1969) has calibrated the temperatures of A stars by computing the Stromgren indices of model atmospheres; empirically determined blanketing coefficients were included. This last calibration is the most recent, and its agreement with the temperatures determined by interferometric techniques (Brown et al. 1967) is extremely good. These four calibrations are shown as a function of (b - y) in Figure 3.

At the outset of this project, the Matsushima results were not available. For this reason, and because ionization equilibrium considerations seemed to favor a shallow temperature-color calibration, we chose the "intermediate" scale of Morton and Adams for the assignment of temperatures to our program stars. We note, however, that the results of Matsushima and of Brown et al. were determined by independent techniques, and their agreement is impressive. This agreement together with the steeper slope of the Hβ calibration for F stars (see Powell 1969) would argue in favor of the Matsushima scale. These differences affect derived abundances primarily in only the hottest A stars ($T_{eff} > 8500^{o}K$). We shall return briefly to this question in the next chapter. For the meantime we note that these differences underscore the present uncertainties in the temperature calibration of stars.

Temperatures derived for the program stars from the individual colors are listed in the second, third, and

Figure 3. Recent stellar temperature calibrations

The calibration represented by ——— is that of Morton and Adams (1968) (adopted herein); - - - - represents that of Wolff, Kuhi, and Hayes (1968); — —, that of Oke and Conti (1966); — - —, that of Matsushima (1969). The ordinate scale is $\theta_{eff} = 5040/T_{eff}$.

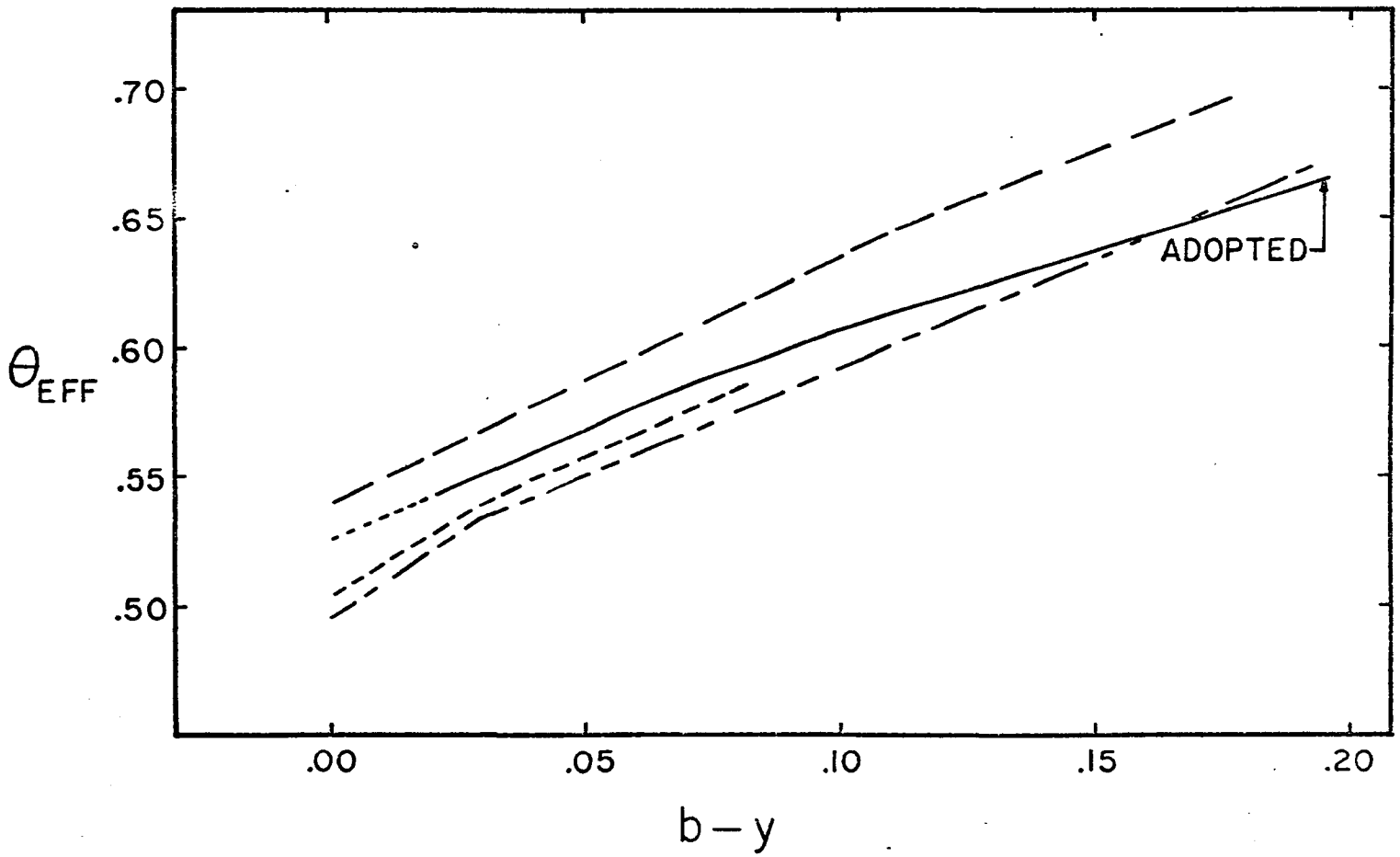

Figure 3. Recent stellar temperature calibrations

fourth columns of Table 2. The actual effective temperature assigned is the average of these and is given in column five. The internal dispersion among the color temperatures T_{V-R}, T_{b-y}, and $T_{H\beta}$ is $\pm 60^{\circ}K$, which sets a lower limit to random errors in the assigned temperatures. This satisfactory agreement among them, however, is actually only a cross-check on the precision of the photometry, since all three color temperatures rely on the same Morton-Adams calibration.

Procurement and Reduction of the Spectrograms

Spectrograms of the program stars were obtained at the Coude focus of the 84-inch telescope of the Kitt Peak National Observatory near Tucson, Arizona. The f/4.1 Schmidt camera was used in conjunction with a 600 grooves/mm double-diamond Bausch and Lomb grating. We obtained three spectrograms of each star[1] on Kodak IIa-0 ("blue") plates at second order (8.9 A/mm) and two plates each on IIa-D ("yellow") plates at first order (17.8 A/mm). For sharp-lined stars the slit width used was 0.10 mm, which projects to 13.7 μ on the plate. For mildly rotating stars a slit width of 0.11 or 0.12 mm was used. The spectrograms were widened to 0.66 mm. The plates were then developed in

---

1. We wish to thank Dr. Frederic Chaffee for his permission to use his plate material for η Lep and γ Vir N. Thanks are also due to Dr. Helmut Abt for kindly taking a blue plate of 16 Ori and a yellow plate of 8 Com.

Table 2. Inferred Temperatures of Program Stars

HR (HD)	T_{b-y}	$T_{H\beta}$	T_{V-R}	T_{eff}
4685	8550°K	8650°K	8625°K	8625°K
(108486)	8425	8525	--	8500
4750	8375	8450	8500	8400
4751	8200	8400	8500	8350
4780	8775	8800	9000	8850
1368	7550	7600	7500	7550
1376	7750	7800	7525	7700
1389	9300	9000	--	9100
1428	8050	8100	7900	8050
1458	8375	8325	8325	8350
1519	8450	8400	8300	8400
1672	8050	8175	8150	8125
2291	8100	8250	8100	8125
5055	8525	8950	--	8800:
7850	8300	8325	8400	8350
8410	8225	8150	8300	8225
114	7750	7600	--	7700
906	8550	8700	8625	8625
2085	7400	7350	7400	7400
4825	7100	7000	7500	7100

Kodak D-76 for thirteen to fifteen minutes, depending on the measured temperature in the developer.

The plate material was taken with the aid of an exposure meter that contained a mirror behind the spectrograph slit. This mirror periodically flipped into the beam in order to sample the stellar light intensity. The spectrograms were exposed such that the densest portion of each has a transmission of approximately 25%. If the plates were more densely exposed, then the slope of the characteristic curve appropriate to these higher densities becomes steep, and direct intensity errors become excessively large. Moreover, the spectral lines tend to "fill in" due to photographic turbidity. This effect tends to reduce the apparent line strengths. If the spectra are underexposed, then lines of a wavelength region on the edge of the emulsion sensitivity are unreliable, for weak lines tend to become lost in the grain noise while strong lines tend to "bottom out." The latter effect leads to spuriously large line strengths. Therefore, in order to insure a homogeneous scale of line strengths, or "equivalent widths," the densities of spectrograms of a given spectral region must be as uniform as possible.

The spot sensitometer of the 84-inch was used to obtain photographic calibrations in four spectral regions. This instrument contains thirteen spots. Its quantitative reliability has been established by Chaffee (1968), who

compared it with a more elaborate, forty-spot device. Calibrations of O-plates were taken with Corning types 5-62 and 5-75 filters, which peak at λ4000 and λ4600, respectively. For the D-plates the 4-105 and 3-110 filters were used; these peak at λ5100 and λ5800, respectively.

The relative spot intensities were taken from photoelectric measures by Chaffee (1968). These permitted the construction of characteristic curves for each of the four spectral regions. These curves were normalized to an arbitrary number of intensity units at a transmission of 40%. This procedure was employed to compensate for small systematic differences between characteristic curves of different spot plates. When normalized, characteristic curves determined from several plates invariably showed only small variations, in accord with Chaffee's (1968) findings. We found that by developing two spot plates simultaneously that we could obtain virtually identical characteristic curves. This observation indicates that most small variations in characteristic curves probably arise from small differences in darkroom temperature and development time. This, in turn, suggests that short of having the plate calibration on the stellar spectrogram plate itself, the most advisable procedure is to reduce the stellar spectrograms by means of a mean characteristic curve. Accordingly, mean curves were used. These mean curves were constructed from curves of four to six spot plates per filter region for

each photographic "batch." In addition, one or two sets of spot plates were exposed and developed along with the stellar plates during each observing run. The spot plates were always cut either from the same plate or from the same box of plates as the spectrogram plates. In all cases, the characteristic curves derived from these spot plates were compared to the appropriate mean curves in order to insure that their shapes did not change from run to run.

The actual reduction of the spectrograms was carried out with the Kitt Peak Hilger-Watts microphotometer and with the Moseley "Autograph" x-y plotter. The Moseley unit has a curve-following attachment which automatically follows the constructed characteristic curve and converts the measured plate density to direct intensity. The direct intensity data are recorded in spectral tracing form by a Brown chart recorder.

The microphotometer was run at a speed of 0.5 mm/min, which yields chart scales of 0.87 and 1.73 A/mm for the 0- and D-plate data, respectively. The microphotometer scanning slit was set at a width of 10 to 12 μ on the plate and at a height of 0.66 mm (the spectrogram width). The intrinsic resolution of the microphotometer with a virtually closed slit is 8 μ (Abt, 1969).

Prior to making a tracing, the curve-follower was normalized to zero transmission by placing an opaque screen in front of the scanning slit beam. The "zero intensity"

was set by locating the clearest available fog level on the plate. Immediately before the tracing was made, the fog level was measured adjacent to the spectrogram along its entire measured length. It was discovered that measured equivalent widths are very sensitive to the "slit focus" setting. If this adjustment is slightly out of focus, the lines become blended and abnormally weak. Therefore, in practice this focus was determined by scanning a comparison line at a slow speed and noting the adjustment setting for which the largest deflection was achieved.

The characteristic curves used for the 0-plate material were those of the 5-75 filter between Hγ and Hβ, and of 5-62 shortward of Hγ. For the yellow plate material the 3-110 curve was used between λ5400 and λ6250, while the 4-105 curve was used between Hβ and λ5400.

Choice and Measurement of the Spectral Lines

Occasionally two investigators obtain different abundances for the same star when nearly identical atmospheric parameters are chosen for the curve of growth analyses. The source of such discrepancies can sometimes be traced to the different lists of lines used by the investigators. In the present analysis we shall derive abundances of elements in some cases based on a very few lines. It therefore becomes imperative to define a homogeneous sample of lines which may be used commonly for

all stars investigated. Otherwise, if a line which systematically indicates an abundance different from the mean for that ion is omitted, the computed mean abundance will be affected by this non-abundance effect. In practice this "homogeneity criterion" for selecting a list of lines means that not many lines should be excessively weak for high temperature stars, nor should many become blended with nearby strong lines with the onset of mild rotation. In reality, this criterion is difficult to fulfill and must be compromised with the obvious requirement that one include as large a number of lines as possible. Moreover, weak lines on the linear portion of the curve of growth must be included in order to determine the abundance best.

Our line identifications were principally obtained from other studies of Am or F stars, such as those of Conti (1965a), Miczaika et al. (1956), Greenstein (1948), Preston (1961), Praderie (1967), Wright et al. (1964), and Chaffee (1968). In addition, several lines were identified with the aid of Moore's (1945) Multiplet Table. However, in all such cases lines were used only when other lines of the same multiplet were clearly visible in the expected ratios. From this procedure we compiled a list of approximately 500 lines of all possible elements. The equivalent widths of these lines were measured in four stars and read into the abundance program described in The Model Atmosphere and Equivalent Width Programs section of this chapter. Those

lines which indicated abundances differing systematically from the mean ionic abundance in all four stars were eliminated from the line list. In addition, a number of easily blendable lines were excluded, as were several strong lines in the λλ5000-5300 spectral region, where the sensitivity of the D emulsion decreases. Finally, all D-plate (hereinafter "yellow") Fe I lines were eliminated because of a wavelength-dependence of Fe I oscillator strengths (see next section). Such lines are practically dispensible since of the final list of 341 lines, 119 are Fe I and 34 are Fe II. Such large numbers insure that random equivalent width errors will virtually cancel and not affect the mean abundance calculated for the ion.

The line elimination procedure just outlined was carried out primarily to eliminate bad blends, and also those lines with particularly inaccurate oscillator strengths.

Experience showed that the effects of spurious photographic effects could be minimized by drawing the estimated continuum levels on the two or three spectral tracings of a star simultaneously. This procedure no longer allows the individually measured equivalent widths to be considered strictly as independent data, however we feel that it does insure the best interpretation of the information available on the tracings.

The equivalent widths of nearly all the stars were measured by considering the lines as triangles and by multiplying their central residual depths with their half-intensity widths. For three of the fastest rotating stars a central depth-equivalent width relation was found for each tracing from twenty to thirty well-defined lines. This relation was used to estimate the equivalent widths for the other lines not completely blended. This procedure reduces the apparent scatter in the equivalent widths considerably.

The equivalent widths of the different tracings of each star were plotted together in order to check the scatter and the scale of the absolute equivalent width system. If the scales differed by less than 10%, the equivalent widths from the tracings were averaged together. For those blue plate scales which differed by more than 10%, presumably because of small differences in exposure or development times, the equivalent width scale of the "deviant tracing" was adjusted to that of the other two. The individual equivalent widths were then averaged together. The equivalent width data are tabulated in Appendix A.

The errors in photographically determined equivalent widths are considerably larger than those obtained by high-resolution photoelectric scanning techniques. The internal root-mean-square error in our best sharp-lined case increases from $\pm$0.03 dex (7%) for 200 mA lines to $\pm$0.09 dex

(23%) for 15 mA lines. In the broadest lined stars, the average scatter becomes as large as ±0.09. These figures refer to equivalent widths larger than 10 mA and 20 mA for the "blue" and "yellow" data, respectively. Measurement of weaker lines was generally avoided.

There are several lines just blueward of Hβ that can be measured on either the O or D plates. Comparisons of such measures show similar equivalent width averages from both types of plate material, but a somewhat larger scatter than that just quoted. We shall show that the same result obtains from a comparison of our data with those of other observers.

A comparison of equivalent width data is often desirable to insure that possible systematic errors arising from the reduction techniques are not present. In Figures 4, 5, 6, and 7 we compare the equivalent width data of this study with those of, respectively, the Victoria system (3.4 A/mm) for 68 Tau (Wright et al. 1964), the Mt. Wilson system (4.5 A/mm) for 8 Com (Greenstein 1948), the Lick system (10 A/mm) for 16 Ori (Conti 1965a), and the Mt. Stromlo system (6.7 A/mm) for η Lep (Bessell 1969). The yellow plate data are compared in Figures 5 and 6. In these figures we find average dispersions of ±0.07 dex for the blue data and ±0.11 dex for the yellow data. This scatter tends to increase for broader lined stars in the case of the blue plate data. In practice, the more uncertain yellow

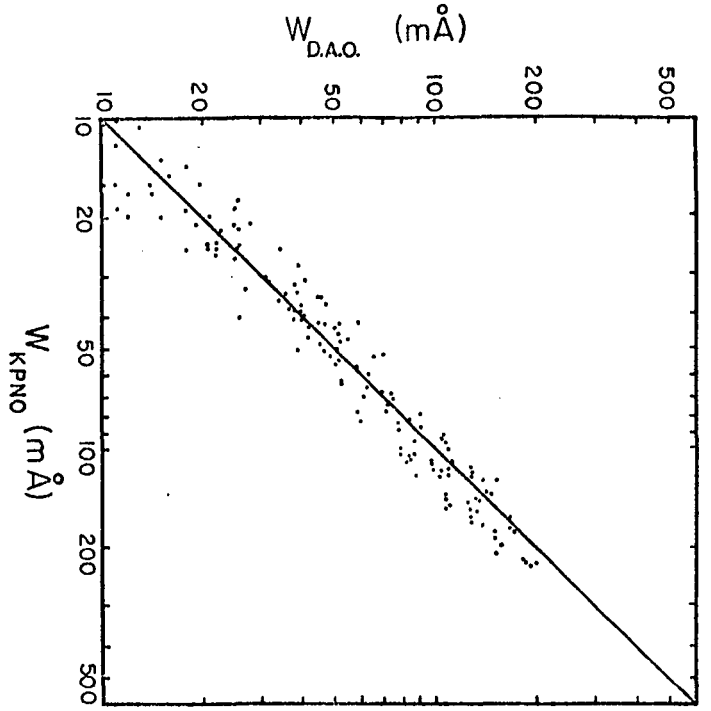

Figure 4. Equivalent width comparison between the D.A.O. (Victoria) and K.P.N.O. systems for 68 Tau

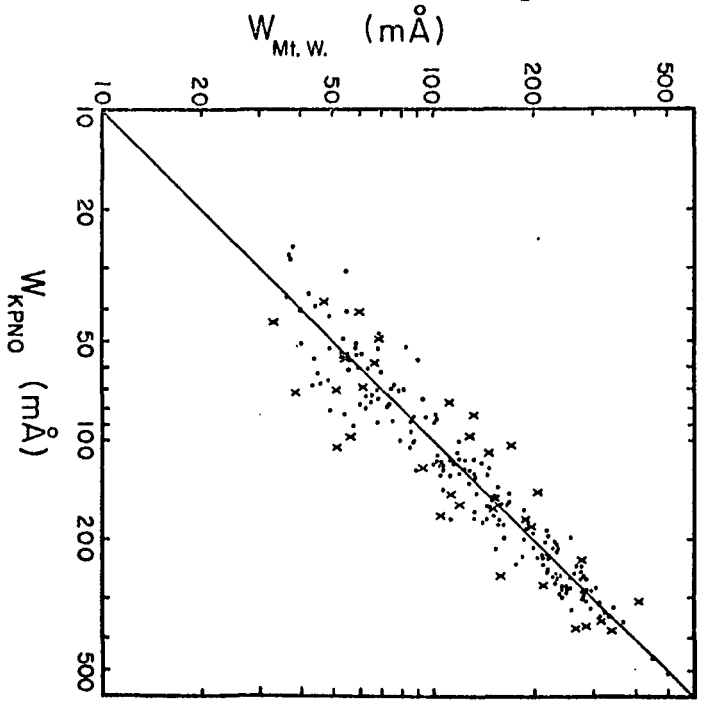

Figure 5. Equivalent width comparison between the Mt. Wilson and K.P.N.O. systems for 8 Com

Yellow plate lines are represented by crosses.

Figure 6. Equivalent width comparison between the Lick and K.P.N.O. systems for 16 Ori

Yellow plate lines are represented by crosses.

Figure 7. Equivalent width comparison between the Mt. Stromlo and K.P.N.O. systems for η Lep

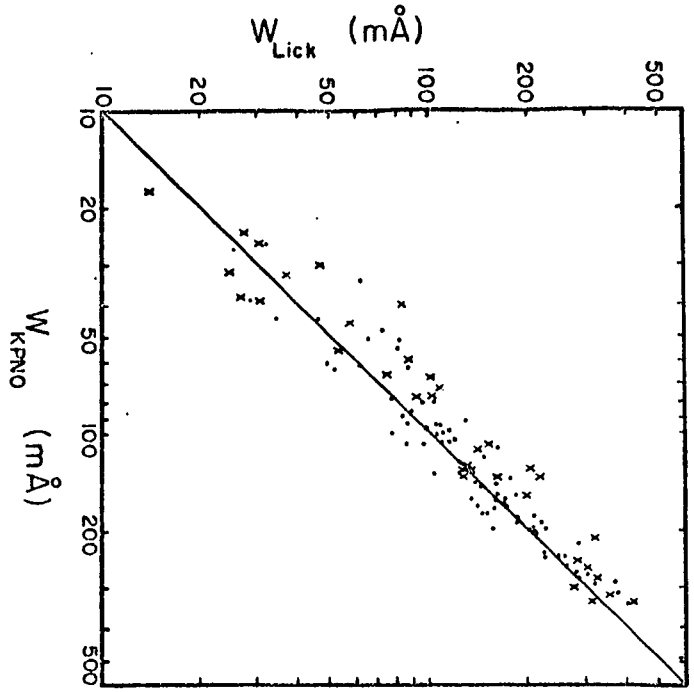

Figure 6. Equivalent width comparison between the Lick and K.P.N.O. systems for 16 Ori

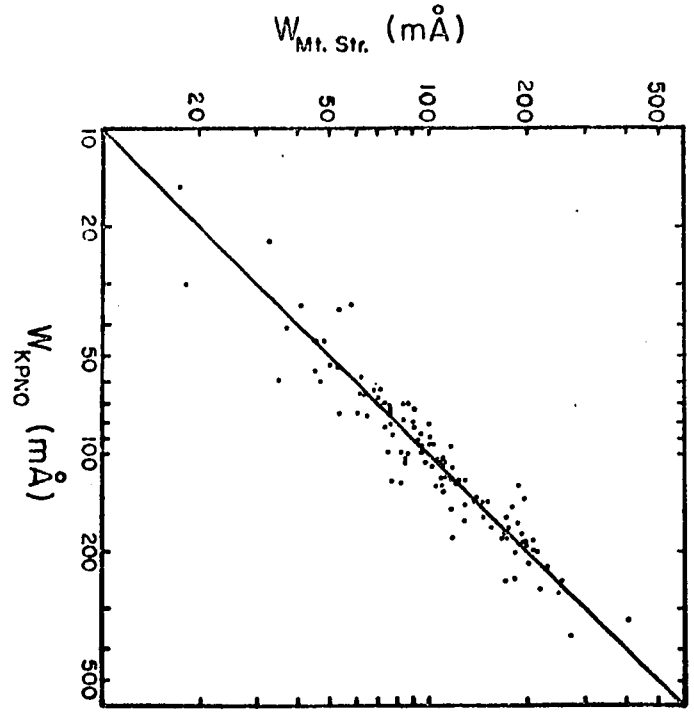

Figure 7. Equivalent width comparison between the Mt. Stromlo and K.P.N.O. systems for η Lep

yellow lines are often not measured, and the scatter remains much the same. These error estimates are slightly larger than those quoted above. However, they are probably more representative of the true errors in equivalent widths.

The larger scatter among the yellow data can be accounted for by certain unfortunate characteristics of the D emulsion. First, because its sensitivity is less than that of the 0 emulsion, one is obligated to take spectra on D plates with only one-half the spectral dispersion. This fact alone makes accurate line measurement more difficult. Second, many of the yellow lines used in this study occur in the spectral region where the D emulsion sensitivity dips, i.e., in the λλ5000-5300 range. In future studies we suggest that such data be obtained on at least three plates or else at higher dispersion. In this study we consider the scatter in the yellow data the weakest link in our analysis.

The scale of the Kitt Peak equivalent width system agrees very well with those to which it is compared in Figures 4 through 7. The only systematic deviations evident are, first, that our equivalent widths are 8% smaller than Conti's for 16 Ori (Figure 6), and second, that our stronger lines are about 10% larger than Wright's for 68 Tau. To five per cent, we feel that the Kitt Peak equivalent width system agrees with the mean of these four systems.

Oscillator Strengths

In order to compute the abundances of elements in stellar atmospheres from observed equivalent widths, the transition probabilities, or "oscillator strengths," of the lines must first be known. We have taken oscillator strengths from several comparatively recent sources. For a given ion we have selected these from a single source, wherever possible. Oscillator strengths of all Fe I lines were taken from Corliss and Warner (1964, hereinafter "CW"). For SI I lines oscillator strengths from Miller and Bengston (1969) were used. Oscillator strengths for Ti II, V II, Cr II, Fe II, and Ni II were obtained by Warner (1967), while those of Na I, Al I, S I, Ca I, Sr II, Ba II were taken from Lambert and Warner (1968a, 1968b, 1968c, 1968d). Except for a few oscillator strengths taken from a list compiled from the literature by R. Kurucz, most others were taken from Corliss and Bozman (1962, hereinafter "CB"). These values and their sources are listed explicitly in Appendix A.

Present values of oscillator strengths should be treated with a certain degree of caution. Very precise measurements have so far been restricted to a small number of resonance transitions. In astrophysically related studies, where oscillator strengths of a large number of weaker lines are measured, indirect procedures are often used to relate these results to the precise, absolute

determinations of the resonance transitions. The great bulk of oscillator strengths currently available has been obtained from observations of emission lines in freely burning arc furnaces. With such a technique, errors can arise from several sources (Takens 1970). First, the persistence of (i.e., time spent by) ions in the vicinity of the arc depends on several factors. Even if the persistence can be accurately estimated, it is usually found that it is of shorter duration than the time needed for the upper atomic levels of the ions to come into equilibrium. Therefore, departures from LTE must also be estimated. The geometry of the arc can affect the derived oscillator strength values, as can the concentration differences of the ions between hot and cool regions. Finally, the measured line strengths must be corrected for the effects of self-absorption through the plasma. In practice, oscillator strengths are first calculated from simplified assumptions. These values are then corrected for the above effects by applying a "normalization function" to them.

The authors mentioned above determined the scales for their oscillator strengths either from theoretical considerations, such as the coulomb approximation or the f-sum rule, or secondarily by adopting the scale of the CB study. In the CB study a single normalization function was determined which was applied to the CW data as well.

While it is advantageous to use such a great body of homogeneously determined data as that of CB and CW, the effects of systematic errors can have far-reaching consequences in astrophysical-abundance applications. Investigators using CW oscillator strengths for Fe I have noticed that several difficulties frequently arise from their use.

First, several investigators (Wright 1967, Conti et al. 1965) have derived excitation temperatures for the atmospheres of middle main sequence stars that are actually lower than their predicted boundary temperatures. Such a phenomenon could arise from the dilution of the line source functions (non-LTE). However, other authors (Warner 1968, Rogerson 1969) have used other oscillator strength sources for weak and intermediate Fe I lines in the sun; they have found that any non-LTE effects must be small.

Use of the CW oscillator strengths has also presented problems in the solar interpretation. Cowley and Warner (1967) have found that the derived gradient in excitation temperature through the solar photosphere is steeper than that given by solar models. It has also been pointed out (Jefferies 1966) that the iron abundance determined from coronal line observations is about ten times larger than that found from photospheric lines.

Elste (1969) has studied equivalent width data of the sun and o Peg and finds that whereas Fe II lines all fit a common curve of growth, multiplets of Fe I lines do not.

On the other hand, if one uses oscillator strengths for Fe I from the recent shock tube study of Huber and Tobey (1968), one obtains a far better agreement.

Elste also pointed out that when the difference between CW and Huber and Tobey oscillator strengths is plotted against the excitation potential of the upper atomic level, χ_u, he finds that the difference grows (in the sense that the CW values are larger) with increasing χ_u, until χ_u = 5.5 ev. It then becomes smaller. A similar effect was found accidentally in the present study. It was observed that when the derived abundances from all Fe I lines (including the yellow data) are plotted against their lower excitation potentials, that a distinctly parabolic distribution results between 0 and 3 ev. Now the energy of the photons of these lines is about 3 ev., so that one finds that the behavior of these data mimics very closely the "parabolic segment" of the plot described by Elste. Put another way, our data would probably exhibit a very uniform iron abundance with χ if Huber and Tobey oscillator strengths were used. Unfortunately, they measured only 38 Fe I lines in the ultraviolet, where stellar work becomes precluded by line blending problems.

Connected with the problem of excitation potential-dependent errors in oscillator strengths is the problem of their wavelength dependence. Various authors have noted systematic wavelength-dependences (Byard 1968, Huber and

Tobey 1968, Grasdalen, Huber, and Parkinson 1969). In our own initial investigations of the iron abundance of four stars, it was found that the yellow Fe I data indicate abundances which are too large by a factor of three to four, relative to the blue data. The Fe II data showed no such effect, so we suspected that this was not an error connected with equivalent width measurement. For this reason, as already noted, the yellow Fe I lines were eliminated from our line list. Recent studies (Huber and Tobey 1968, Grasdalen et al. 1969), however, indicate that the CW oscillator strengths above λ5000 are probably more correct than those in the blue.

The systematic errors mentioned in the CB and CW oscillator strengths probably arise from the effect of the assumption of a uniform isothermal arc plasma; the over-simplified assumption leads to an error in determining the normalization function (Warner and Cowley 1967). Cowley and Warner (1967) have also concluded that these errors arise in part from the improper use of a common normalization function for different ions. Takens (1970), in a recent review of the problem of obtaining oscillator strengths in arc furnaces, has also argued that these errors arise largely for these two reasons. Takens also criticized the homogeneity of the revised oscillator strengths given by Corliss and Tech (1968) and recommends that they not be used at all.

The more recent determinations of oscillator strengths, based on results from arcs (Garz and Kock 1969), shock tubes (Byard 1967, 1968, Huber and Tobey 1968, Grasdalen et al. 1969), and beam foils (Whaling et al. 1970) now appear to be in relatively close agreement. These lists, however, are not as complete as are the CB or CW studies, so that for the present one must use some form of the latter. It has been suggested that the scale of the CB and CW studies is too large by about 0.90 dex (Garz et al. 1969, Grasdalen et al. 1969). When such a correction is made, the photospheric solar abundance of iron is brought into close accord with the coronal value. As noted, it is also likely that excitation potential-dependent errors in these studies are present. Since this type of error tends to mimic a weak line-strong line effect, it propagates into the determination of the microturbulence in curve of growth analyses. Garz et al. (1969) found that use of their oscillator strengths, rather than the CW values, reduces by about 1/2 km/sec the apparent microturbulence derived in the sun. If this is correct, our microturbulence values should be reduced by comparable amounts. In the present analysis, however, we shall report only those abundances and microturbulence values directly calculated from the oscillator strengths chosen.

The Model Atmosphere and Equivalent Width Programs

The curve of growth analysis was carried out by means of a complete LTE model atmosphere treatment described herein. The procedure entails use of two computer programs, one which computes a desired model atmosphere and a second which calculates abundances from line strength data.

The first version of the model atmosphere program was written by Dr. Stephen Strom, and is described more fully elsewhere (see Strom and Avrett 1965). The present version, ATLAS3, was written by Mr. Robert Kurucz of the Harvard-Smithsonian group.

ATLAS3 is meant to be a versatile program capable of calculating non-gray model atmospheres hotter than $T_{eff} \simeq 4000^{o}K$. Several features are added which can be easily included or left out by means of simple ON or OFF statements on control cards. One may include any of twenty continuous opacity sources, a depth-dependent turbulent support term, and convection. The abundance of "the metals" may be arbitrarily scaled, and the abundance of hydrogen or helium may be altered. As originally written, ATLAS3 included the effects of departures from LTE in hydrogen, however this feature could not be fit into the memory core of the Controlled Data Corporation 6400 Kitt Peak computer used. In any case, recent studies have shown that these

departures in dwarf or giant stars must be small (see Auer and Mihalas 1970).

The solution of the basic radiation parameters in ATLAS3 has been described by Kurucz (1969). He solves for the source function by first representing it as a vector in the equation relating the source function and its Planckian and scattering components; the mean intensity here is written as the matrix product of a first moment operator and the source function. The resulting matrix equation is then inverted and solved by Gauss-Seidel iteration. This gives $S_\nu(\tau)$. Matrix operators are then applied to solve the moment integral equations for the monochromatic mean intensity and flux at each depth.

The solution of the physical parameters of the atmosphere is carried out by conventional procedures. The assumptions of plane-parallel geometry, total flux conservation, and hydrostatic equilibrium are made. One starts with a gray temperature-optical depth relation or with the parameters of a previously calculated model. The calculations are started by assuming a pressure at a depth and then computing the electron pressure and ionization equilibria of atoms from the fractional ionization and Saha equations. With P_e known, the number density of each absorber is found, and the continuous opacities are calculated explicitly. These values are inserted into the equation of hydrostatic equilibrium, which is integrated to give a revised value of

the pressure. This process is iterated until convergence of the pressure values is attained. All physical parameters are calculated for each of forty depths. Separate subroutines calculate the convective flow velocity and the convective flux. An Avrett-Krook procedure is used to correct the initial $T(\tau)$ relation. The models are iterated until the desired accuracy is achieved.

In our set of models forty optical depths were chosen in steps of $\sqrt[6]{10}$ down to $\tau = 100$. Here τ refers to the optical depth at $\lambda 5000$. We used a fifty-five point frequency set appropriate to the effective temperature range under consideration. These frequencies represent the continuum and the major hydrogen discontinuities. The frequencies are also chosen such that one point represents each of the major hydrogen lines. Therefore, while no hydrogen line profiles are calculated, approximate equivalent widths for these lines are computed from their triangular shapes. It thus becomes possible to correct the temperature distribution for the effect of these lines.

In our models we allowed for continuous opacity from hydrogen (bound-free), hydrogen lines, H^-, H_2^+, Si I, Mg I, CI, Al I, He I, He II, electron scattering, and Rayleigh scattering. The program has the capability of including metallic lines opacities in a picket fence representation, however the lack of empirical line blanketing coefficients precluded their inclusion. The presence of increased

metallic lines could be important through their effect of atmospheric backwarming.

Praderie (1967) has shown that besides the two predominant opacity sources in the visual (H I and H^-), C I, Mg I, and Si I are in fact dominant in the ultraviolet region just above the Lyman limit. Models chosen for the normal standard stars were calculated using the "cosmic abundances" tabulated in ATLAS3. For the program Am stars, initial investigations showed that carbon tends to be mildly deficient; magnesium and silicon tend to be either normal or deficient, or normal or enhanced, respectively. Therefore, models for Am stars were calculated with one-half the normal carbon abundance and with normal magnesium and silicon abundances. We shall show in the next chapter that such changes only have small effects on the derived abundances.

In order to calculate a model, we inserted a control card specifying the desired effective temperature and an estimate of the gravity. Convection was included in all cases; a mixing length of one scale height was chosen. The number of iterations was specified, and the program was run on the CDC 6400. Each iteration required one minute of computing time. The iterations were continued until the flux and flux derivative errors became of the order of a per cent or less. The program output from the last iteration was both printed on computer paper and punched on cards.

These cards were then used either in the equivalent width program described below or as a starting set of physical parameters for another model.

The final step in the curve of growth analysis is the use of the WIDTH4 program to calculate equivalent widths. The basic function of this program, also written by Kurucz, is to assume a trial abundance for an element, to calculate an equivalent width for a given line, and to compare it with the measured equivalent width. This is repeated until the measured value is bracketed and duplicated through successive interpolations. This procedure yields an abundance for that line; in so doing it generates a curve of growth for that line.

To do these calculations, WIDTH4 reads in the physical parameter cards from the ATLAS3 program. These cards contain the runs of temperature, pressure, and electron density through the atmosphere. Other parameters needed are calculated via subroutines in WIDTH4 which are identical to those in ATLAS3. Quantities needed for regions between the tabulated optical depths are determined through parabolic interpolation.

An outline of the calculation of the equivalent width of a line is as follows. First, the equivalent width is defined from the equation

$$W = \int_0^\infty (1 - F_L/F_C)d\nu, \qquad (1)$$

where πF_L and πF_c are the observed net fluxes in the line and at a neighboring continuum frequency, respectively. F_c is therefore already known from the model calculations. The flux in the line is calculated from the second moment integral equation:

$$F_{L_\nu} = 2 \int_0^\infty S(t'_\nu)\, E_2(t'_\nu)\, dt'_\nu, \qquad (2)$$

where E_2 is the second exponential integral, S is the line source function, and t'_ν is the total optical depth at frequency ν in the line. The latter consists of the sum of the individual optical depths due to the continuum and line absorption coefficients. In a more rigorous analysis, the source function for each line can only be obtained after the structure of the atomic levels is specified. Only in this way can scattering and other non-LTE effects be included. In these dwarf atmospheres, however, we shall assume LTE in the lines, i.e., that $S_\nu = B_\nu$ locally. In order to proceed with the integration of equation (2), one must tabulate the product $S(t'_\nu)\, E_2(t'_\nu)$ as a function of t'_ν for each frequency in the line. Now the optical depth due to the line alone, t_ν, is given by

$$t_\nu = \int_0^{x_o} k_\nu\, \rho\, dx, \qquad (3)$$

where k_ν is the line mass absorption coefficient, ρ the local density, and x_o and dx a fiducial point and

incremental pathlength, respectively. In practice dx is broken up into subintervals corresponding to the distances between the forty continuum optical depth levels. They are already tabulated in the model atmosphere. The corresponding densities are also known. Therefore the calculation of t_ν rests with the calculation of the line absorption coefficient k_ν. This quantity is in turn given by

$$k_\nu = \frac{\pi^{1/2}\ e^2}{m\ c}\ \frac{N^* gf}{\Delta\nu_D}\ H(a,u)\ (1 - \exp[h\nu/kT]). \qquad (4)$$

Here e and m are the charge and the rest mass of an electron; c, the speed of light; g and f the statistical weight and oscillator strength of the line in question; h, Planck's constant; and k, the Boltzmann constant. The quantity $\Delta\nu_D$ is the Doppler width and is given by $(V_{Doppler}/c)\ \nu_o$. H(a,u) is the broadening function of the line, and in this case is the Voigt function. The parameter u represents the number of Doppler widths between the line center frequency, ν_o, and the frequency of interest. The letter a is related to the atomic damping constant, γ, through the relation $a = \gamma/2\pi\Delta\nu_D$. Unless otherwise specified, γ is assumed by WIDTH4 to be ten times the classical value. Finally, we note that N* is the density of atoms producing the line of interest.

In these calculations one first makes use of the Saha and Boltzmann equations to calculate N* from an assumed

N_{total} for the element. This is a straightforward computation since the local excitation temperature and ionization equilibrium are known from the model atmosphere. The Doppler width is calculated from the component thermal and (input) microturbulent velocities.

One then considers one of several frequencies along the line profile. Since a is known from the assumed damping, and since u comes from the frequency chosen, H(a,u) is specified. The product gf is known from the input data, so that k_ν and in turn t_ν may be calculated at each continuum optical depth level through equations (4) and (3). The monochromatic flux in the line may then be calculated by assigning the appropriate line source functions, $B(t'_\nu)$, by computing $E_2(t'_\nu)$, and finally by integrating their products, as in equation (2). This procedure is repeated for fifteen points distributed along one side of the line profile which is presumed symmetric. The equivalent width of the line is then calculated via equation (1). The calculation of one line requires normally four iterations or approximately 3-1/2 seconds on the CDC 6400. We note parenthetically that one may also solve for the mean (continuum) optical depth value by noting that depth for which $t'_\nu = 1$ for each frequency in the line. The "mean depth of formation" then becomes the equivalent width-weighted mean of these values for the entire line profile.

The WIDTH4 program reads in line data needed for these computations. For each line, a data card lists the line center wavelength, the ion, the lower excitation potential, the quantity log gf, and the measured equivalent width. The program prints the apparent abundance and mean depth of formation of each line separately. It then computes the mean abundance for an ion and the r.m.s. scatter about this mean.

The final task of the program is to plot the apparent abundances against the lower excitation potentials, the equivalent widths, and the mean depths of formation of the lines. The purpose of these plots is to aid in the elimination of spurious non-abundance components which enter into the observed line strengths. In theory, one should be able to modify the effective temperature of the model atmosphere used such that in a successive run there is no correlation between the apparent abundances of the lines and their excitation potentials. In reality, as was demonstrated in the last section, excitation potential-dependent errors in oscillator strengths are present, and they make difficult this application. In the second plot, however, one may demand that there be no correlation between the apparent abundances and the equivalent widths. One assures this by selecting a microturbulent velocity value such that no correlation persists. When this occurs one assumes that the value is the correct value for the microturbulence and that

the microturbulence is the same for all elements. The tabulated abundances are then considered "real." In the present study, we used about 100 lines of Fe I to obtain microturbulent velocities in this manner.

There are several advantages which accrue from the use of these computer programs in determining abundances. The method treats line formation in a much more rigorous fashion than single-parameter analyses. Moreover, the calculation of abundances and of microturbulence may be made in an objective and systematic fashion in different stars. A particularly important advantage, however, is that it permits the direct comparison of abundances of stars with very different temperatures and/or surface gravities.

A limitation of the WIDTH4 program is that it does not allow for the blending of weak lines within the profile of the line of interest. This is in reality a serious problem. It was also found that a single-frequency representation for each hydrogen line in ATLAS3 is inadequate for the accurate computation of the quasi-continuous opacity along the wings of these lines. The resulting calculated quasi-continuous opacity is so crude that often the line opacity becomes too small. As a result, negative equivalent widths are calculated for metal lines in the wings of the hydrogen lines, and the program aborts. It was therefore necessary to run WIDTH4 without the effects of hydrogen line blanketing. Both of these limitations have also been common

to the analyses of most previous authors. It is expected that detailed blanketed atmospheric models will soon be available in order to circumvent these problems.

CHAPTER IV

RESULTS AND CONCLUSIONS

The Derived Physical Parameters

In this chapter the equivalent width data are exhibited and evaluated by means of the ATLAS and WIDTH computer programs described in the previous chapter. In this first section results are presented which underscore the remarks in Chapter II concerning the normality of the atmospheres of Am stars.

In Figure 8 a plot of mean depth of line formation, $\overline{\tau}$, against wavelength is shown for all Fe I, Fe II, Ca I, and Sc II lines used in a "typical" Am star, HR 2291 (RR Lyn). All mean depths of formation are normalized with respect to the optical depth at λ5000. The depth of continuum formation, $\tau_\nu = 1$ is shown as a solid line. Attention is drawn to the fact that most all the Ca I and Sc II lines are formed uniformly in the region below $\overline{\tau} = 0.5$. This region is also where the weak Fe I lines, on the linear portion of the curve of growth, are formed. This observation confirms Conti's (1965a) finding that since Ca I (and Sc II) lines are formed in the same physical location as the Fe I lines, no stratification effect in these atmospheres can change the derived abundance ratios, Ca/Fe or Sc/Fe, significantly.

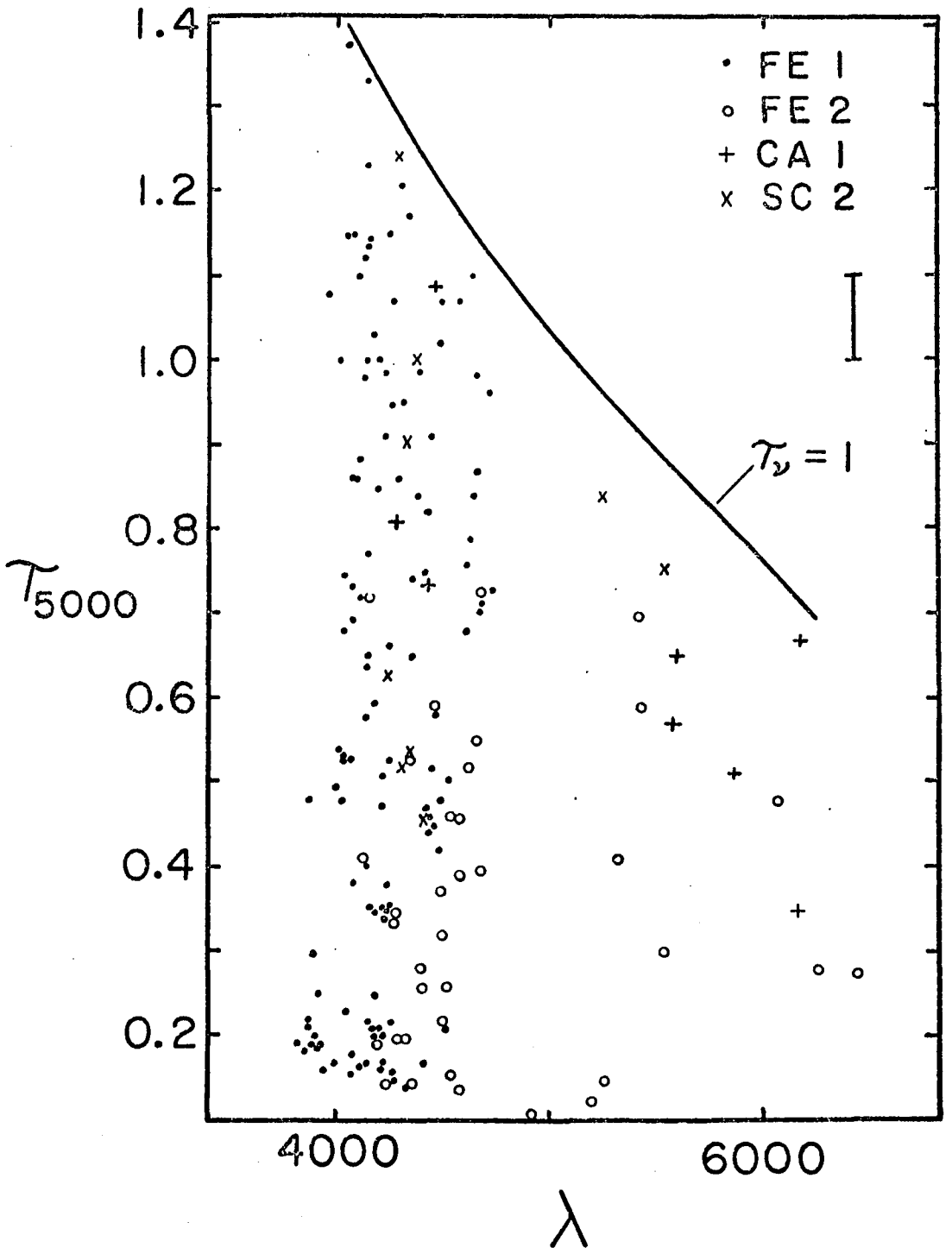

Figure 8. Distribution of mean depths of line formation with wavelength for several ions

Approximate error bars are shown.

In all cases the equivalent width data were run with model atmospheres having effective temperatures given in the last column of Table 2. For the surface gravities of these stars we chose an initial value of log g = 4.0 (c.g.s.) based on the recent results discussed in Chapter II. Because of the lack of photoelectric scanning data and because no trend exists between Stromgren Δc_1 and (b - y), it was considered inappropriate to pre-assign differential values of surface gravity as a function of effective temperature.

In anticipation of future improvements in the calibrations in the effective temperature scales and surface gravity estimates for A stars, we have used a grid of model atmospheres to run the same equivalent width data for several effective temperatures and surface gravities. In Table 3 the logarithmic abundance data of RR Lyn, run for a standard model atmosphere, are compared with the results run for these different models. This particular star was chosen because it has easily measurable sharp lines and has an intermediate effective temperature, iron abundance, and microturbulence for the sample of stars chosen. The numbers in parentheses refer to the logarithmic difference in an element's computed abundance, from lines of a given ion, relative to the change in the iron abundance for that model. Except for C I lines, which vary with T_{eff} and log g more

Table 3. Comparison of Abundances Run with a Standard Model (8125°K, log g = 4.0, ξ = 7 km/sec), with Models Having Varying Parameters

Element	ξ_T=6	No Conv.	No H-line Blank.	8125° 4.5	7500°	7500° 4.5	8000°	8500°	9000°	9000° 4.5
C I	.03	.00	.00	.07 (-.09)	-.02 (+.09)	.11 (.05)	-.01 (+.01)	.11 (.01)	.34 (.06)	.28 (-.11)
Na I	.08	.03	-.01	-.03 (-.02)	-.31 (-.08)	-.34 (+.07)	-.05 (+.02)	.25 (-.03)	.62 (-.09)	.51 (-.09)
Mg I	.11	.02	-.01	-.01 (.00)	-.29 (+.10)	-.27 (+.14)	-.05 (+.02)	.25 (-.03)	.63 (-.08)	.52 (-.08)
Al I	.20	-.01	-.02	.00 (.01)	-.41 (-.02)	-.42 (-.01)	-.09 (-.02)	.30 (.02)	.73 (.02)	.62 (.02)
Si I	.01	.01	-.02	-.04 (-.03)	-.28 (+.11)	-.31 (+.10)	-.05 (+.02)	.24 (-.04)	.58 (-.13)	.45 (-.15)
Si II	.14	-.07	.04	.20 (.04)	.30 (.41)	.51 (.45)	.07 (.09)	-.15 (-.25)	-.22 (-.50)	-.11 (-.50)
S I	.00	-.01	-.01	.01 (.02)	-.16 (-.23)	-.09 (+.32)	-.03 (+.04)	.18 (-.10)	.48 (-.23)	.38 (-.22)
Ca I	.02	.01	-.03	-.05 (-.04)	-.38 (+.01)	-.42 (-.01)	-.07 (.00)	.31 (.03)	.78 (.07)	.60 (.00)
Sc II	.02	.01	-.01	.15 (-.01)	-.26 (-.15)	-.11 (+.17)	-.04 (-.02)	.20 (.10)	.50 (.22)	.57 (.16)

Table 3.--Continued Comparison of Abundances Run with a Standard Model (8125°K, log g = 4.0, ξ = 7 km/sec), with Models Having:

Element	ξ_T=6	No Conv.	No H-line Blank.	8125° 4.5	7500°	7500° 4.5	8000°	8500°	9000°	9000° 4.5
Ti I	.02	.01	-.03	-.04 (-.03)	-.45 (-.06)	-.49 (-.08)	-.08 (-.01)	.33 (.05)	.79 (.08)	.66 (.06)
Ti II	.13	-.01	-.01	.17 (.01)	-.21 (-.10)	-.05 (-.11)	-.04 (-.02)	.17 (.07)	.48 (.15)	.53 (.14)
V II	.02	-.01	-.01	.15 (-.01)	-.18 (-.07)	-.02 (-.08)	-.03 (-.01)	.14 (.04)	.35 (.07)	.45 (.06)
Cr I	.07	.01	-.02	-.02 (-.01)	-.43 (-.04)	-.47 (-.06)	-.07 (.00)	.31 (.03)	.76 (.05)	.65 (.05)
Cr II	.06	.03	.03	.18 (.02)	-.04 (+.07)	.13 (.07)	.02 (.04)	.11 (.01)	.26 (-.02)	.36 (-.03)
Mn I	.11	.01	-.02	-.02 (-.01)	-.43 (-.04)	-.46 (-.05)	-.07 (.00)	.31 (.03)	.76 (.05)	.65 (.05)
Fe I	.12	-.01	-.02	-.01	-.39	-.41	-.07	.28	.71	.60
Fe II	.13	-.01	.00	.16	-.11	.06	-.02	.10	.28	.39
Co I	.02	.00	-.03	-.04 (-.03)	-.47 (-.08)	-.51 (-.10)	-.08 (-.01)	.33 (.05)	.78 (.07)	.67 (.07)

Table 3.--Continued Comparison of Abundances Run with a Standard Model (8125°K, log g = 4.0, ξ = 7 km/sec), with Models Having:

Element	ξ_T=6	No Conv.	No H-line Blank.	8125° 4.5	7500°	7500° 4.5	8000°	8500°	9000°	9000° 4.5
Ni I	.05	.01	-.02	-.02 (-.01)	-.32 (+.07)	-.35 (+.06)	-.05 (+.02)	.26 (-.02)	.63 (-.08)	.52 (-.08)
Ni II	.07	.01	.00	.16 (.00)	-.04 (+.07)	.13 (.07)	-.01 (+.01)	.06 (-.04)	.18 (-.10)	.29 (-.10)
Cu I	.01	.02	-.03	-.04 (-.03)	-.46 (-.07)	-.49 (-.08)	-.08 (-.01)	.33 (.05)	.77 (.06)	.65 (.05)
Zn I	.02	-.01	-.01	-.03 (-.02)	-.39 (-.28)	-.41 (.00)	-.07 (.00)	.28 (.00)	.69 (-.02)	.57 (-.03)
Sr II	.23	-.01	-.01	.14 (-.02)	-.35 (-.24)	-.19 (-.25)	-.06 (-.04)	.28 (.18)	.80 (.52)	.80 (.41)
Y II	.16	.00	-.01	.17 (.01)	-.30 (-.19)	-.14 (-.20)	-.05 (-.03)	.25 (.15)	.62 (.34)	.66 (.27)
Zr II	.09	.00	-.01	.16 (.00)	-.22 (-.11)	-.07 (-.13)	-.04 (-.02)	.19 (.09)	.46 (.18)	.54 (.15)
Ba II	.22	.02	-.02	.09 (-.07)	-.46 (-.35)	-.36 (-.42)	-.09 (-.07)	.34 (.24)	.87 (.59)	.84 (.45)
La II	.01	.00	-.02	.14 (-.02)	-.29 (-.18)	-.14 (-.20)	-.05 (-.03)	.21 (.11)	.51 (.23)	.59 (.20)

Table 3.--Continued Comparison of Abundances Run with a Standard Model (8125°K, log g = 4.0, ξ = 7 km/sec), with Models Having:

Element	ξ_T=6	No Conv.	No H-line Blank.	8125° 4.5	7500°	7500° 4.5	8000°	8500°	9000°	9000° 4.5
Ce II	.02	.00	-.01	.14 (-.02)	-.27 (-.16)	-.12 (-.18)	-.04 (-.02)	.21 (.11)	.52 (.24)	.58 (.19)
Nd II	.01	.01	-.02	.13 (-.03)	-.30 (-.19)	-.15 (-.21)	-.05 (-.03)	.24 (.14)	.61 (.33)	.64 (.25)
Sm II	.01	.01	-.03	.08 (-.08)	-.38 (-.27)	-.27 (-.33)	-.07 (-.05)	.32 (.22)	.79 (.51)	.74 (.35)
Eu II	.05	.00	-.04	.03 (-.13)	-.57 (-.46)	-.51 (-.57)	-.11 (-.09)	.39 (.29)	.97 (.69)	.89 (.50)
Gd II	.01	.00	-.02	.13 (-.03)	-.31 (-.20)	-.17 (-.23)	-.06 (-.04)	.25 (.15)	.62 (.30)	.64 (.25)

like Fe II than Fe I lines, these abundance differences are referred to the common ionization stage of iron.

In columns 2, 3, and 4 we also present the abundance differences run with models with ξ_T = 6.0 (to be compared to the actually computed 7.0 km/sec), with an atmosphere model having no convection, and with one having no hydrogen line opacity included, respectively. From the very small differences apparent in column 2, one may conclude that the convection added to our actual model changes the computed abundances almost negligibly at T_{eff} = 8125°K. Similarly, the effect of the inclusion of the hydrogen line opacity on the standard atmosphere actually used is extremely small, even though these lines occur largely near the stellar flux maximum for these temperatures. This last point is significant because the effects of atmospheric backwarming due to the excessive line blanketing in these stars has been ignored up to now in computing the temperature stratification. This observation implies, however, that the effect does not greatly change the abundances of the high metal-content Am stars with respect to the normal metal-content ones. In any case it changes virtually all abundances in the same direction. This point will be taken up again below.

The existence of Table 3 permits the estimate of errors in the assigned T_{eff} and log g values through an indirect use of the Saha equation. The number of lines

representing the iron abundance from Fe I and Fe II lines is sufficiently large in either case that one may assume that random equivalent width measurement errors will cancel to a high degree. Therefore, the mean abundance determined from either ion is quite precise. It follows that variations from star to star in the difference in the iron abundance from the two ions (designated "Fe I-Fe II") will reflect differences in the ionization equilibrium of iron arising from small errors in the assumed effective temperature and surface gravity. The mean Fe I and Fe II difference for all our twenty stars (see Table 4) is +0.11 dex, with a r.m.s. scatter of $\pm$0.10 dex. We note a difference of +0.1 dex in the solar iron abundance derived from the CW and Warner studies. Therefore the mean derived spectroscopic gravity for our stars is almost exactly that assumed, i.e., log g = 4.0. According to the Fe I and Fe II entries in columns 4 and 7, a scatter of $\pm$0.10 dex corresponds to an error of $\pm 250^{\circ}K$, if no error in log g is assumed, or to $\pm$0.3 in log g, if none in T_{eff} is assumed. Since a common value in log g was initially assigned to all Am stars, it is presumed that most of the error is in this parameter. On the other hand, from The Temperature Calibration of Chapter III it is recalled that the previous error estimate in temperature was that $\Delta T_{eff} \simeq \pm 60^{\circ}K$. Therefore we estimate random errors of $\pm 100^{\circ}K$ in T_{eff} and $\pm$0.2 dex in log g for the stars in this study.

Table 4. Microturbulence Values Determined for the Program Stars

Star HR (HD)	ξ_T (km/sec)	Star HR	ξ_T (km/sec)
4685	7.2	2291	7.0
(108486)	(6.0)	5055	7.2
4750	7.5	7850	(7.8)
4751	7.0	8410	9.0
4780	6.2		
		Standards	
1368	7.8	114	5.0
1376	7.0	906	6.5
1389	5.0	2085	6.0
1428	6.0	4825	5.0
1458	(6.0)		
1519	(8.5)		
1672	7.2		

Of the four standard stars, the iron ionization equilibrium of only one indicated a substantially different gravity. This star is HR 114 (28 And). As previously noted, it is an apparent δ Scuti variable and has a Δc_1 = 0.15.

In the course of this investigation it was found that the (Fe I - Fe II) differences of all the program stars exhibit a systematic trend with T_{eff} in the sense that the hotter stars exhibit the algebraically larger values. This relation is shown in Figure 9. This effect can not be explained by the consideration that hotter stars near cluster evolutionary turn-offs have lower surface gravities than do the cooler stars closer to the zero age main

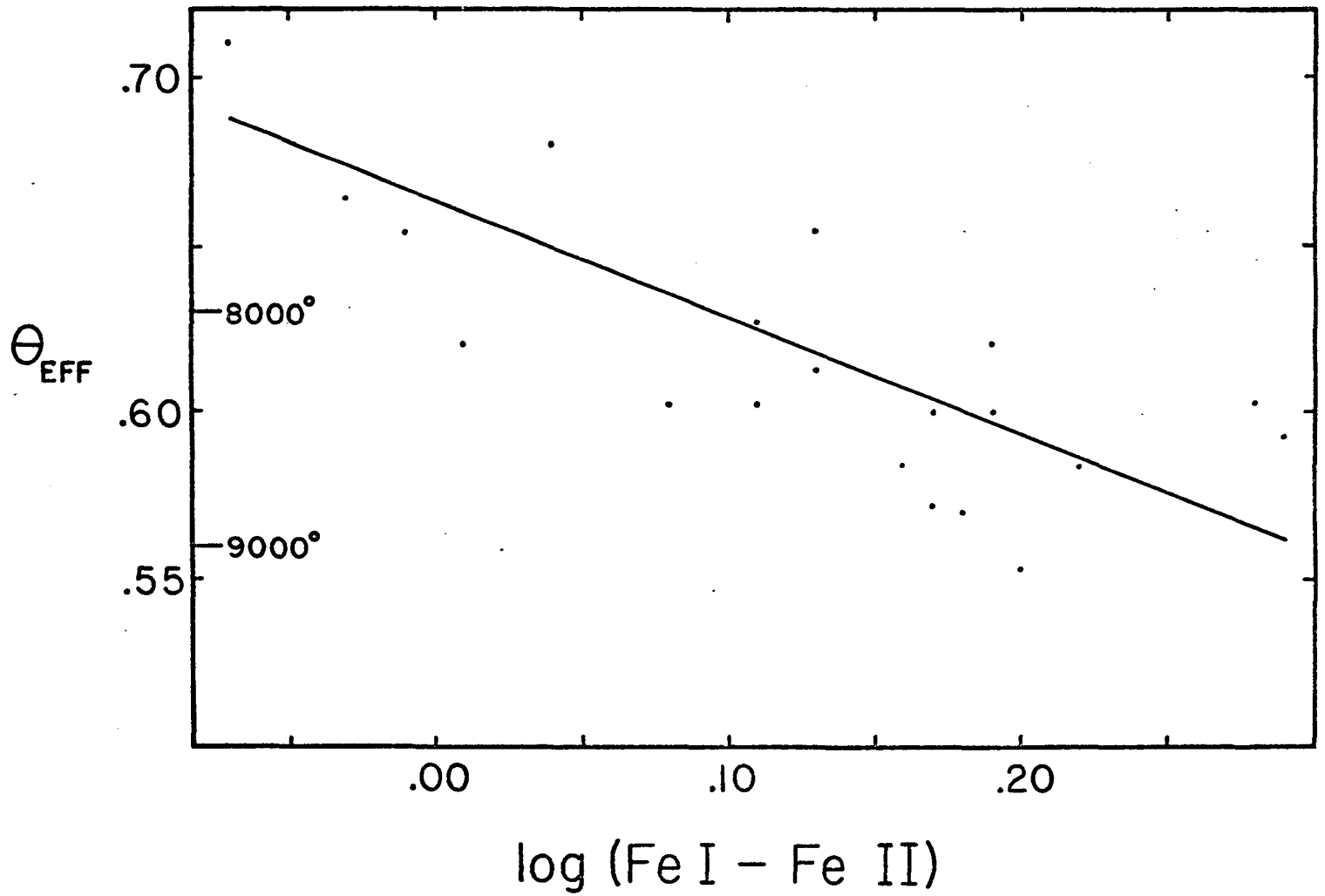

Figure 9. Effective temperature versus the (Fe I - Fe II) abundance discrepancy

sequence because the sense of the correlation is incorrect. Reference to Table 3 shows that in order to decrease the (Fe I - Fe II) difference, one must employ a model of higher gravity. We note further that use of a steeper temperature-color calibration, such as that of Matsushima in Figure 3, would serve to augment the discrepancy. A possible explanation for this effect is that the neglect of metallic line blanketing would produce excessively shallow temperature gradients in the cooler model atmospheres. According to this interpretation, the weak Fe I lines, which primarily determine the iron abundance, would be formed in deep layers which are calculated too cool. An excessively low abundance of iron from Fe I lines would therefore be derived. The Fe II lines are formed high in the atmosphere (see Figure 8) and would not be so affected. One may see in fact from the Fe I and Fe II entries in column 3 of Table 3 that an inclusion of additional blanketing in the models would produce a shift in the desired direction, toward increasing (Fe I - Fe II) for the cool stars. If this explanation is correct, then the mean spectroscopic gravity of these stars should actually be taken from the (Fe I - Fe II) values of the hottest stars, which are least affected by metallic line blanketing. In that case we would derive a mean spectroscopic gravity intermediate between 4.0 and 4.5 for both the Am and normal A stars in this study.

The Microturbulence in Metallic Line Stars

Microturbulence values (ξ_T) have been assigned to all program stars according to the procedure outlined in The Model Atmosphere and Equivalent Width Programs of Chapter III. The Fe I data from Appendix A were used for this purpose. These values are presented in Table 4. The numbers in parentheses refer to uncertain ξ_T values chosen for mildly rotating stars.

After having chosen microturbulent parameter values that insure the lack of correlation of apparent abundance with equivalent width, the plots of abundance versus mean depth of line formation were examined in a few sharp-lined program stars for microturbulence stratification. In no case was there convincing evidence of an apparent variation of microturbulence with depth in the atmosphere. Such a variation would be expected to be related to changes in density, and since the range of the latter is small in line formation regions of dwarf atmospheres, this observation is not surprising.

In Figure 10 the microturbulence values derived for these stars are shown as a function of effective temperature. Dots refer to the program Am stars, while the circles represent the standards used in this study. The crosses represent seven normal A stars taken from Chaffee (1970), including our standards HR 2085 and HR 4825. In these

Figure 10. The microturbulent parameter as a function of (b - y)

Dots represent program Am stars; circles, program standards; crosses, Chaffee's (1970) normal A and F field stars. Parentheses denote uncertain ξ_T values of rapid rotators. Solid line designates the sonic velocity in the atmosphere. Approximate error bars are shown.

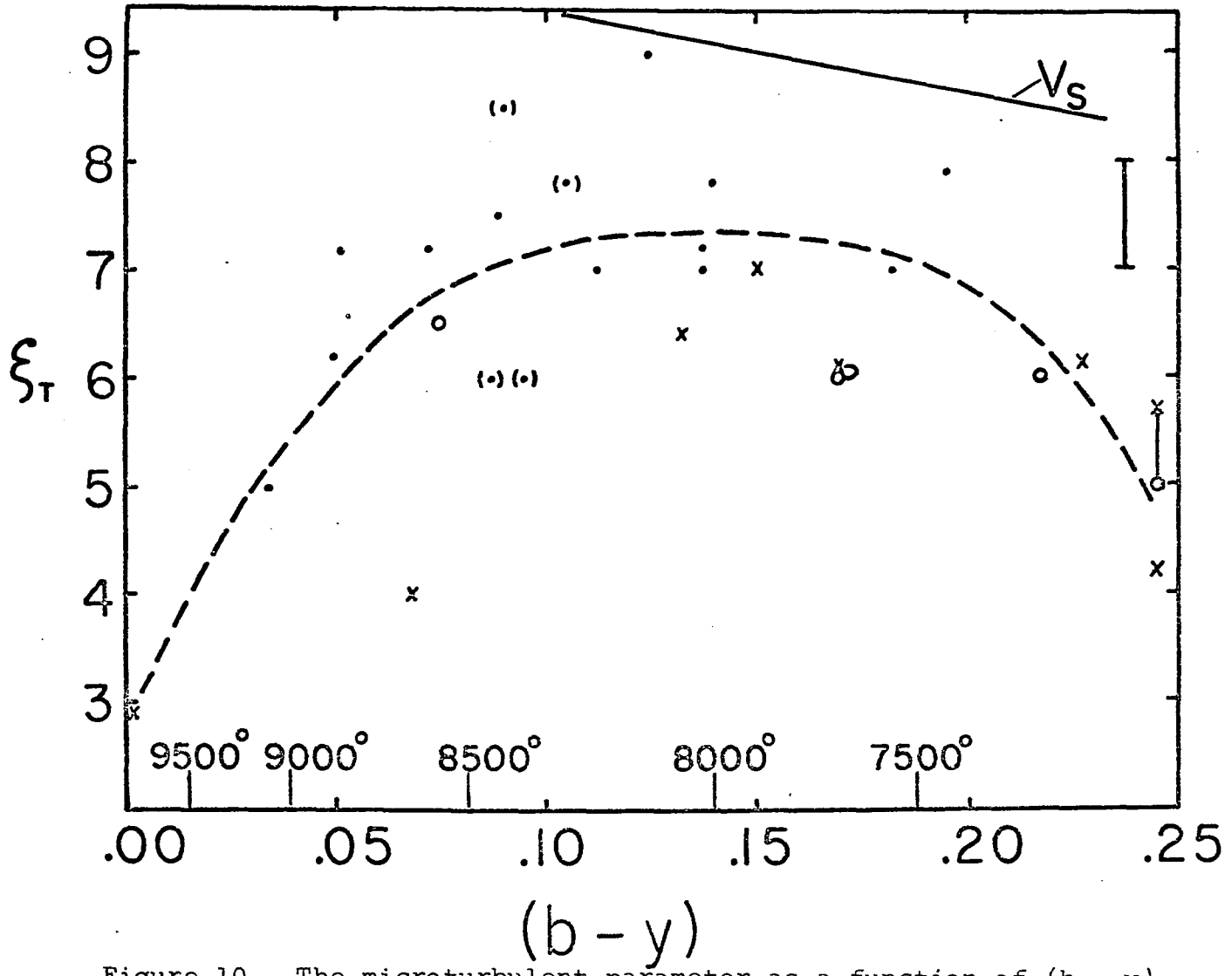

Figure 10. The microturbulent parameter as a function of (b - y)

cases ξ_T was derived on the basis of his equivalent widths of about 60 Fe I lines in common with our line sample.

Inspection of Figure 10 indicates a run of ξ_T such that it rises from 3 km/sec at $T_{eff} = 9700^{\circ}K$, rises to 7 km/sec at $8500^{\circ}K$, remains constant to $7600^{\circ}K$, and decreases again to 4 km/sec at $7000^{\circ}K$. This general pattern appears to be followed by both Am and normal A stars. Therefore, in concert with the results of Baschek and Reimers, we conclude that there appears to be no significant difference in microturbulence between Am and normal A stars of the same temperature. The reality of this peak in the late-A region may be confirmed by reference to other studies showing low (~3 km/sec) microturbulence values for early A or middle F stars (Strom et al. 1968, Conti and Strom 1968a, 1968b, Chaffee 1970).

It should also be pointed out that the peak in ξ_T indicated in Figure 10 occurs in the color range $.09 \leq (b - y) \leq .18$. This region coincides precisely with the domain of the H-R diagram in which the instability strip intersects the main sequence (Breger 1970b). One interpretation of this coincidence is that at least a large component of the computed microturbulence is due to real turbulent motions in the atmospheres of these stars, perhaps arising from local incipient pulsational instabilities. The physical theory dealing with such a postulated phenomenon is, however, presently lacking.

There are a few other observations which can be drawn from Figure 10. First, we note that in no case is the derived microturbulence as high as the speed of sound ("V_s") in the atmospheres, denoted by the solid line in the upper right portion of the diagram. We also note that there is no apparent correlation of ξ_T with rotation up to V sin i = 59 km/sec.

We estimate the random error in the determination of ξ_T for a sharp-lined Am star to be $\pm$0.5 km/sec, that also estimated in the Conti and Strom studies. We note, however, that the error for a mildly rotating star, or for an early A star with weak lines is apt to be somewhat larger. Based on these estimates, one may show that the distribution of points about the mean relation in Figure 10 indicates that the observed scatter is entirely attributable to observational or ξ_T-measurement errors. These data imply, therefore, that microturbulence is a <u>unique</u> function of effective temperature along the A star domain of the main sequence. A strictly observational consequence of such a conclusion would be the following: since the sensitivity of Δm_1 to line strengths increases as we go to later types along the main sequence, a good correlation of Δm_1 with ξ_T (the "Conti-Deutsch effect" [Conti and Deutsch 1966, 1967]) ought not to be possible for A stars. Stars of the same temperature and sensitivity to metallic line blanketing would all have the same microturbulence, according to our result.

The Absolute Iron Abundances in Am Stars

In Figure 11 the absolute iron abundances of all program stars are presented as a function of effective temperature. All abundances designated are on the log (Hydrogen) = 12.00 scale. These abundances are the means of those computed from Fe I and Fe II lines, which are given in Table 5 of the next section. As in Figure 10 above, the iron abundances of Chaffee's normal field A stars are represented. In these latter cases, however, the iron abundance was derived solely from Fe I lines so that it was necessary to synthesize Fe I - Fe II quasi-means by assuming the appropriate (Fe I - Fe II) differences according to Figure 9. In no case, however, did this correction exceed 0.1 dex. We have also represented the iron abundance of Conti's (1965a) standard, 45 Tauri, by the symbol "(C)." For this star we chose twenty equivalent widths from Conti's study which are very near his empirical curve of growth. Conti's parameters, T_{eff} = 7100°K and ξ_T = 4.0 km/sec, were used to determine the 45 Tau abundance shown.

Except for HR 906,[1] represented as a square, Figure 10 shows that the iron abundances of the metallic line stars exhibit very little overlap with those of the normal stars. All Am stars studied exhibit iron

---

1. HR 906 has a Stromgren Δm_1 of -0.01, so that its derived high iron abundance is nor surprising. The abundances of this star will be treated in more detail in the next section.

Figure 11. Calculated iron abundances as a function of effective temperature

Same stars and symbols as in Figure 10. The arrow represents the trajectory resulting from small temperature modifications.

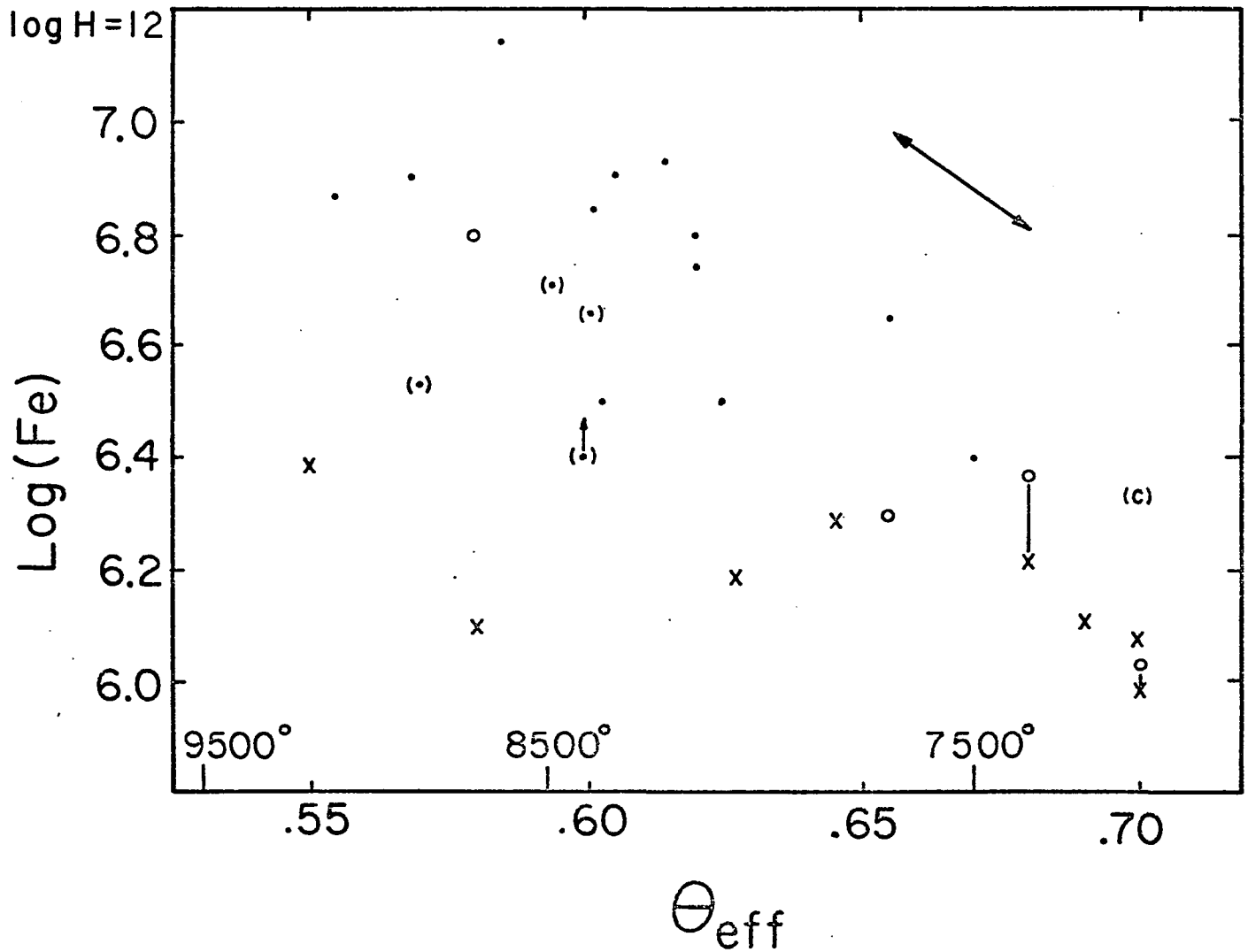

Figure 11. Calculated iron abundances as a function of effective temperature

enhancements which vary from several per cent to a factor of five, or even greater in the case of HR 4685 (8 Com). The great bulk of the scatter in log (Fe) at a given temperature in Figure 11 must be intrinsic to the stars themselves, since we estimate errors in log (Fe) to be ± 0.1. It appears, therefore, that Am stars exhibit real variable enhancement factors of iron and of other elements, as will be shown in the next section. A consequence of this conclusion may be that Conti's (1970) "subgroup b" of Am stars (those with normal iron abundances) is merely the low iron enhancement extension of the general Am class.

As would be expected, the absolute iron abundance determined for the normal stars is the same for all temperatures. There is, however, a trend for the Am stars in the sense that the hotter ones have larger iron enhancements. If the star HR 1458 (88 Tau, denoted by the upward arrow) is excluded on the basis of its apparent line dilution, one finds that this "trend" is in fact a statistically significant correlation with a 95% confidence coefficient. The double-headed arrow represents the direction in which a data point would be changed for small adjustments in temperature, according to Table 3. Since the slope of this trend is nearly parallel to this arrow, it follows that one cannot explain this correlation by systematic changes in assigned T_{eff} values unless one accepts the unlikely possibility that all stars actually have nearly the same temperature.

Moreover, use of a steeper temperature-color calibration such as Matsushima's would actually improve the correlation. A change in gravity at T_{eff} = 9000°K would produce no change in the computed iron abundance. Since errors in the assigned physical parameters cannot explain the observed trend, we conclude that Am stars have iron abundances which tend to be progressively enhanced with increasing effective temperature.

Discussion and Interpretation of the Derived Am Abundances

From the equivalent width data in Appendix A, we present abundance results in Table 5 for twenty-nine elements. The three numbers in each column correspond, respectively, to the logarithm of the abundance, on the log H = 12.00 scale, the number of lines actually measured (in parentheses), and the indicated logarithmic r.m.s. scatter. Asterisks are included in a few cases for the abundances from Si II, Nd II, and S I. This symbol indicates that an adjustment of the mean abundance was made because only one of two lines was measured. The adjustment compensates for the fact that each of the two lines for these ions gives a systematically different abundance from the other. Abundances in parentheses represent those in which the scatter is somewhat larger than average or for which the number of lines measured is inordinately small.

Table 5. The Computed Mean Abundances and R.M.S. Scatter (log H = 12.0)

	HR 114	HR 906	HR 2085	HR 4825	HR 4685
C I	8.37 (4) .17	8.60 (4) .19	8.50 (5) .18	8.25 (4) .17	8.27 (4) .12
Na I	5.96 (3) .15	6.32 (4) .21	6.05 (4) .20	5.96 (4) .14	6.80 (4) .20
Mg I	6.78 (4) .16	7.57 (4) .35	7.46 (4) .29	6.97 (4) .36	7.70 (4) .28
Al I	4.86 (2) .11	5.56 (2) .16	5.10 (2) .24	4.85 (2) .11	5.77 (2) .35
Si I	6.89 (4) .08	7.44 (6) .20	7.02 (4) .14	6.95 (5) .13	7.66 (7) .18
Si II	7.00*(1) --	7.22*(1) --	7.18 (2) .10	7.13*(1) --	8.11 (2) .12
S I	6.60 (4) .20	7.25 (3) .18	6.98 (2) .19	6.61 (2) .30	7.30 (4) .22
Ca I	6.09 (8) .07	6.58 (8) .10	5.98 (8) .14	5.81 (8) .24	6.72 (8) .12
Sc II	2.73 (7) .23	3.12 (8) .35	2.60 (8) .25	2.29 (8) .30	3.10 (8) .25
Ti I	4.66 (4) .14	5.39 (3) .15	4.69 (4) .15	4.18 (4) .23	5.63 (3) .30
Ti II	4.24 (33).30	4.64 (34).35	4.23 (34).26	3.92 (33).34	5.10 (31).37
V II	3.12 (7) .08	3.55 (7) .15	3.51 (7) .25	3.17 (5) .33	4.28 (7) .18
Cr I	5.21 (10).31	5.72 (9) .32	5.20 (10).31	4.79 (11).33	6.22 (11).24
Cr II	5.43 (13).35	5.78 (13).24	5.44 (13).24	5.32 (12).33	6.14 (13).22
Mn I	4.89 (6) .25	5.33 (9) .25	5.05 (8) .21	4.54 (8) .29	5.76 (7) .28
Fe I	6.36(118).19	6.89(117).24	6.38(117).26	5.99(117).28	7.25(117).27
Fe II	6.23 (33).25	6.67 (34).25	6.34 (33).26	6.06 (33).36	7.09 (33).24

Table 5.--Continued The Computed Mean Abundances and R.M.S. Scatter (log H = 12.0)

	HR 1672	HR 2291	HR 5055	HR 7850	HR 8410
C I	8.04 (5) .12	7.98 (4) .27	7.93 (4) .11	8.20 (4) .07	8.17 (5) .13
Na I	6.63 (4) .13	6.19 (4) .26	6.05 (2) .05	6.14 (3) .13	6.56 (3) .07
Mg I	6.75 (4) .03	6.93 (4) .29	7.11 (4) .23	6.69 (4) .34	6.73 (4) .17
Al I	5.46 (2) .28	(5.39)(2) .50	5.37 (2) .16	5.20 (2) .28	5.38 (2) .40
Si I	7.40 (7) .15	7.11 (6) .10	----------	7.14 (4) .14	7.47 (7) .19
Si II	7.79 (2) .12	7.82 (2) .14	6.94*(1) --	7.33 (2) .28	7.89 (2) .20
S I	7.31 (4) .10	6.82 (4) .15	(7.13)(2) .31	7.13*(1) --	7.13 (2) .14
Ca I	5.97 (8) .26	5.97 (8) .22	5.96 (4) .15	6.09 (7) .27	6.03 (7) .14
Sc II	2.29 (7) .27	2.27 (8) .19	2.34 (5) .24	2.60 (6) .29	2.51 (7) .24
Ti I	5.13 (4) .32	4.97 (4) .42	5.28 (3) .33	5.07 (2) .19	5.47 (3) .16
Ti II	4.45 (31).22	4.44 (33).28	4.13 (25).28	4.32 (26).31	4.59 (33).22
V II	3.73 (6) .24	3.66 (7) .15	3.26 (2) .04	3.41 (4) .12	3.90 (7) .20
Cr I	5.79 (10).27	5.56 (10).24	5.43 (4) .05	5.48 (4) .28	5.78 (10).23
Cr II	5.93 (13).18	5.72 (12).30	5.70 (9) .28	5.56 (8) .19	5.98 (13).33
Mn I	5.40 (9) .29	5.38 (8) .31	5.23 (6) .19	5.20 (6) .29	5.54 (8) .27
Fe I	6.89(116).26	6.74(117).24	6.66 (65).26	6.53 (67).28	6.98(117).27
Fe II	6.70 (31).27	6.73 (34).19	6.49 (27).24	6.45 (27).25	6.85 (34).25

Table 5.--Continued The Computed Mean Abundances and R.M.S. Scatter (log H = 12.0)

	HD 108486	HR 4750	HR 4751	HR 4780	HR 1368
C I	8.15 (3) .11	8.04 (5) .09	8.06 (4) .13	8.31 (4) .13	8.02 (4) .23
Na I	6.80 (4) .20	6.25 (3) .11	6.64 (4) .11	6.80 (3) .08	5.94 (4) .21
Mg I	7.37 (4) .28	6.87 (4) .14	7.07 (4) .24	7.40 (4) .22	6.53 (4) .31
Al I	5.73 (2) .28	5.63 (2) .33	5.54 (2) .33	5.53 (2) .25	4.92 (2) .28
Si I	7.64 (4) .05	7.40 (6) .19	7.61 (5) .10	(7.52)(4) .27	6.91 (3) .14
Si II	7.38 (2) .19	7.68 (2) .18	7.73 (2) .22	7.38 (2) .23	7.58*(1) --
S I	7.10 (2) .05	7.12 (4) .15	7.01 (2) .26	7.39 (2) .01	6.71 (2) .16
Ca I	6.38 (7) .14	6.00 (6) .19	6.34 (7) .27	6.76 (6) .07	5.61 (5) .19
Sc II	2.42 (5) .13	2.39 (5) .25	2.67 (7) .20	3.42 (7) .16	2.25 (4) .11
Ti I	5.10 (3) .25	5 14 (3) .32	5.12 (2) .01	5.52 (4) .28	4.74 (1) --
Ti II	4.30 (30).31	4.52 (33).25	4.57 (38).32	4.76 (30).29	4.17 (28).28
V II	3.48 (6) .25	3.67 (6) .26	3.72 (4) .17	3.51 (5) .19	3.39 (4) .20
Cr I	5.69 (8) .29	5.74 (11).16	5.92 (9) .20	5.92 (6) .34	5.22 (7) .29
Cr II	5.68 (13).28	5.78 (12).26	5.90 (12).24	5.89 (12).32	5.71 (10).31
Mn I	5.34 (7) .28	5.52 (9) .21	5.61 (8) .30	5.44 (8) .20	4.98 (8) .35
Fe I	6.83(101).26	6.92(113).23	7.05(104).27	6.95(101).25	6.38 (91).27
Fe II	6.54 (28).30	6.73 (34).25	6.77 (34).29	6.77 (31).24	6.41 (28).26

Table 5.--Continued The Computed Mean Abundances and R.M.S. Scatter (log H = 12.0)

	HR 1376	HR 1389	HR 1428	HR 1458	HR 1519
C I	7.88 (5) .31	8.23 (5) .14	7.98 (4) .29	8.11 (4) .17	7.98 (4) .23
Na I	6.16 (4) .17	6.54 (4) .23	6.36 (3) .15	6.17 (2) .14	6.27 (4) .31
Mg I	6.53 (4) .37	7.13 (4) .20	6.58 (4) .44	6.60 (4) .29	6.75 (4) .24
Al I	5.17 (2) .31	5.88 (2) .39	5.05 (2) .22	5.16 (2) .15	5.43 (2) .29
Si I	7.13 (4) .17	7.50 (3) .03	6.96 (4) .22	7.26 (3) .05	7.35 (3) .10
Si II	7.86 (2) .17	7.68 (2) .22	7.12*(1) --	7.24 (2) .25	7.33*(1) --
S I	6.76 (2) .23	7.42 (2) .19	6.68*(1) --	----------	6.95 (2) .32
Ca I	5.35 (8) .23	6.26 (6) .14	5.96 (7) .19	6.08 (5) .23	5.94 (6) .13
Sc II	2.20 (8) .17	2.58 (6) .32	2.33 (6) .18	2.60 (5) .23	2.40 (3) .06
Ti I	4.62 (4) .40	5.45 (2) .43	4.78 (2) .23	----------	5.61 (2) .18
Ti II	4.22 (33).25	4.70 (34).24	4.21 (32).37	4.09 (27).45	4.26 (26).29
V II	3.65 (7) .22	3.80 (6) .08	3.41 (3) .19	3.46 (4) .33	(3.38)(1) --
Cr I	5.53 (10).25	6.00 (10).26	5.41 (8) .21	5.29 (4) .26	5.59 (7) .15
Cr II	5.95 (13).29	5.99 (13).34	5.72 (10).27	5.67 (10).28	5.75 (8) .35
Mn I	5.10 (9) .25	5.68 (8) .31	5.15 (8) .22	5.10 (8) .29	5.35 (8) .29
Fe I	6.66(119).26	6.97(115).24	6.54(100).27	6.42 (81).30	6.73 (73).31
Fe II	6.67 (34).24	6.77 (32).21	6.43 (32).27	6.31 (31).33	6.56 (27).32

Table 5.--Continued The Computed Mean Abundances and R.M.S. Scatter (log H = 12.0)

	HR 114	HR 906	HR 2085	HR 4825	HR 4685
Co I	4.90 (3) .60	(5.16)(3) .65	4.99 (3) .77	4.52 (3) .67	5.90 (3) .47
Ni I	5.22 (9) .24	5.82 (11).26	5.29 (11).22	5.01 (11).23	6.22 (11).26
Ni II	4.96 (4) .17	5.31 (3) .27	5.34 (3) .28	5.14 (3) .13	6.09 (4) .25
Cu I	4.45 (1) --	5.12 (2) .08	4.20 (1) --	4.01 (1) --	5.14 (2) .03
Zn I	2.84 (2) .01	3.15 (2) .09	3.05 (2) .05	2.81 (2) .06	4.10 (2) .02
Sr II	2.72 (2) .15	3.51 (2) .05	3.25 (2) .00	2.57 (2) .32	4.52 (2) .33
Y II	2.34 (7) .23	2.87 (7) .19	2.41 (7) .20	2.03 (7) .30	3.56 (7) .35
Zr II	3.00 (7) .17	3.38 (7) .33	2.96 (7) .29	2.55 (6) .32	4.09 (6) .27
Ba II	1.92 (4) .26	2.61 (4) .21	1.80 (4) .28	1.52 (4) .51	3.27 (4) .17
La II	1.66 (6) .47	2.38 (8) .54	1.94 (8) .34	1.39 (4) .31	3.07 (7) .28
Ce II	1.83 (6) .39	2.48 (7) .37	2.03 (6) .25	1.77 (6) .25	3.13 (8) .24
Nd II	1.69*(1) --	2.33 (2) .15	1.77 (2) .21	1.54 (2) .22	2.91 (2) .29
Sm II	1.40 (2) .03	2.26 (1) --	1.77 (1) --	1.47 (2) .01	2.93 (2) .01
Eu II	1.27 (2) .07	1.96 (1) --	1.20 (2) .17	0.84 (2) .03	3.23 (2) .21
Gd II	1.39 (1) --	2.16 (1) --	1.11 (1) --	1.09 (1) --	2.92 (1) --

Table 5.--Continued The Computed Mean Abundances and R.M.S. Scatter (log H = 12.0)

	HD 108486	HR 4750	HR 4751	HR 4780	HR 1368
Co I	5.45 (3) .72	5.53 (3) .52	5.63 (3) .60	5.72 (3) .62	5.01 (3) .62
Ni I	5.87 (11).26	5.95 (11).19	6.00 (10).21	6.07 (10).21	5.50 (9) .29
Ni II	5. 51 (4) .20	5.80 (4) .19	5.84 (3) .22	5.41 (3) .04	5.51 (2) .31
Cu I	5.32 (2) .03	5.35 (2) .03	5.31 (2) .02	5.76 (2) .11	4.88 (1) --
Zn I	4.08 (2) .00	3.90 (2) .05	3.98 (2) .06	4.17 (2) .04	3.11 (2) .01
Sr II	4.08 (2) .05	4.23 (2) .05	4.11 (2) .17	3.85 (2) .06	3.68 (2) .15
Y II	3.06 (7) .31	3.25 (6) .25	3.11 (7) .34	3.14 (7) .24	2.80 (7) .30
Zr II	3.47 (5) .25	3.62 (7) .19	3.09 (5) .15	3.53 (5) .11	2.98 (3) .17
Ba II	2.69 (3) .34	2.62 (4) .14	(2.73)(4) .37	2.81 (4) .16	2.06 (4) .33
La II	2.34 (6) .31	2.68 (8) .28	2.62 (7) .21	2.68 (4) .35	2.28 (6) .25
Ce II	2.51 (8) .23	2.68 (8) .18	2.84 (7) .22	2.62 (4) .08	2.43 (5) .24
Nd II	2.44 (2) .19	2.59 (2) .15	2.62 (2) .12	2.64 (2) .28	2.17 (2) .24
Sm II	2.44 (2) .04	2.57 (2) .04	2.47 (2) .08	2.75 (2) .11	2.21 (1) --
Eu II	2.34 (2) .16	2.60 (2) .01	2.62 (2) .06	2.58 (2) .10	1.93 (2) .14
Gd II	2.41 (1) --	2.45 (1) --	2.41 (1) --	2.58 (1) --	1.88 (1) --

Table 5.--Continued The Computed Mean Abundances and R.M.S. Scatter (log H = 12.0)

	HR 1376	HR 1389	HR 1428	HR 1458	HR 1519
Co I	5.32 (3) .65	(5.81)(3) .57	5.33 (3) .54	5.29 (3) .54	5.28 (3) .47
Ni I	5.99 (11).35	6.18 (10).37	5.74 (10).27	5.77 (7) .36	5.78 (9) .27
Ni II	5.87 (4) .17	5.76 (4) .11	5.48 (3) .15	5.18 (3) .05	5.67 (3) .20
Cu I	4.93 (2) .19	(5.59)(1) --	4.74 (2) .22	5.16 (2) .17	4.98 (2) .03
Zn I	3.60 (2) .06	4.06 (2) .07	3.50 (2) .04	3.18 (2) .02	3.51 (2) .04
Sr II	3.92 (2) .22	4.03 (2) .05	3.75 (2) .13	3.22 (2) .16	3.82 (2) .33
Y II	3.02 (7) .33	3.14 (7) .19	2.82 (7) .24	2.67 (7) .25	3.20 (5) .18
Zr II	(3.05)(7) .34	3.50 (6) .17	3.16 (4) .16	3.06 (4) .19	3.50 (4) .29
Ba II	2.62 (4) .11	2.94 (4) .21	2.68 (4) .24	2.31 (4) .45	2.75 (4) .39
La II	2.63 (8) .23	2.54 (5) .39	2.51 (7) .26	2.28 (4) .22	2.38 (5) .17
Ce II	2.62 (8) .19	2.77 (8) .29	2.57 (6) .19	2.36 (4) .22	2.53 (6) .24
Nd II	2.53 (2) .24	(2.44)*(1) --	2.40 (2) .29	2.06 (2) .39	2.22 (2) .38
Sm II	2.43 (2) .07	2.95 (2) .02	2.43 (2) .00	2.31 (2) .04	2.31 (1) --
Eu II	2.48 (2) .07	2.79 (2) .21	2.37 (2) .10	2.01 (2) .01	2.73 (2) .17
Gd II	2.28 (1) --	2.82 (1) --	2.23 (1) --	2.30 (1) --	2.41 (1) --

Table 5.--Continued The Computed Mean Abundances and R.M.S. Scatter (log H = 12.0)

	HR 1672	HR 2291	HR 5055	HR 7850	HR 8410
Co I	5.56 (3) .57	5.34 (3) .56	5.20 (2) .27	5.36 (3) .58	5.74 (3) .47
Ni I	6.04 (11).21	5.88 (11).28	5.71 (9) .21	5.95 (6) .32	6.00 (11).25
Ni II	5.92 (4) .17	5.72 (4) .24	5.18 (3) .09	5.37 (3) .13	5.97 (4) .21
Cu I	5.35 (2) .00	4.93 (2) .09	5.33 (2) .08	5.14 (2) .12	5.38 (2) .05
Zn I	3.91 (2) .03	3.72 (2) .02	3.54 (2) .11	3.69 (2) .04	3.80 (2) .02
Sr II	3.93 (2) .41	3.99 (2) .13	3.53 (2) .15	3.39 (2) .27	4.21 (2) .36
Y II	3.09 (7) .28	3.21 (7) .33	2.95 (7) .18	2.95 (7) .28	3.43 (7) .27
Zr II	3.47 (7) .32	3.77 (7) .21	3.33 (4) .27	3.30 (6) .18	3.94 (6) .20
Ba II	2.67 (4) .29	2.92 (4) .30	2.79 (4) .30	2.69 (4) .37	3.07 (4) .20
La II	2.82 (8) .34	2.62 (8) .23	2.38 (5) .34	2.16 (4) .31	2.98 (7) .25
Ce II	2.87 (7) .24	2.58 (8) .20	2.45 (4) .19	2.59 (5) .19	2.97 (8) .22
Nd II	2.69 (2) .34	2.51 (2) .20	2.19 (2) .35	2.20 (2) .24	2.72 (2) .18
Sm II	2.75 (2) .04	2.39 (2) .02	2.30 (1) --	2.36 (1) --	2.68 (2) .02
Eu II	2.75 (2) .03	2.54 (2) .09	2.26 (2) .26	2.34 (2) .28	2.97 (2) .15
Gd II	2.50 (1) --	2.45 (1) --	2.06 (1) --	----------	2.76 (1) --

The data in Table 5 are represented in Figures 12a and 12b and are plotted in absolute abundance form. In Figure 13 the data are replotted relative to iron on an expanded scale. In the latter diagrams the abundances from all ionized elements are plotted relative to those given by Fe II, while all neutral element abundances (except for C I) are referred to those from Fe I. By this procedure we hope to minimize the influences of the small ionization equilibrium errors that do exist. In both diagrams the Ti I data are not included because so many more lines of Ti II are given.

In these figures dots denote individual abundances in metallic line stars. The abundances in three of them, HR 4780 (22 Com), HR 1458 (88 Tau), and HR 7850 (θ Cep), are represented as crosses. These stars are apparent "marginal" Am stars, according to Figure 13, for they show normal Ca/Fe, Sc/Fe and near-normal C/Fe, Mg/Fe, whereas their heavy elements, including the iron peak, are enhanced as in Am stars. Abundances of three standards HR 114, HR 2085, and HR 4825 are represented as circles. Those of the fourth, HR 906, are represented as squares; this star will be discussed in more detail subsequently. Finally, we note that any abundance points surrounded by horizontal bars are the relatively more uncertain ones parenthesized in Table 5.

In general those abundances represented by the large numbers of lines are most reliable. Those data are

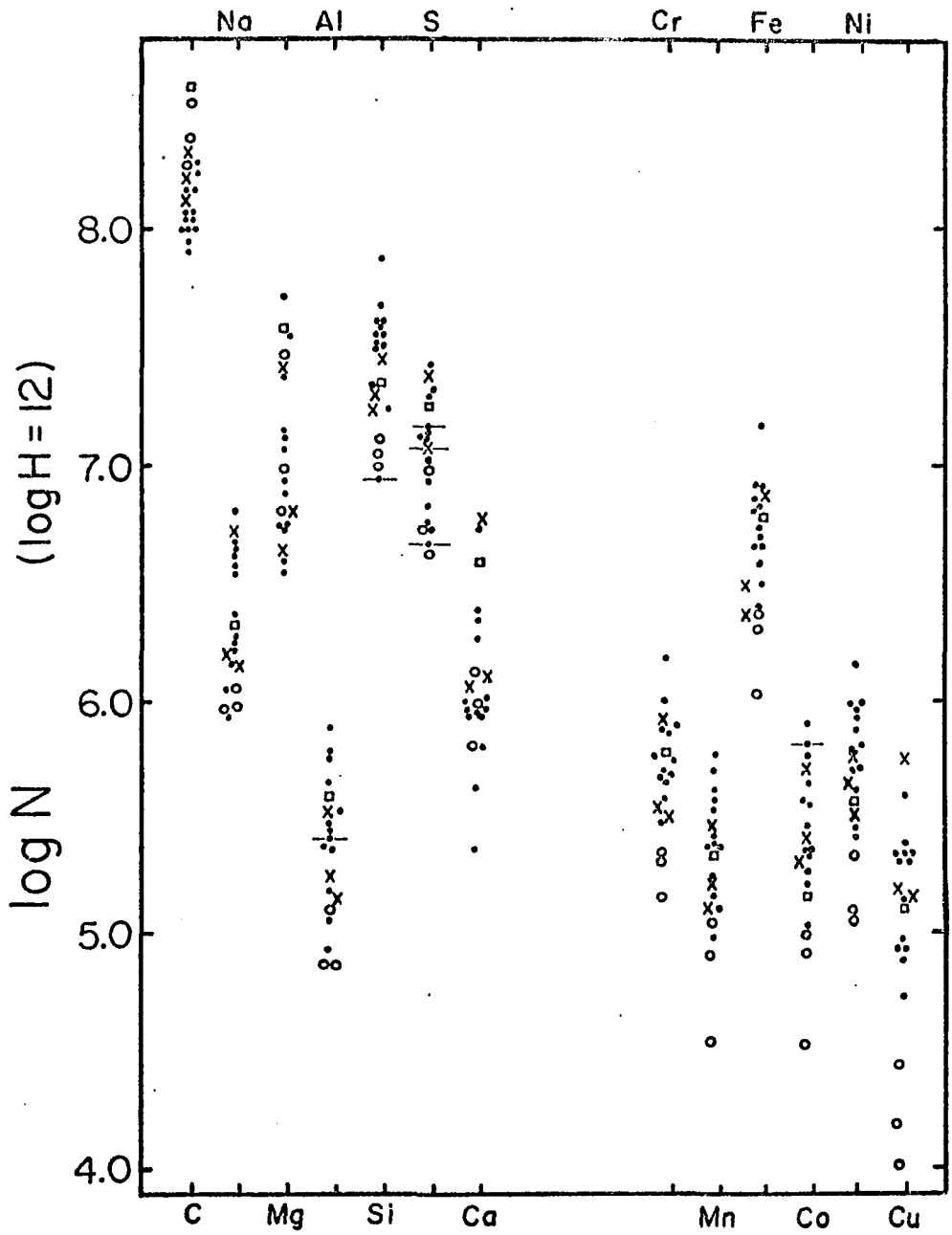

(a) The light elements

Figure 12. The calculated absolute abundances of the elements

Dots represent Am stars; crosses, "marginal" Am stars; circles, normal standards; squares, HR 906.

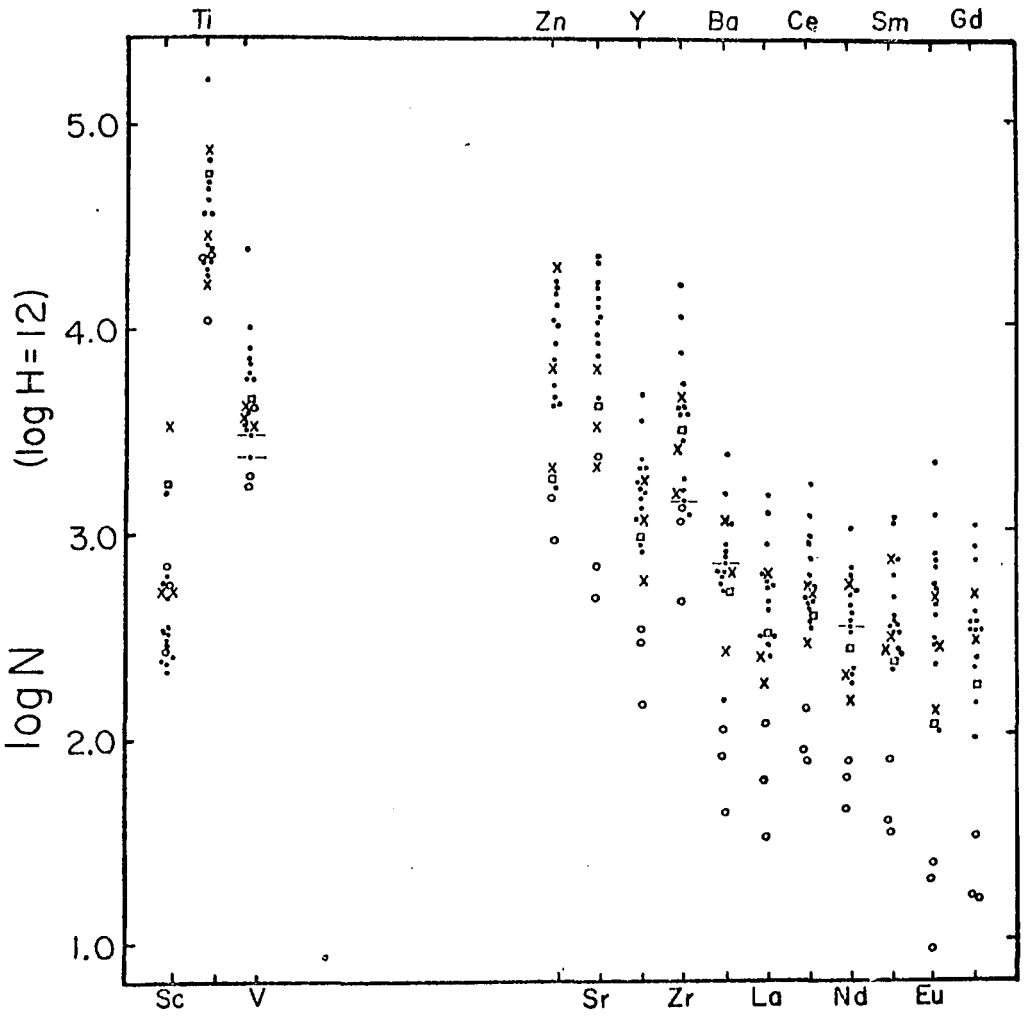

(b) The heavy elements

Figure 12.--Continued

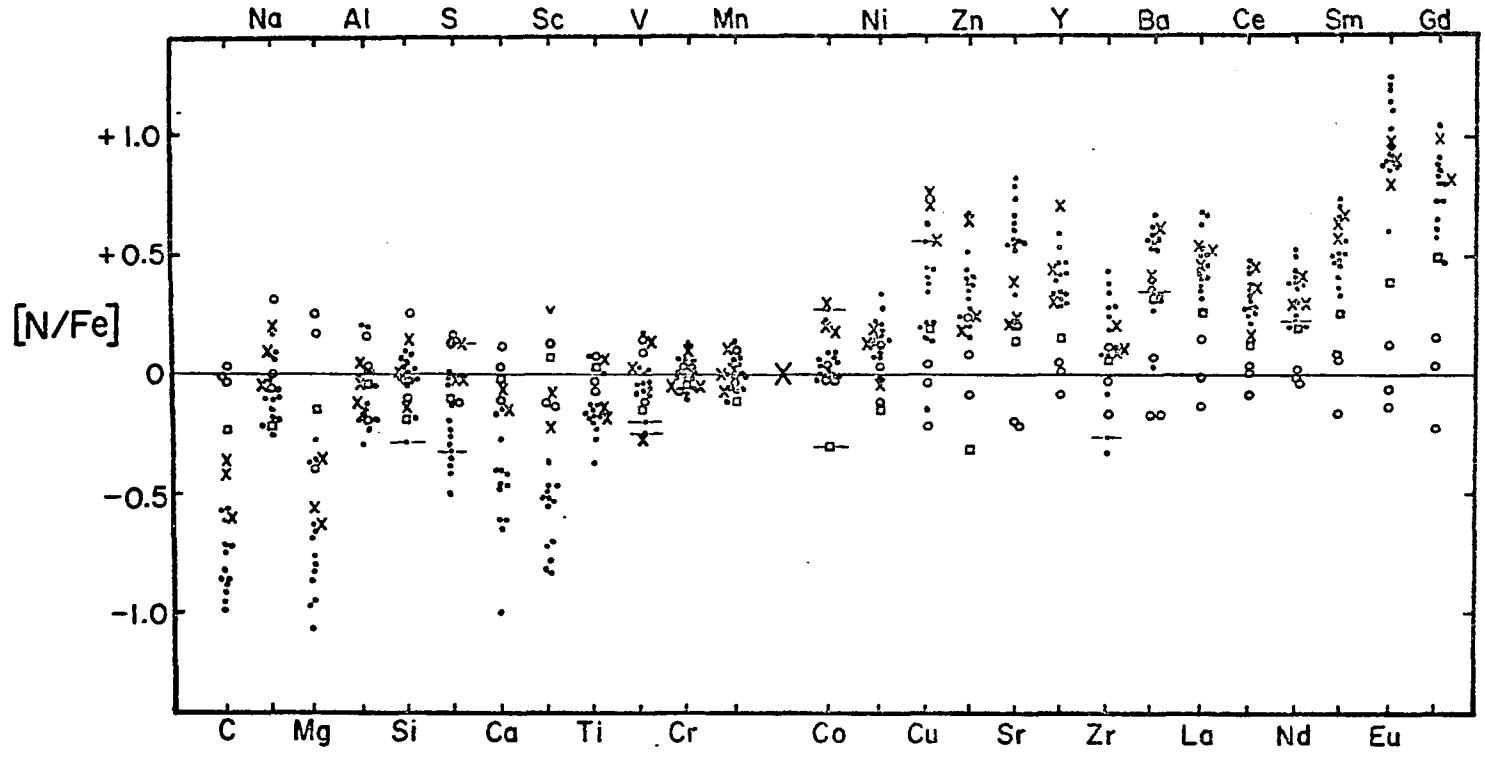

Figure 13. The relative abundances of the elements

The ordinate represents logarithmic abundance ratios with respect to iron and relative to the means of the standards. Same symbols as in Figure 12.

least reliable which contain only a few very strong or very weak lines taken from the D plates. Examples of such are Mg I, Si I, S I, and Cu I. In addition, the heavy elements Nd II, Sm II, and Eu II are represented by two lines, and Gd II by only one. The Sr II ion is represented by two very strong resonance lines which are formed on the horizontal portion of the curve of growth where the logarithmic slope is about one-sixth. They are therefore likely to exhibit large errors in their individual computed abundances. Inspection of internal errors in Sr II from star to star indeed shows that their individual abundance differences show large fluctuations. We estimate that except for Fe I, Fe II, and Ti II, most abundances are subject to errors arising from equivalent width errors in the range of 0.05 to 0.10 dex, or possibly more in the above mentioned cases.

A brief general description of the pattern of abundances in Am stars relative to the normal stars follows. It has already been shown that iron is enhanced in Am stars. For reasons apparent below, the behavior of the elemental abundances relative to iron, as in Figure 13, are described.

Starting with the lightest element examined, carbon, one sees that C/Fe is low in Am stars. According to Figure 13, this is also true of the absolute carbon abundance. Marginal deficiencies of this order have been noted by a few previous authors, however we feel that further attention should be drawn to this point since carbon is cosmically

very abundant. From our data it appears that a carbon deficiency in metallic line stars is a group property. Although C/Fe is difficult to measure because of the location of only a few C I lines near Hβ, it might be used, like Ca/Fe or Sc/Fe, as an Am star indicator.

Of the remaining elements, three others, Mg, Ca, and Sc, often show appreciable deficiencies relative to iron. Hereinafter, C, Mg, Ca, and Sc will be referred to as "the deficient elements."

We note that S/Fe and Ti/Fe also appear marginally deficient. The other light elements studied scale with iron from star to star. The iron peak elements V, Cr, Mn, and Co are also enhanced along with iron. The iron peak element Ni may be slightly more enhanced than iron, however. The heavy elements, from Cu and Zn out to the rare earths Eu and Gd, exhibit super-enhancements relative to iron.

The large abundances of Ca and Sc depicted in Figures 12 and 13 merit a brief digression. In general the Ca and Sc deficiencies which obtain in this study are more moderate than those found by previous investigators. Conti's (1965a) study of Am stars in the Hyades, for example, shows larger deficiencies than we derive for the same stars. Analysis of the data for his standard, 45 Tau, shows, however, that the Ca and Sc abundances are larger by factors of about three and two, respectively, than those in our standards (other than HR 906). Our three standards

also appear to be slightly metal deficient relative to the sun.

Detailed checks of the WIDTH program have been made by attempting to reproduce the results of the abundances of these elements found in the Conti and Strom studies. It was found that our abundance scales for Ca and Sc are 0.3 and 0.1 dex, respectively, larger than theirs.

The apparent result that the absolute abundance of calcium and occasionally scandium is actually enhanced in some Am stars was completely unanticipated. Examination of the literature, however, demonstrates similar results from other studies. The equivalent width of the K-line of 8 Com measured by Miczaika et al. (1956) can be shown to be indicative of enhanced calcium abundance, as Henry's (1969) photometry also indicates (see Figure 17). Further, the absolute calcium abundance in Sirius may actually be higher than in Vega (Strom et al. 1968). In such stars, however, the Ca/Fe ratio is low.

In Figures 12 and 13 the abundance results have been presented in both absolute and relative forms. The advantage of the absolute presentation is that it enables the investigator to determine how much of each element is added or subtracted from a normal composition mixture. If a nucleosynthetic or a chemical separation process were responsible for the Am traits, then one would expect common enhancements or deficiencies of a selected group of processed elements.

Such an effect would be readily discernible in Figure 12. Moreover, this presentation facilitates a check on the possible conservation of heavy particles, which would be expected to be obeyed by any nucleosynthetic process. The advantages of a relative comparison, on the other hand, are that it would be most appropriate if an element separation process, e.g., by diffusion, were responsible. In such a case a large number of elements, unrelated chemically or nucleosynthetically, would be affected since the chances of a perfect balance of forces for any one ion would be small. Such a representation also tends to minimize spurious effects in T_{eff}, log g, ξ_T, and equivalent width errors, the magnitudes of which have been previously estimated. Finally, it enables a convenient comparison to be made with what the spectroscopist actually observes, relative line strengths.

In order to determine the more appropriate facets of each representation, and to make indirect inferences on the general nature of the Am phenomenon, we shall state and then consider three general criteria:

1. Does the pattern of correlations among the elements follow from known nucleosynthetic processes? For example, do the elements with a "magic number" of nucleons show larger enhancements than their neighbors?

2. For each element, which representation minimizes the scatter of the Am abundances relative to the scatter of the standard star abundances? (It is assumed that any incorrect representation will add to the apparent scatter.)
3. Are there simple or ordered patterns arising from either representation?

Toward consideration of the first criterion, we recognize that there are five general nucleosynthetic processes responsible for the genesis of the elements investigated herein (Arnett et al. 1968): helium burning (to carbon); the α-process (addition of α particles to light elements in order to form Na, Mg, Al, Si, S, Ca, Ti); the e-process (an equilibrium set of reactions at high temperatures and densities forming the iron peak elements V, Cr, Mn, Fe, Co, Ni); the s-process (neutron capture on a slow timescale relative to that of β-decay, forming Sc, Cu, Zn, Sr, Y, Zr, Ba, La, Ce, Nd); and the r-process (neutron capture on a rapid timescale, leading to the formation of Sm, Eu, Gd). We note parenthetically that calcium is a "doubly magic number" element with 20 protons and 20 neutrons; other magic number elements are Sr, Y, Zr (50 neutrons), and Ba, La, Ce (82 neutrons). None of these processes is presently thought to be operative in the interiors of main sequence A stars.

By means of a large number of diagrams not shown here, we have attempted to correlate the Am star abundances of adjacent elements, elements common to the same nucleosynthetic process, and elements of the different processes. The great bulk of these results may be summarized by the simple statement that except for the deficient elements, most all elements correlate well or very well with one another and with iron. These correlations occur irrespective of the nucleosynthetic group of which the elements are members and regardless of their positions in the periodic table. In addition, those stars with the largest iron peak enhancements tend to show the largest enhancements for most other elements; the converse is true for those stars with small iron peak enhancements.

The deficient elements, particularly C, Ca, and Sc, are well correlated together, both in their absolute abundances and in their "anomalies" (i.e., abundances relative to iron). Correlations with the more uncertain Mg results are weaker. In Figures 14 and 15 we exhibit, respectively, the correlations between Ca and Sc and between Ca/Fe and Sc/Fe. When allowance is made for observational errors in the abundance determinations, it is concluded that these correlations are good, however imperfect. It is to be further mentioned that the absolute abundances of the deficient elements do not show significant anti-correlations

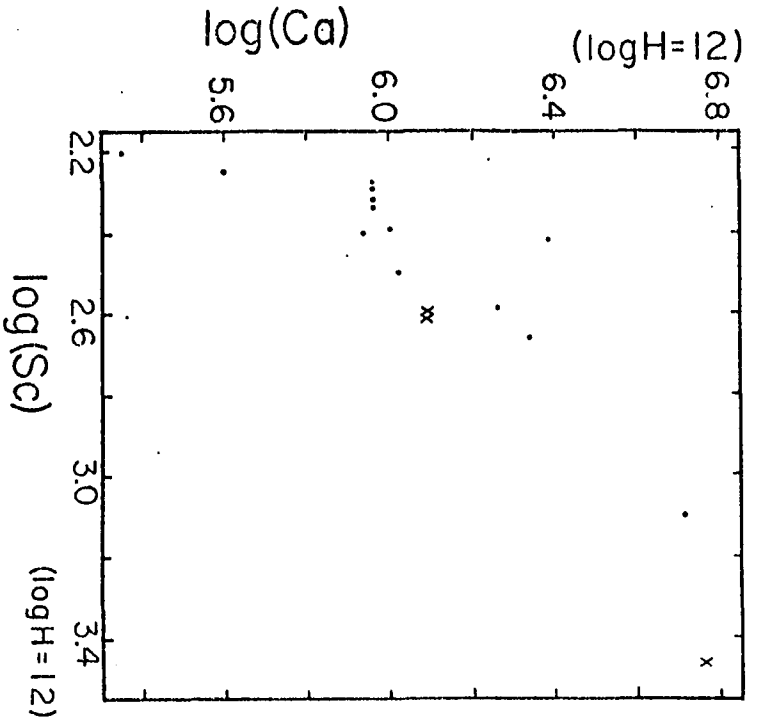

Figure 14. The log(Ca), log(Sc) diagram
Same symbols as in Figure 12.

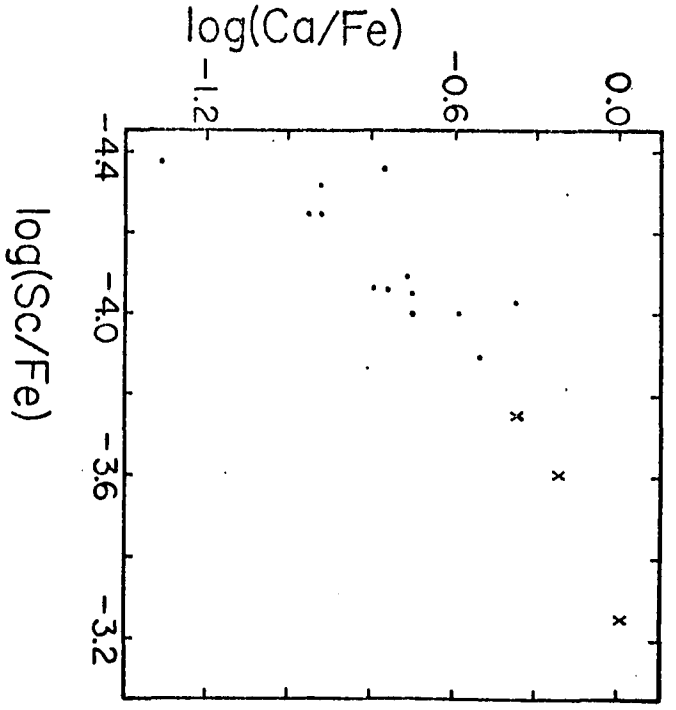

Figure 15. The log(Ca/Fe), log(Sc/Fe) diagram
Same symbols as in Figure 12.

with any of the enhanced elements. However, we shall return to this point in consideration of Figure 19.

The scatter in abundances from star to star in Figures 12 and 13 is next considered. In Figure 13 most all the enhanced elements exhibit N/Fe scatter no larger among the Am stars than the three standards HR 114, HR 2085, and HR 4825. The obvious exceptions to this rule are Zr/Fe and Cu/Fe, which will be treated later. Those elements showing larger scatter among the Am stars are principally the deficient elements, as can be seen in Figure 13 by the large range in Am ratios C/Fe, Mg/Fe, Ca/Fe, Sc/Fe, and S/Fe. In Figure 12 the absolute abundance representation exhibits almost the reverse situation. Here the enhanced elements exhibit the large scatter among the Am group, whereas the deficient elements show the smaller scatter among them.

If one requires for each element that the apparent Am scatter be minimized relative to the standard scatter (Criterion #2), then a possible interpretation of the above observations is that two subprocesses may be operative: one for the deficient elements, and the other for the enhanced elements, including the iron peak. Other interpretations will be suggested below.

Two general points emerge from consideration of the scatter criterion. First, the data suggest that a general enhancement process is occurring to different degrees among most elements. Further, the degree of enhancement,

conveniently measured in iron, apparently varies from one Am star to another. As already suggested in reference to Figure 11, this "degree of enhancement" may be partially correlated with effective temperature. The second point is that there is a great uniformity in relative abundances among the elements. For most all enhanced elements (except for a few discussed near the end of this chapter), the metallicism process does not seem to tolerate real N/Fe variations by more than a factor of two. Most of the observed scatter in these elements, as exemplified by the scatter in the standard stars for these elements, can be explained on the basis of errors in assigned atmospheric parameters, equivalent width errors, and small differences in primordial composition mixtures. The deficient anomalies show more variation, a point to which we shall return presently.

It will now be demonstrated that the relative abundance representation in Figure 13 lends an apparent order to the abundance results which Figure 12 does not (Criterion #3). First, it can be seen that for Am stars in Figure 13 the group abundance behavior of any one element is similar to that of the neighboring elements. The rise to super-enhancements from the post-iron peak elements copper and zinc to the rare earths is gradual. The super-enhancements are shared by both r- and s-process elements. The iron peak elements exhibit nearly identical behavior, a

fact which is manifested in Figure 13 by the extremely small scatter. Anomalies on both sides of the deficient Ca, Sc element group (such as Ti/Fe, S/Fe, and K/Fe [Conti 1965a]) show lesser degrees of deficiencies. However, this latter point may not be applicable to elements adjacent to C and Mg. From these considerations, the anomaly pattern seems related to atomic number. There is, moreover, no sharp enhancement for the magic number elements as in nucleosynthesis. A possible interpretation of this adjacency pattern will be taken up in the final chapter.

The final order coming out of the Figure 13 representation lies in the consideration of possible transition cases of Am stars. Earlier, a class of three "marginal" Am stars was defined on the basis of their normal Ca/Fe and Sc/Fe and near-normal C/Fe and Mg/Fe. With the exception of Sr/Fe (which exhibits only a weak super-enhancement in these three stars), the heavy elements in these stars show the characteristic Am enhancements, both in the absolute abundance of iron and in the N/Fe-ratios. We note further that the fourth "standard," HR 906, shows a pattern of anomalies in Figure 13 which suggests that it is a possible link between the normal stars and these "marginal" Am cases. This star shows intermediate C/Fe and Mg/Fe anomalies, normal Ca/Fe and Sc/Fe, enhanced iron, and slight enhancements relative to iron for the post-iron peak elements. The apparent patterns of weak Am anomalies in three stars taken

with the very weak anomalies in HR 906 suggest that the relative abundance representation yields additional order to the interpretation of Am stars.

This discussion may be summarized by stating that the consideration of all three criteria offered above points toward the relative abundance representation being the more appropriate and meaningful one. Therefore, it is inferred that the property of enhanced iron abundance and the anomalies exhibited by Am stars in Figure 13 typify the pattern of abundances of the Am star family. A generalized definition of "metallicism" could therefore be made in terms of this pattern.

The abundances of Conti's prototype "early type" Am star can be seen to coincide very well with the mean anomalies of the other Am stars. It is concluded that except for the deficient elements, which will be discussed later, there are no significant differences in the relative anomalies between the "hot" and "cooler" types of Am stars. Presumably the distinction between them lies in the ease at detecting their metallicism on low dispersion spectra.

The suggestion that different Am stars possess varying degrees of metallicism was advanced earlier. To pursue this idea, we felt it would be desirable to determine whether one might be able to synthesize an "index of metallicism" in order to compare different "Am" stars quantitatively. We started with the deduction that the

absolute enhancement of a "standard" element (iron) must be significant; it is actually this enhancement which provides the photometric "metallicity" discriminant for Am stars. It was also noticed that those Am stars in Figure 11 with the largest iron enhancements for their temperatures also have the largest Sr/Fe values. Moreover, two Am stars with weak iron enhancements, and the three "marginal" Am stars show Sr/Fe values intermediate between those of "stronger" Am stars and those of the standard stars. Finally, it was noticed that those Am stars with the largest iron enhancements for their temperatures tend to have the largest C/Fe, Mg/Fe, Ca/Fe, and Sc/Fe deficiencies, a fact that is only partially due to the behavior of the iron component in these ratios. With no a priori justification other than the above observations, an "index of metallicism," f(Am), was formulated as follows:

$$f(Am) = [Fe] + [Sr/Fe] - 1/4\{[C/Fe] + [Mg/Fe] + [Ca/Fe]\,[Sc/Fe]\} \quad (5)$$

The anomalies were referred to the means of relative abundances of the standards. For [Fe] and [C /Fe], however, HR 906 was not considered a standard. In Table 6 the computed f(Am) indices are listed in descending order for the Am stars. HR 906 and the standards are included separately.

Table 6. Computed Values of the f(Am) Index

Star HR (HD)	f(Am)	Star HR	f(Am)
4750	2.16	1428	1.40
8410	2.15	1368	1.28
4685	2.13	5055	1.18
4751	2.04	4780	1.13
1376	1.90	7850	0.82
1672	1.88	1458	0.60+
2291	1.79		
1389	1.77	906	0.68
(108486)	1.66		
1519	1.58	114	-0.25
		2085	0.38
		4825	-0.40

The "+" symbol associated with the f(Am) value of HR 1458 is noted. Since this star shows apparent line dilution, following Figure 11 any absolute abundance parameter associated with it must be considered a lower limit.

In Figure 16 the f(Am) values for the 16 Am stars and for HR 906 are plotted against their apparent rotational velocities from Table 1. In those cases where two V sin i values are given, our personal determinations were adopted in order to ensure a greater degree of homogeneity. In this diagram one finds a dichotomy in the sense that the eight "pronounced" Am stars are sharp-lined, whereas all but one of the eight "weak" ones show measurable rotation. This dichotomy is strengthened upon consideration of the

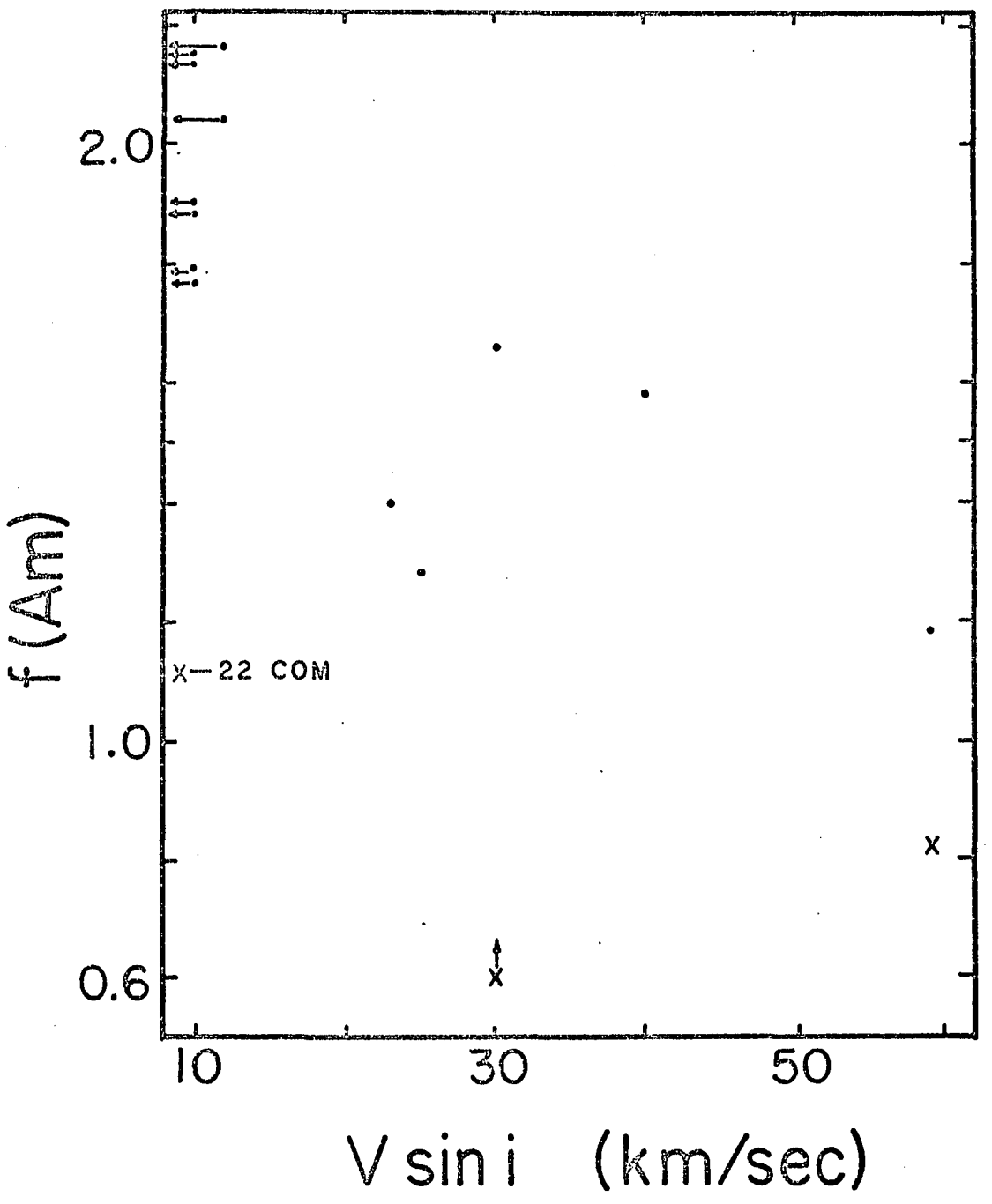

Figure 16. The f(Am), V sin i diagram

Same symbols as in Figure 12.

inclination factor in the abcissa. Were f(Am) plotted against the actual rotational velocity alone in Figure 16, one might expect the "weak" Am stars to occupy the envelope region in the lower right of the diagram. HR 1458 (= 22 Com), for example, is conceivably a pole-on rotator. In view of the present meager statistics, however, we are reluctant to press this interpretation too far.

The relation shown in Figure 16 is significant in two respects. First, it constitutes an a posteriori verification that f(Am) as constituted is a real measure of fundamental attributes of metallicism. Second, the apparent correlation with rotation strongly suggests that the latter serves to attenuate these attributes. A few ramifications of these conclusions follow.

If the f(Am) index is indeed physically meaningful, then the distribution of the values in Table 6 appears continuous. This suggests that "metallicism" is present to a variable degree, which in turn implies that the distinction of three of the Am stars as being "marginal" is artificial. Further, it suggests that it may be difficult to define a real division between "normal" and "metallic line" stars, even if accurate abundance data are available for them. HR 906 may be an example of a star difficult to categorize because of its "trace" Am anomalies. However, studies of more stars will be first required to determine

whether an actual transition exists between the two groups of stars.

The observation that mild rotation serves to reduce the apparent degree of metallicism is an extension of the conclusion in Chapter I that a low rotational velocity in an A star is a fundamental prerequisite for the onset of metallicism. Since mild rotation in a star would induce circulation currents, which would in turn mix material in the atmosphere and just below the surface, we suggest that metallicism exists in greatest degrees in those stars with the most stable surface layers.

Further evidence that metallicism may only be compatible with conditions of stability in surface zones of stars may be found from consideration of Henry's (1969) K-line photometry of metallic line stars. In Figure 17 his Δk index, a measure of [Ca], is plotted against the Stromgren Δc_1 index for those stars classified as Am by Cowley et al. (1969). A correlation exists in the sense that those presumably slightly evolved stars with large Δc_1 values also show nearly normal calcium abundances. A similar relation has been found previously by Abt (1966) between Δc_1 and a calcium defect indicator. It thus appears that as an Am star begins to evolve off the main sequence, its calcium abundance becomes normal. We interpret this effect as evidence that instabilities arising from the more fully developed convection zones in these slightly evolved stars

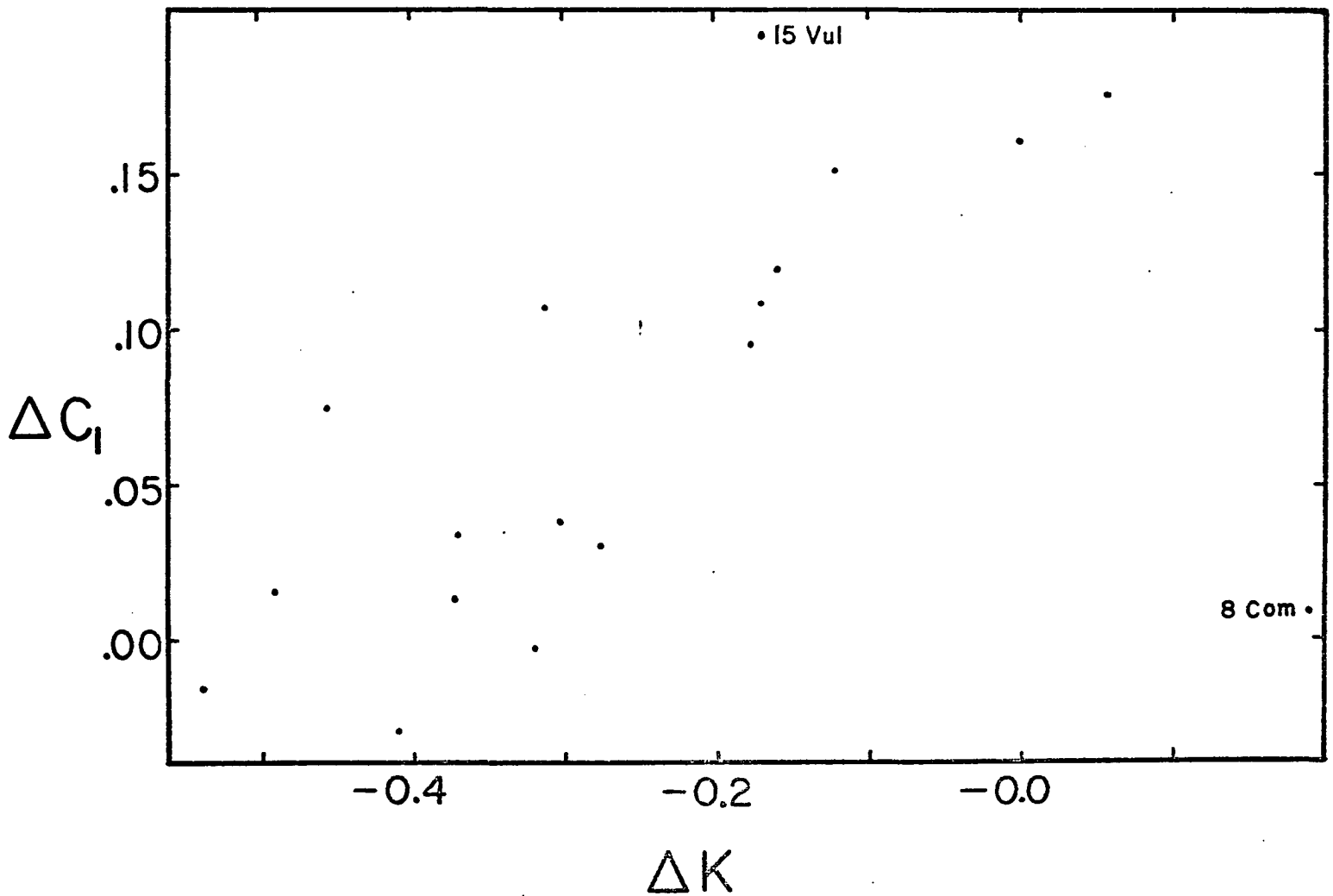

Figure 17. The Δc_1, Δk diagram for bright Am stars

serve to moderate at least some deficient anomalies. This evidence also appears in accord with the statement in Chapter I that convection has apparently "normalized" three A stars in binaries which one would expect otherwise to be Am according to Abt and Bidelman (1969).

It has been thus shown from two independent considerations that metallicism must be intimately related to conditions of quiescence or stability in the surface zones of A stars.

In the last section it was noted that the iron enhancement of the Am stars investigated is correlated with effective temperature. The question arises as to whether the anomalies relative to iron may similarly be correlated. It was found that no temperature dependence exists for the enhanced or super-enhanced elements. In contrast, dependences were found for the deficient elements such that their anomalies are less pronounced in the hotter stars. This trend is least evident for C/Fe and most evident for Ca/Fe and Mg/Fe. In Figure 18 a plot of effective temperature relative to Ca/Fe is shown. The trend depicted here confirms the suspicion expressed by Conti (1970) that hot Am stars do not show as extreme deficiency anomalies as cool ones. These results imply in turn that large amounts of the scatter in the deficiency anomalies may be ascribed to their dependence on effective temperature. They also imply that the effect of effective temperature on increasing

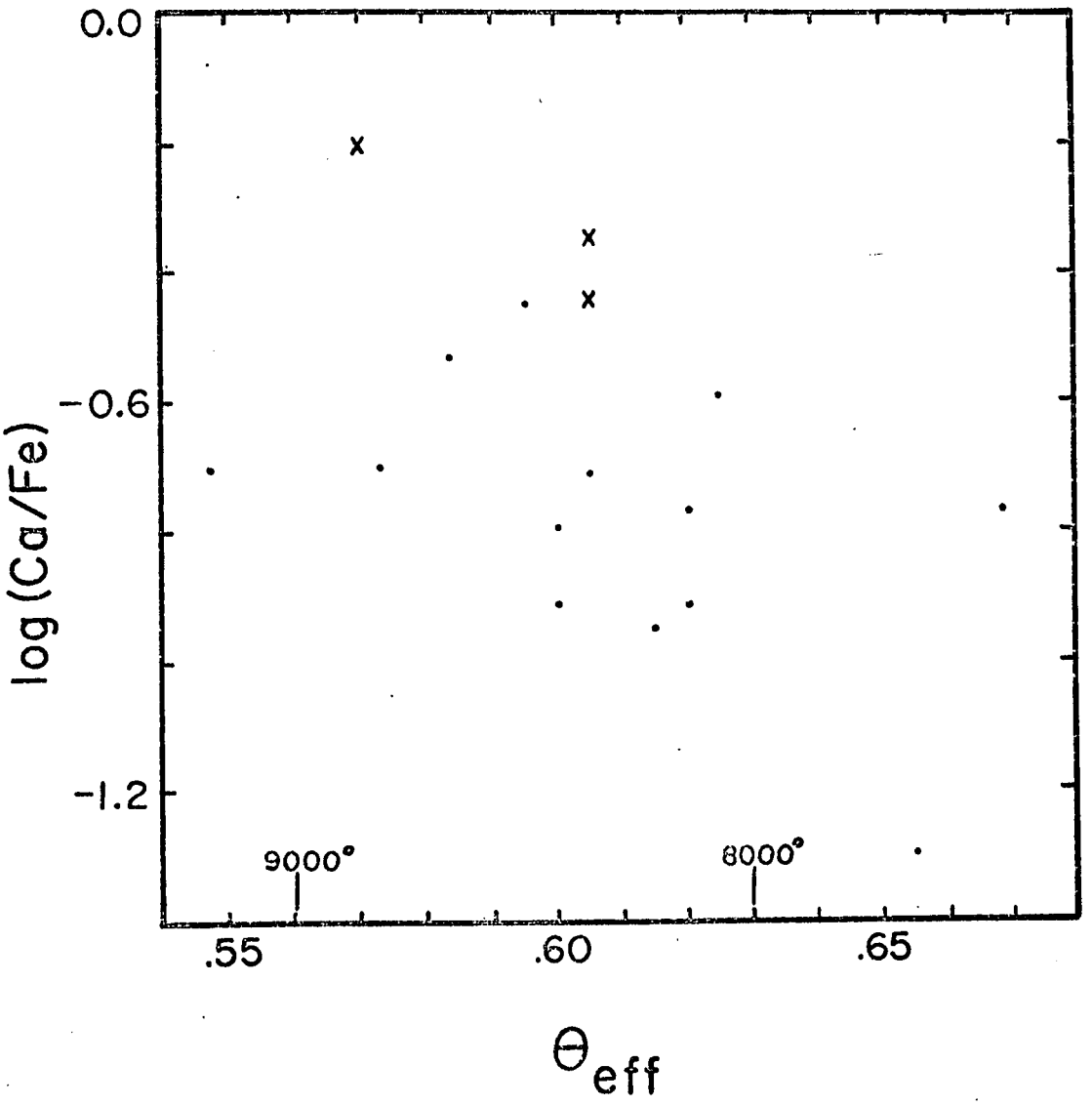

Figure 18. The log(Ca/Fe), θ_{eff} diagram

Same symbols as in Figure 12.

[Fe] is compensated by its moderating influence on the deficiency anomalies, so that f(Am) as defined in equation (5) is insensitive to T_{eff}.

Further insight into the behavior of the calcium anomaly may be seen in Figure 19, where the (absolute) calcium abundance is plotted relative to that of iron. In this diagram the eight "strong," sharp-lined Am stars from Figure 16 are represented as dots, while the "weak," moderately rotating Am stars, including 22 Com, are represented as circles. The effective temperatures assumed in this study are also exhibited. While this diagram is redundant in that it represents information already given in Figures 11, 16, and 18, it offers other informative aspects more clearly. First (as in Figure 16), a dependence of the calcium and iron abundances on rotation is evident. While the present data do not allow an interpretation as to the precise relative effect of rotation on these quantities, it is clear that the abundances of each are moderated. Second, with two exceptions there is a monotonic relation between the abundances of both elements and temperature in the sense that they both increase with the latter. Thus it appears that the observed calcium anomaly is a function of both rotational velocity and temperature. Moreover, the great bulk of scatter in this anomaly, and presumably of the other deficient elements, can evidently be eliminated when these observed physical parameters are allowed for.

Figure 19. The log(Ca), log(Fe) diagram

Dots represent sharp-lined ("strong") Am stars; circles, moderately rotating ("weak") Am stars, including 22 Com. Numbers refer to assigned effective temperatures in degrees Kelvin.

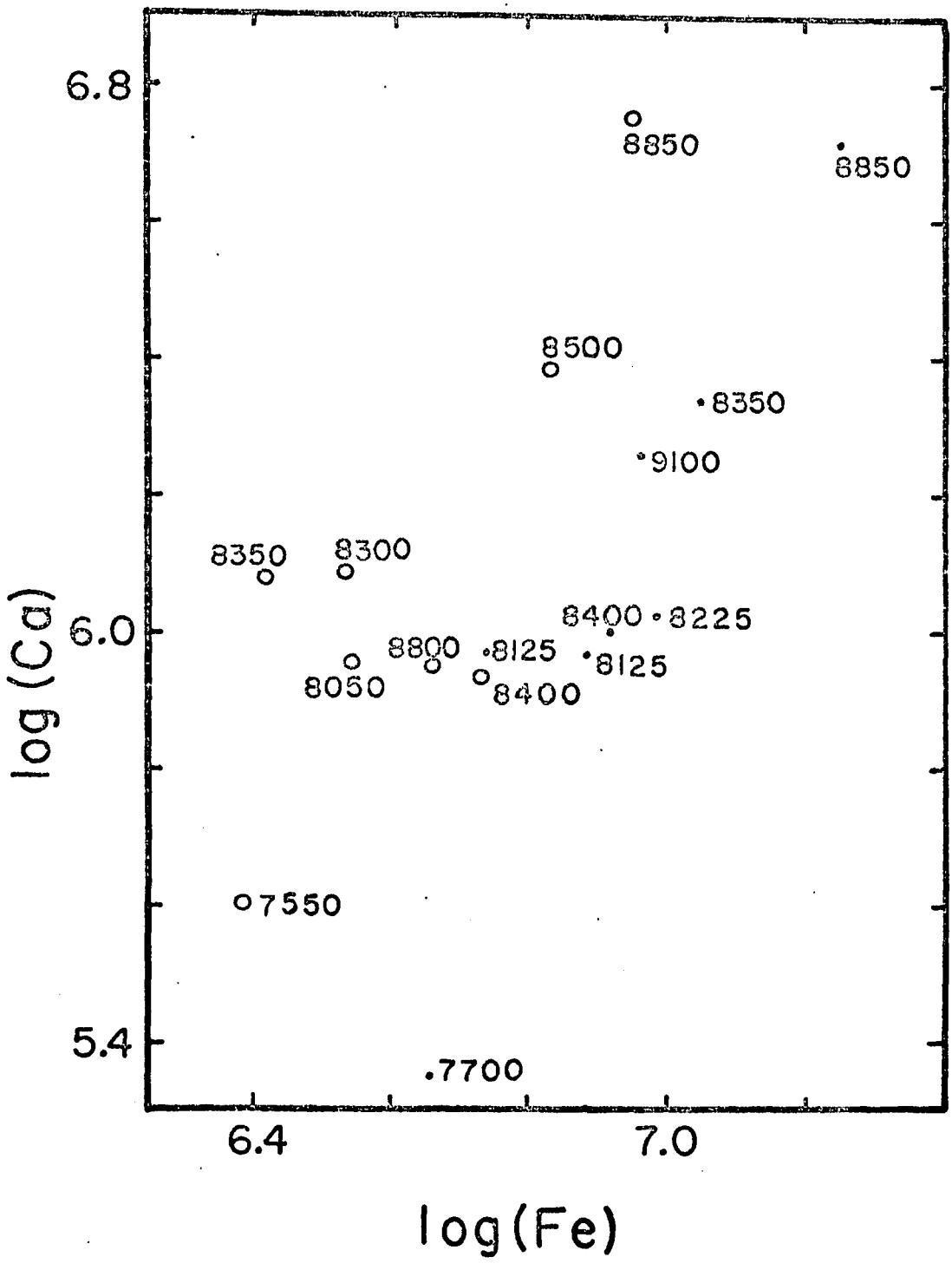

Figure 19. The log(Ca), log(Fe) diagram

We have pointed out that the effects of temperature, rotation, and possibly convection appear to be responsible for much of the observed scatter in the anomaly diagrams through their opposite effects on deficient and enhanced element anomalies. It is difficult to see how the behavior of the individual anomalies could be explained in terms of a few independent subprocesses since the same physical parameters appear to influence most all the abundances to variable degrees. Alternatively, the suggestion is that either some anomalies suffer different sensitivities to disruption before others or that they arise in different localities of the star.

We now proceed by drawing brief attention to possible abundance correlations not mentioned in the above discussion of the more general Am abundance properties.

First, we mention that no other anomaly was found to correlate with the f(Am) index. We conclude that we are unable to improve significantly on its definition (equation [5]) from the present data.

It was previously remarked that the Zr/Fe ratios among Am stars show substantially larger scatter than that of the standard stars in Figure 13. Although some "strong" Am stars, such as 8 Com, 32 Aqr, and RR Lyn, exhibit large Zr/Fe values, other "strong" cases have small values; such stars as 63 Tau and HR 4751, for example, actually show nearly normal absolute zirconium abundances. In Figure 20

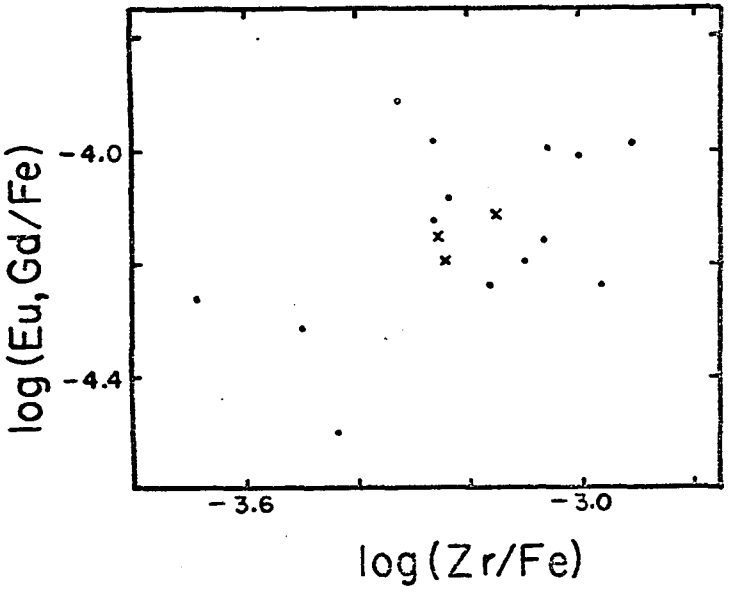

Figure 20. The log(Eu, Gd/Fe), log(Zr/Fe) diagram

Same symbols as in Figure 12.

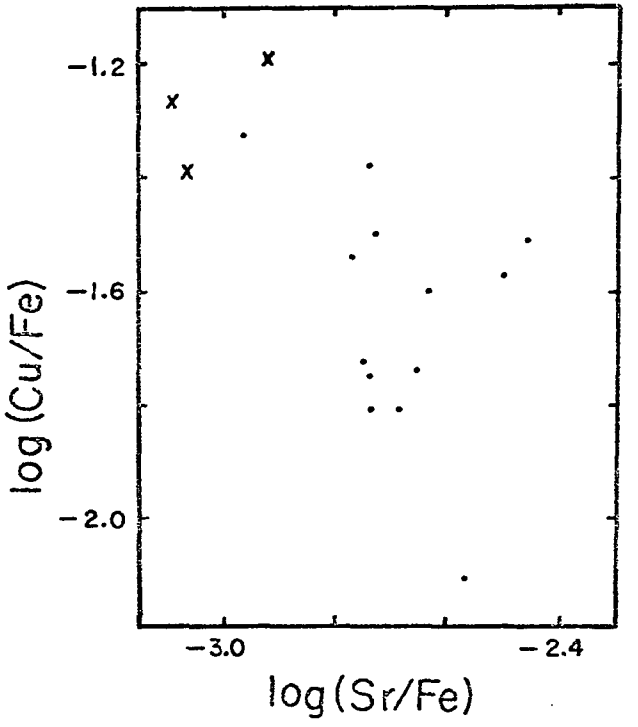

Figure 21. The log(Cu/Fe), log(Sr/Fe) diagram

Same symbols as in Figure 12.

evidence is presented that the Zr/Fe ratio may in fact be correlated with the ratio of the mean rare earth anomalies ([Eu, Gd]/Fe), which also appear to exhibit small variations.

The significance of the marginal correlation of this diagram is unclear at this writing, and any interpretation would be premature. However, in another context an important conclusion may be drawn from the zirconium results: The apparent random behavior of Zr/Fe, the more orderly behavior of Sr/Fe, and the lack of scatter in Y/Fe among the Am stars, all indicate together that the abundances of the "magic number" elements of the Sr, Y, Zr peak do not correlate well in detail. This is a strong argument against the interpretation of their enhancements by s-processing nucleosynthesis.

In Figure 21 what might be an anti-correlation between Cu/Fe and Sr/Fe is shown. Such a result would be surprising since copper is an enhanced element, and one would not expect to find the Cu/Fe ratio highest in "weak" Am stars. Although the copper lines measured are weak and difficult to measure at higher temperatures, it is found that our Cu/Fe values are not related to effective temperature. The apparent effect is therefore probably not an observational error. Nevertheless, we consider the apparent anti-correlation in this diagram highly uncertain and suggest that it be investigated further in future studies.

Jaschek and Jaschek (1960) have examined a large number of Am stars at intermediate dispersion to investigate the possibility of subfamilies occurring among Am stars and abundance correlations. They found no evidence for subgroupings. Their data suggested, however, that an inverse correlation exists between calcium and manganese and between manganese and silicon as well as a positive correlation between strontium and yttrium and between strontium and silicon. From our data we find little evidence for the inverse correlations between manganese and calcium or silicon. However, the (absolute) abundance of strontium does correlate with those of yttrium and silicon. In our study we have chosen to interpret this as a common rise, by different amounts, of these elements with the iron peak elements. Our failure to confirm the first two correlations is not understood. The Jascheks noted, however, that their relations are not transitive. We therefore suspect that their apparent correlations are not statistically significant.

From a comparison of abundance anomalies, we find no evidence for "subgroups" of Am stars. Other than those used to formulate the f(Am) index, and a few others already discussed, most anomalies show very little variation from star to star. If indeed f(Am) is a meaningful measure of metallicism, then our evidence indicates that Am stars in any one cluster <u>do not</u> differ systematically from those in

others, despite the small apparent differences in primordial composition between the clusters. Examination of Figure 10 shows that the mean enhancement of iron in the Hyades Am stars is actually lower than that of the Coma Am stars. This is true evidently because the sample of Am stars examined happens to be cooler in the mean for the Hyades stars, and therefore the heavier elements are less enhanced. Small apparent differences in the deficient element anomalies between the Coma and Hyades Am stars we similarly interpret in terms of their dependences on effective temperature. Since Am stars in each cluster show a wide range in f(Am) values, or simply in their iron enhancements or deficiency anomalies, it appears that metallicism occurs in variable degrees among A stars of different clusters. These degrees are evidently primarily determined by local physical conditions on the stars themselves.

Summary

In this section we state briefly the major conclusions drawn from this chapter:

1. The spectroscopic gravities found for all Am stars investigated are dwarf-like (log g = 4.0), confirming the results of recent investigations.
2. The microturbulence shows a maximum in the temperature region coinciding with the intersection of the instability strip with the main sequence. It

appears that high microturbulence is a universal attribute of both Am and normal late A stars alike.

3. The microturbulence of A stars along the main sequence is apparently a unique function of effective temperature. From this observation a negative result is predicted for a test of the Conti-Deutsch effect with the m_1 index.
4. The absolute abundance of iron (and the iron peak elements) in Am stars is enhanced by a variable factor of up to five or more.
5. The iron enhancement of those Am stars examined shows a weak positive correlation with their effective temperatures and a negative correlation with apparent rotational velocity.
6. Examination of the abundances of Am stars shows that in addition to calcium, scandium, and magnesium, carbon is deficient by a small factor in Am stars.
7. From several considerations it was concluded that it is most appropriate to interpret the abundance data of Am stars in terms of their anomalies relative to iron. According to this representation, most all the enhanced elements exhibit very uniform anomalies from star to star. The deficient elements show considerably larger scatter in their anomalies (see point #11).

8. No evidence has been found to support the hypothesis that the abundance anomalies in Am stars are produced by well-understood nucleosynthetic processes. Conclusion #7 furnishes indirect evidence that a process involving many or all the elements, such as diffusion, is operative in Am stars.

9. An index of metallicism, f(Am), was formulated to measure a postulated "degree of metallicism." We used the criteria of enhanced iron abundance, the strontium anomaly, and the deficiency anomaly, such criteria as suggested by several early investigators of Am stars. The correlation of f(Am) with apparent rotational velocity is significant in that it implies f(Am) measures physically important attributes of metallicism, and also in that the highest degree of metallicism occurs in those stars with the most stable surface zones. This conclusion is confirmed by the tendency of slightly evolved Am stars with large convection zones to show normal abundances of the deficient element calcium.

10. It is not altogether clear whether it may always be possible to determine whether a star is normal or a "marginal" Am star. An example of an intermediate type of star may be HR 906. More studies are needed, however, to determine whether in fact a real transition occurs between these two groups of stars.

11. The effects of effective temperature, rotation, and presumably convection are responsible for most of the apparent scatter in the deficient element anomalies through their opposite effects on the abundances of both deficient elements and iron. These considerations coupled with the fact that these moderating effects do not cause significant variations in heavy element anomalies implies that the various anomalies either have different sensitivities to disruption by local physical conditions or that they do not originate in a common locality.

12. There appears to be no justification for a subgrouping of Am stars of different temperature ranges. The apparent differences between "hot" and "classical" Am stars noted by Conti can be explained in terms of a correlation of the deficient anomalies with effective temperature and in terms of extended convection zones in those normal A stars observed in close binaries.

13. There is no evidence for subgroups among the Am stars or that abundances in Am stars of various clusters differ systematically from one another. The "degree of metallicism" which an Am star may have appears to be an attribute related more to

conditions of outer layer stability than to primordial composition.

CHAPTER V

INTERPRETATIONS OF THE METALLICISM PHENOMENON

Is Nucleosynthesis Responsible for Metallicism?

In Chapter IV it was pointed out that the general pattern of enhanced abundances in Am stars, as well as the detailed behavior of the Sr, Y, Zr "magic number" elements in them, do not seem compatible with the operation of nucleosyntehtic processes. It is nevertheless instructive to ask whether another class of stars with abundances reminiscent of those of Am stars might exist which can be understood in terms of such processes.

In this connection it has been suggested by a few investigators (e.g., by Chromey et al. 1969) that barium ("Ba II") stars may be the antecedents of Am stars despite the lack of evidence that the incidence of duplicity in the former group is high (Warner 1965, see his Table 1).

Ba II stars occur in the late G to middle K giant region of the H-R diagram. They are identified principally by their strong Ba II line at λ4554, their strong Sr II lines, and their strong CH band. In classic papers on the subject, Burbidge and Burbidge (1957) and Warner (1965) have advanced the now widespread view that the apparent over-abundances responsible for the strengths of these spectral features are due to s-process nucleosynthesis. According to

this picture, these stars have recently terminated the helium-burning evolutionary phase and have just entered carbon-burning. Protons from the envelope region have mixed with C^{12} in the core during thermal relaxation cycles (Sanders 1967) to form C^{13}. Neutrons are released on a slow timescale through the subsequent reaction $C^{13}(p,n)O^{16}$. These neutrons bombard principally iron-peak nuclei to form the intermediate-heavy s-process products (Fowler et al. 1965).

A detailed comparison of the typical anomalies present in Ba II stars and Am stars shows that although a few similarities exist, several differences also exist which should not go unmentioned. First, carbon is enhanced in Ba II stars, apparently as a result of the recent helium burning to carbon (Warner 1965), whereas this element has been shown to be deficient in Am stars. Moreover, with the exception of lithium (which appears to exhibit normal or deficient abundances in Am stars [Praderie 1968, Wallerstein and Conti 1969]) and Na, no light elements are enhanced in Ba II stars. In the preceding chapter it was found that several light elements are enhanced in Am stars. The remaining peculiar attribute of Ba II stars is the enhancement pattern of all s-processed elements, perhaps including scandium. Am stars, in contrast, show enhancements for all those s-processed (except scandium) and r-processed elements which have been examined. Finally, it should be noted that

the abundances of the iron peak elements appear normal in Ba II stars whereas it has been shown that the corresponding abundances are enhanced in Am stars.

From the foregoing comparison it can be seen that Ba II star peculiarities may be explained in terms of a few well understood nucleosynthetic processes. On the other hand, the abundances of several α, e, s, and r processed elements in Am stars are enhanced. It is difficult to imagine that all of these processes should occur together in them since the slightly different interior conditions likely to occur among the different Am stars would be expected to yield widely disparate abundances. Further, the enhancement of heavy elements by s- or r-processing would in fact entail an (unobservable) 1% depletion of the iron peak seed nuclei, which contradicts the observation that the iron peak nuclei are present in surplus in the atmospheres of Am stars. In any case the e-processing necessary to explain these enhancements would be difficult to justify in these stars in view of the extreme conditions ($T = 4 \times 10^{9}{}^{o}K$, $\rho = 10^{6}$ gm/cm^{3} [Arnett et al. 1968]) for which this process is thought to be operative.

There are further problems which arise from an explanation of metallicism in terms of nucleosynthesis. In Figure 12 it was shown that the absolute abundance of carbon is deficient by a factor of two. Since carbon is so cosmically abundant, it could more than provide the heavy

particles needed to build heavy element enhancements. In fact the question arises that if carbon is so depleted by transmutation to other elements then where do these atoms go? Other elements into which carbon might be expected to be transformed are those of comparable cosmic abundances such as nitrogen, oxygen, or neon (unobservable). The data on the "CNO" element abundances are presently very limited, however the available evidence (Strom et al. 1968, Praderie 1968) does not point toward heavy particle conservation among the CNO elements. Under nucleosynthesis one would expect such particle conservation.

In order to understand best the objections to nucleosynthesis in relation to metallicism, however, it is perhaps most advisable to examine the basis for which the nucleosynthesis explanation was advanced. The initial proposal was made by van't Veer-Menneret (1963) on the grounds of the "striking analogy" of the abundance anomalies of the Am star 63 Tau and the Ap star α^2CVn.

As with the Ba II stars, there are important detailed differences between the abundances of Am stars and α^2CVn or other Ap stars. It was mentioned that the iron peak elements Cr, Mn, and Fe are all enhanced by the same amounts in the case of Am stars. This trait is not held by Ap stars especially of the Mn or Cr variety. In addition, Fe in Ap stars is often normal (Sargent 1964). Further, the abundances of Ca and Sc are not correlated in Ap stars, and

Sc is usually found to be normal (Sargent 1964). Ba tends to be normal in Ap stars, including α^2CVn (van't Veer-Menneret 1963), but is always enhanced in Am stars. Finally, among the Sr, Y, Zr "magic number" elements, Zr is most enhanced in α^2CVn, which is not true among the Am stars.

The suggestion that Am anomalies arise from nucleosynthetic processes was popular at a time (see Chapter I) when Am stars, or their companions, were thought to be in a late stage of evolution. The discovery of Am stars in very young clusters has, however, removed the basis for this argument. Similarly, the apparent lack of magnetic fields of appreciable strength (Conti 1969a) casts doubts on the plausibility of the operation of surface nuclear reactions.

Because of the negative aspects of comparisons of Am star abundances with those of stars which are likely to have undergone nucleosynthesis, the unevolved stage of evolution in which metallicism seems to occur, and the lack of detailed correspondence of the observed Am anomalies with expectation, it is concluded that it is very doubtful that metallicism may be interpreted in terms of well-understood nucleosynthetic processes.

We note parenthetically that it has been suggested that the abundances found in Am stars are the result of the chemical separation of some elements from a stellar protocloud and the selective transfer of these elements on to the

surfaces of A stars, where they would not be efficiently mixed with the envelope material of slowly rotating stars. It is difficult, however, to understand how different abundances could result on the surfaces of two components in a binary system, as is observed (see Chapter I). In addition, the predicted sequence of element condensation from the protostar environment (Larimer and Anders 1970) is not in accord with observed Am anomalies. It is concluded that a chemical separation mechanism, also, is an unlikely origin of metallicism.

Boundary Conditions on a Metallicism Mechanism

As it has been concluded that metallicism may not be interpreted within a context of nucleosynthesis or chemical separation, the explanation must be found elsewhere. We proceed by discussing two boundary conditions which any proposed mechanism must satisfy besides the general run of abundance anomalies themselves.

First, it is to be noted that young Am stars often exhibit spectral peculiarities as pronounced as those of older ones. Glaspey (in prep.) has found m_1 indices for two Am stars in the (young) Scorpio-Centaurus association to be 0.25 and 0.27. These are among the largest m_1 values found for any Am stars in the Stromgren-Perry Catalogue. The implied high degree of metallicism of such stars argues strongly that metallicism does not entail a time-dependent

process building up with time but that it is a steady state phenomenon.

Second, from the discussion in Chapters I and IV of the kinds of stars that do develop Am properties, one may conclude that the Am mechanism requires surface zone stability. The mechanism can apparently withstand dynamic atmospheric effects but cannot withstand massive stellar perturbations such as pulsation, deep convection zones, or high rotation. This statement deserves expansion since it carries the important implication that the atmosphere itself cannot be the seat of the Am peculiarities. Accordingly, we list the following reasons as justification for the statement that the atmospheres of Am stars are often not quiescent:

1. The fact that microturbulence is observed to be a function of temperature over a small temperature range together with the coincidence of the ξ_T-rise with the instability strip in the H-R diagram implies strongly that at least a large component of the observed ξ_T arises from real physical motions in the atmospheres of these stars. Such motions would be expected to keep the atmosphere well mixed.
2. The proximity of the convection zone to the photosphere and the probable existence of some convective overshooting would also cause atmospheric mixing.

3. Meridional circulation currents are presently thought (see e.g., Smith 1966) to increase toward the surface as $1/\rho$ and to approach the sonic velocity in the upper layers.
4. Abt (1961) has observed gaseous streaming between components of spectroscopic binary systems containing Am stars.
5. Investigation of the β Ari system shows that it contains a weak or "marginal" Am star. This system has a high eccentricity of 0.89 (Batten 1967b) and a small periastron distance of four stellar radii. Such a close passage by the secondary would set up substantial surface tides and local convective currents.

From this evidence we accept the working hypothesis that any mechanism requiring atmospheric stability, such as the element separation process proposed recently by Michaud (1970) for Ap stars, is not directly applicable to the atmospheres of Am stars. It is emphasized, however, that since Ap stars have very low rotational velocities and microturbulent velocities, and have less developed surface convection zones generally, none of these objections may in fact be appropriate to the Ap case.

A Proposed Mechanism: A Subsurface Element-Separation Zone

In this section we propose that the observed abundance anomalies in Am stars may arise from a highly quiescent region located under the surface convection zone. According to this picture, atoms of certain elements would diffuse upward through the quiescent zone and be swept up to the surface when they enter the convection zone. Here they would be observed as "enhanced element anomalies." The depletion of other elements would occur from the sinking of atoms in this zone and the resulting diffusion force or drag acting on those atoms in the convection zone material. Since the stability of the postulated "quiescent zone" is critical to element separation, it follows that the mechanism would be destroyed in those stars where turbulence-induced mixing penetrated this zone.

We list several reasons which lead us to the above picture:

1. A subsurface mechanism is strongly implied by the second boundary condition on metallicism discussed above. If the inferred stability conditions are correct, then metallicism results from an envelope rather than a surface phenomenon.
2. The interpretation that metallicism is present to degrees similarly implies a depth or volume dependent effect. This picture implies that stars of the same

effective temperature and having the most stable surface zones should exhibit maximum and similar Am anomalies, as is observed.

3. The Am domain appears to end abruptly at the low temperature boundary (T_{eff} = 7200°K). This boundary can be interpreted as being due to the penetration of the surface (H I and He I ionization) convection zones of F2 and later stars into the otherwise quiescent, element-separating regions beneath them. The penetration by these turbulent zones would destroy the latter through mixing.
4. In Chapter IV it was inferred that rapid rotation or extended convection zones in Am stars have the effect of moderating the degree to which anomalies are present. These observations, too, are consistent with the idea of turbulent zones penetrating and disrupting a quiescent region below them. The different temperature dependences of the anomalies argues strongly that the turbulent surface zones are not serving merely to dilute contaminated surface abundances, as suggested by Stromgren (1963).

There are several effects that can limit the position of the postulated quiescent zone. The effect of rotation mentioned above is to induce meridional circulation currents in the stellar envelope. The velocity of these

currents increases as $1/\rho$ toward the surface. Therefore rotation would act to push the point at which laminar flow becomes turbulent deeper into the envelope. Consequently, less volume remains available for element separation, and the anomalies observed at the surface would be expected to decrease, as indeed was found in Chapter IV. The general effect of convection zone growth would be similar. We also note that the meridional circulation velocity goes as $V^4_{rotation}$ (Smith 1966) so that the high sensitivity of some Am anomalies (e.g., as found in Figures 16 and 19) would be readily understood.

A complete hydrodynamical treatment of these effects would be useful in determining whether and where such a quiescent zone may occur. However, in the following we point out where the postulated zone is most likely to exist.

It is probable that in most non-tidally disrupted Am stars a <u>combination</u> of convection and rotation cause a moderation of the anomalies. This can be seen by examining those Am stars for which the rotational velocities and the Δc_1 indices are presently known. It is found that no Am stars exist with both large V sin i ($\gtrsim$ 70 km/sec) values and large Δc_1 indices, although some do exist with large values of either parameter. Therefore it would be easier to investigate these effects separately by examining those stars with the most extensive convection zones but with little apparent rotation (e.g., 15 Vul) and those with the

least developed convection zones but with high rotation (e.g., HR 1403, HD 110500). The available evidence (see Figures 2 and 17) indicates that metallicism is destroyed in A stars which have rotational velocities of about 125 km/sec, and little convection, and in those having Δc_1 values of 0.15 to 0.20 ($\Delta \log g = 0.6$ to 0.8), and little rotation.

On the theoretical side, the calculation of the turbulence inducing zones from these phenomena will provide an upper limit to the placement of the quiescent zone in the envelope. A lower limit may be set by requiring that the mechanism be fully operative in the observed timescale of $\sim 10^7$ years. This timescale corresponds to the ages of the youngest known Am stars (Conti and van den Heuvel 1970). Since the drift velocity of a diffusing particle is inversely proportional to the product of the density and the square root of the temperature (Loeb 1934), the placing of the zone too deep in the star will result in a drift velocity which is too slow to guarantee element separation in the requisite time.

What do model calculations of outer stellar envelopes actually show? In this connection it is interesting to note that stars in the effective temperature range of 7500°K to 10,000°K exhibit a pair of convection zones; the upper is due to H I and He I ionization while the lower is due to He II ionization (Cox and Giuli 1968). These

zones do not intersect. For stars cooler than 7500°K both zones eventually become so extensive that they merge. It is to be underscored that the effective temperature range for which two separate convection zones occurs is almost exactly that in which Am stars are found.

Praderie (1967) has calculated model upper envelopes for a star having T_{eff} = 8000°K and log g = 3.9. In Figure 22 the thermodynamic parameters and depths of the convection zones which she derived are presented along with a schematic diagram of this envelope region. Attention is drawn to the radiative region occurring between the convective ones. Its width is about 13,000 km. If the mixing length is assumed to be one pressure scale height, then this distance corresponds to about 10 mixing lengths. It thus appears unlikely that convective overshooting could transfer material from one convective region to the other. Therefore most of the radiative zone is stable.

On the basis of the above paragraphs, it is suggested that the postulated quiescent element separation zone must lie in the radiative region between the two convective zones. It is supposed that it is the material in this region which rises or sinks due to selective forces on ions. If an average drift velocity of 3×10^{-5} cm/sec is assumed (see remarks below concerning Watson [1970]), then virtually all the material can be scoured out of the radiative zone in the relatively short timescale of 10^6

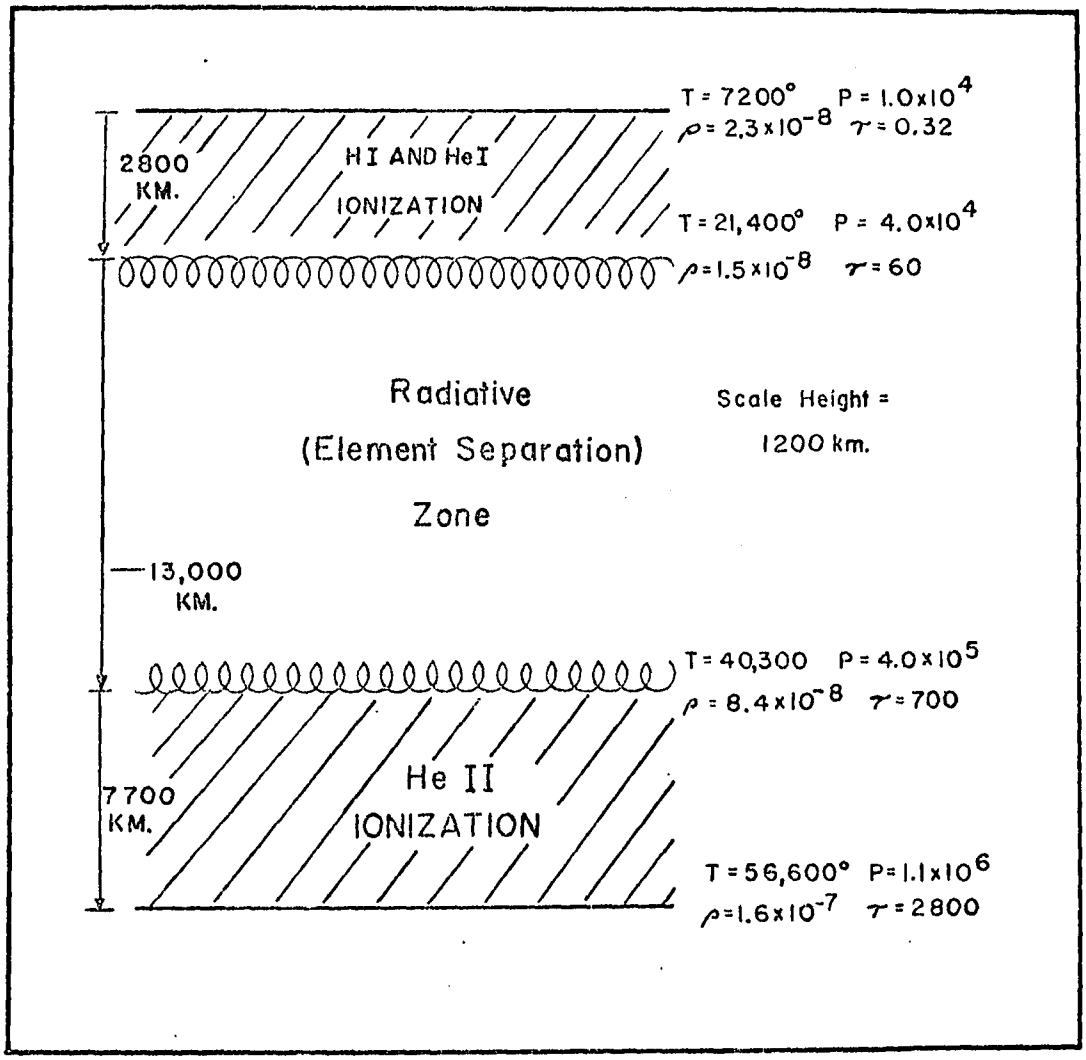

Figure 22. Praderie's envelope model of a T_{eff} = 8000°K, log g = 3.9 star

Shaded zones are (convective) zones of ionization. The appropriate parameters are in c.g.s. units.

years. This fact would explain why older Am stars do not have more extreme anomalies than younger ones (our first boundary condition on metallicism).

We further note that there are enough particles in this radiative region to provide absolute abundance enhancements of a factor of ten or more for metals in the upper convective region. On the other hand, the extreme overabundances of the rare earth elements (about a factor of 50, according to Figure 12) may not be sufficiently accounted for by the corresponding atoms in the radiative zone alone. Perhaps these atoms must first migrate up to the He II convection zone from a lower quiescent zone and must then also migrate up to the surface. Such a possibility may be justified in light of conclusion #11 of Chapter IV. We feel, however, that more extensive model calculations should be made to determine whether a real particle conservation problem actually arises here. Such model calculations would also indicate whether the number of particles in the radiative zone increases with effective temperature, in accord with our observations on the temperature dependences of the anomalies.

It is instructive to investigate the variation of depth of the H I-He I convection zone with gravity. Recent models calculated by de Loore (1970) for the temperature range of interest indicate that the depth of the upper convection zone increases by a factor of ten for a

corresponding decrease in gravity. If, following our estimates on the maximum decrease in gravity permitted for metallicism still to persist, we allow $\Delta \log g = 0.6$, then we find that the upper convective zone just merges with the lower one. It appears therefore that the data available on the dependence of convection zone depths with gravity explains very well the disappearance of metallicism that occurs to a star as it expands and evolves off the main sequence.

The foregoing discussion has referred to any diffusion mechanism capable of imparting drift velocities large enough to ions for them to diffuse efficiently through the ambient medium. To determine what this mechanism might be, one must examine the forces which are operative on ions at these depths in a quiescent medium.

First, the presence of gravitation would cause heavy elements to settle downward relative to the lighter ones. Second, as Aller and Chapman (1960) demonstrated, the temperature and pressure gradients present in a star set up an electrostatic field which causes primarily the heavy ions to diffuse downward. Thus this force reinforces the gravitational settling. Schatzman (1969) has recently shown that these effects alone can cause a very large depletion of the heavy elements in the upper envelope region of an FO star during its lifetime. That such underabundances of the heavier elements are not observed in these stars he

interpreted as evidence that turbulent mixing due to meridional circulation exists in these envelope regions. All these effects go in the wrong direction to explain the Am anomalies.

The question arises as to whether there are upward buoyant forces on the ions which can counterbalance the effect of the forces mentioned above. Such an upward force can arise from selective radiation pressure from the emergent flux. Michaud (1970) has recently shown that the buoyant force of selective radiation pressure is dominant for many ions in the (presumably quiescent) atmospheres of Ap stars. He found that the rising or sinking of different atoms due to all these forces may explain many or all of the peculiarities observed in Ap stars.

According to this mechanism, momentum is transferred from the radiation field to the appropriate ions through either photo-ionization or line absorption. The force due to radiation pressure on an ion is equal to 1/c times the integral taken over frequency of the product of the net flux and the total absorption coefficient. Therefore, the evaluation of this integral for each element necessitates accurate knowledge of where the element separation zone is, so that the correct ionization stages can be specified, and of oscillator strengths of the lines likely to contribute most to the buoyancy. Since accurate oscillator strengths of the more highly ionized atoms likely to occur at these

depths are largely unknown, considerably uncertainties remain in the calculation of these forces for the relevant ions.

If selective radiation pressure is responsible for the postulated upward diffusion of ions through an element separation zone, one may infer that the photo-ionization component contributes little to the total buoyancy of the atom. Since the ionization potentials of Fe and Ca, and of Ba and Sc, are so similar over several ionization stages, then if the photo-ionization effect were important, one would expect the abundances of elements in each pair to behave similarly; however they do not. We conclude that any buoyancy must arise from the line absorptions. Therefore those "heavy" elements that are cosmically rare should only need a few lines in order for them to float. Many light elements are cosmically abundant and would thus have to compete for line-frequency photons to absorb. It follows that only those cosmically abundant elements appearing in an ionization stage having many lines would float. The others would sink.

The element separation zone proposed herein may actually extend over two, three, or even four ionization stages of some elements. Adjacent elements in the periodic table mimic at a higher temperature the electronic configuration of their low-mass neighbors. Therefore, if the buoyancy effects are averaged over the entire zone, one

would expect similar anomalies to occur for adjacent elements in the periodic table. Such an effect was observed and referred to as an "adjacency pattern" in the previous chapter.

We also consider that any ions having a closed electronic configuration would have few lines, like those of the "noble gases," and would be expected to sink. This may be the explanation for the deficiencies observed in the cases of C, Mg, Ca, and Sc. To test this possibility, we have determined for light elements the ionization stages which occur in the postulated separation zone of Figure 22. These stages are exhibited in Table 7. Those stages in which the elements occur principally are underlined. The stages denoted by asterisks have closed electronic shell configurations. With the exception of C^1 (and perhaps Na^1) one may see that the deficient elements are indeed present mainly in the closed-shell stages, whereas the other light (and enhanced) elements are largely present in non-closed shell configurations. This explanation may also apply to the heavy element Ce, which typically shows a more moderate enhancement than its neighbors, according to Figure 13. Evidently these atoms have the necessary number of lines to

---

1. It is possible that these exceptions may be due to their high (for C) and low (for Na) cosmic abundances rel tive to those of the neighboring light elements.

Table 7. Light Element Ionization Stages Present in the Element Separation Zone

Deficient elements		Other light elements	
C	II, III, IV	Na	II*, III
Ca	III*, IV	Al	III, IV*
Sc	III, IV*	Si	III, IV, V*
Mg	III*	S	III, IV, V
		Ti	III, IV, V*

insure their buoyancy, in contrast to the situation of the deficient element atoms.

On the basis of similar considerations, Watson (1970) has independently advanced an explanation of metallicism in terms of a subsurface element separation zone. For a $T_{eff} = 8400^{o}K$ model, he calculated drift velocities for a number of elements at a point under the surface corresponding to $T = 34{,}000^{o}K$ and $\rho = 3 \times 10^{-8}$ gm/cm^3. This point coincides closely with the location of the zone we suggested above. Watson found drift velocities of the order of a few times 10^{-5} cm/sec for the light elements up to several times 10^{-4} cm/sec for the heavier ones. He also found a negative drift velocity "trough" for the Ca and Sc elements and large positive velocities for the heavier ones. While there are a few discrepancies between

his results and our Figure 13, we consider his results very promising. In addition to our inferences based on observations, Watson's is good theoretical evidence that metallicism is indeed caused by a subsurface element separation process.

It should also be pointed out that there still are difficulties with the proposed mechanism. From the present estimates of meridional circulation velocities, it may be difficult to understand how efficient separation can take place, even if these currents flow in a horizontal and laminar fashion under most of the surface of the star. This question may be resolved when the theory regarding meridional circulation becomes more refined.

In a related manner, it remains to be shown rigorously that the separation of the H I, He I and the He II convection zones by several mixing lengths is sufficient to insure quiescence on the order of 10^{-4} cm/sec in the intermediate, radiative zone.

The question also arises that if peculiarities in both Am and Ap stars may be explained in terms of a diffusion process, then how it is that these different groups of stars can co-exist in the same region of the H-R diagram. It may be that their element separations take place in different levels of the surface zones.

Desiderata

In the foregoing section we have suggested that a diffusion mechanism which is operative between the H I, He I and the He II convection zones is responsible for the metallicism phenomenon. Watson's work indicates in particular that selective radiation pressure at these depths is likely to be responsible for the postulated element separation. These ideas suggest several directions for future research.

On the theoretical side, a detailed grid of envelope models should be calculated as a function of effective temperature and surface gravity. Such models would allow both the calculation of element separation at a series of depths in a given envelope and also in envelopes of different effective temperatures and gravities. Studies of the effects of convective mixing, rotational disruption, circulation velocities, and ion migration in stellar envelopes are badly needed. Finally, oscillator strengths of many lines of highly ionized atoms are required. Since the buoyancy effect on atoms no longer increases sensitively when a line saturates, it is possible that the aggregate effect of weak lines will be the most important for an ion. The determination of oscillator strengths for weak lines in such ions would be best carried out using beam foil techniques.

Observationally, it would be most interesting to observe Am stars in the border region of the Am domain. One might examine the stars in the region around and beyond the cool temperature boundary to determine whether in fact vestigial Am anomalies still do persist. One might also attempt to pinpoint the effects of rotation and convection on the different anomalies. Finally, one might test our finding herein that extensive convection zones disrupt metallicism by searching for Am stars in extremely young clusters like I Orionis where the A stars are still in the pre-main sequence contraction phase. Such stars still have comparatively extensive convection zones and would therefore not be expected to show pronounced Am peculiarities.

APPENDIX A

MEASURED EQUIVALENT WIDTHS$_{\odot}$ FOR THE PROGRAM STARS (IN mÅ)

log gf coding:

CB	Corliss and Bozman 1962
CW	Corliss and Warner 1964
W	Warner 1967
LW a	Lambert and Warner 1968a
LW b	Lambert and Warner 1968b
LW c	Lambert and Warner 1968c
LW d	Lambert and Warner 1968d
MB	Miller and Bengston 1969
Pr	Praderie 1967
Sm	Smithsonian gf listing

Appendix A. Measured Equivalent Widths for the Program Stars (in mÅ)

	λ	χ(ev)	log gf	log gf source	HR 114	HR 906	HR 2085	HR 4825	HR 4685
C I									
	4771.72	7.46	-1.70	Sm	69	73	132	70	66
	4775.87	7.46	-2.20	Sm	--	--	47	--	17.0
	4932.00	7.65	-1.92	Sm	51	159	50	23	26
	5052.12	7.54	-1.49	Sm	143	49	152	110	97
	5380.24	7.65	-1.68	Sm	94	73	64	48	--
Na I									
	5682.63	2.09	-0.71	LW a	47	30	52	41	58
	5688.20	2.10	-0.40	LW a	51	33	67	61	76
	5895.92	0.00	-0.19	LW a	248	219	278	291	311
	6160.75	2.10	-1.27	LW a	--	13	32	17	40
Mg I									
	4702.90	4.33	-0.12	Sm	151	180	222	146	229
	5172.68	2.70	-0.40	Sm	294	360	445	350	415
	5183.60	2.70	-0.17	Sm	335	405	485	420	440
	5528.42	4.33	-0.48	Sm	139	149	152	169	170
Al I									
	3944.01	0.00	-0.62	LW a	170	191	240	186	257
	3961.52	0.01	-0.32	LW a	183	188	220	195	198
Si I									
	5645.67	4.91	-1.65	MB	--	16.0	--	16.0	29
	5665.60	4.90	-1.57	MB	--	--	--	--	16.0
	5690.47	4.90	-1.43	MB	16.0	17.2	28	--	--
	5708.43	4.93	-1.11	MB	24	20	53	39	45
	5772.25	5.06	-1.36	MB	--	16.0	--	15.2	31
	5793.12	4.91	-1.56	MB	--	15.5	--	--	15.0

	λ	χ(ev)	log gf	log gf source	HR 114	HR 906	HR 2085	HR 4825	HR 4685
Si I									
	5948.58	4.93	-0.89	MB	30	22	42	67	55
	6254.25	5.59	-0.62	Sm	27	--	48	56	31
Si II									
	4128.05	9.79	+0.22	Sm	--	--	84	--	223
	4130.88	9.80	+0.77	LW b	76	125	77	48	269
S I									
	4694.13	6.50	-1.39	LW a	18.3	15.5	22	7.9	30
	4695.45	6.50	-1.54	LW a	6.5	--	--	--	10.0
	4696.25	6.50	-1.76	LW a	6.0	8.0	--	--	8.0
	6046.04	7.83	-0.78	LW a	14.5	20	22	11.9	25
Ca I									
	4226.72	0.00	-0.55	CB	296	290	312	260	322
	4283.01	1.88	-0.39	LW d	103	96	110	66	122
	4435.69	1.88	-0.69	LW d	85	56	89	63	118
	4455.89	1.88	-0.72	LW d	70	65	94	65	95
	5588.76	2.51	+0.14	LW d	123	89	121	105	150
	5601.29	2.51	-0.54	LW d	54	41	82	63	49
	5857.45	2.92	+0.17	LW d	103	79	99	101	116
	6162.17	1.89	-0.39	LW d	130	121	150	154	105
Sc II									
	4246.83	0.31	+0.09	CB	212	205	198	115	224
	4294.77	0.60	-1.27	CB	43	24	41	22	26
	4314.08	0.62	-0.10	CB	223	196	193	130	241
	4320.74	0.60	-0.22	CB	230	220	188	154	240
	4325.01	0.59	-0.37	CB	139	124	148	111	139
	4374.45	0.62	-0.45	CB	142	190	182	103	125

	λ	χ(ev)	log gf	log gf source	HR 114	HR 906	HR 2085	HR 4825	HR 4685
Sc II									
	5239.82	1.46	-0.50	CB	65	68	65	62	50
	5526.81	1.77	0.03	CB	--	22	31	27	41
Ti I									
	3958.21	0.05	+0.01	CB	75	74	91	63	132
	4286.01	0.82	-0.12	CB	14.5	--	31	13.0	--
	4457.43	1.45	+0.53	CB	20	20.0	50	21	45
	4534.78	0.83	+0.43	CB	28	34	46	18.2	32
Ti II									
	3913.46	1.12	-0.24	W	265	234	283	206	--
	4028.33	1.89	-0.65	W	119	119	123	64	184
	4056.21	0.61	-2.46	W	26	23	24	20	61
	4290.22	1.16	-0.79	W	233	218	213	153	344
	4300.05	1.18	-0.46	W	230	200	228	145	346
	4301.93	1.16	-1.11	W	182	167	170	120	304
	4312.86	1.18	-1.06	W	166	141	145	94	252
	4316.81	2.05	-1.07	W	53	27	45	21	107
	4386.86	2.60	-0.46	W	63	64	70	28	145
	4394.06	1.22	-1.47	W	85	77	107	52	144
	4389.77	1.24	-1.06	W	147	144	144	85	200
	4411.08	3.09	-0.07	W	50	35	59	35	--
	4411.94	1.22	-2.11	W	18.0	14.0	30	16	56
	4417.72	1.16	-1.18	W	150	140	139	75	203
	4418.34	1.24	-1.67	W	67	58	66	39	115
	4421.95	2.06	-1.14	W	50	52	65	42	84
	4443.80	1.08	-0.74	W	193	199	185	107	--
	4450.49	1.08	-1.41	W	136	129	141	89	204
	4468.49	1.73	-0.65	W	190	208	182	117	264
	4488.32	3.12	+0.01	W	72	78	81	47	128

	λ	χ(ev)	log gf	log gf source	HR 114	HR 906	HR 2085	HR 4825	HR 4685
Ti II									
	4501.27	1.12	-0.79	W	185	211	178	113	244
	4533.97	1.24	-0.64	W	256	288	236	149	325
	4544.01	1.24	-2.08	W	26	14.0	31	14.9	55
	4563.76	1.22	-0.86	W	216	206	183	118	255
	4568.31	1.22	-1.93	W	--	10.0	15	--	10.0
	4571.97	1.57	-0.34	W	188	179	218	123	299
	4589.96	1.24	-1.61	W	101	100	103	54	177
	4779.99	2.04	-1.12	W	78	62	64	57	125
	4805.11	2.05	-0.74	W	84	100	68	90	179
	5129.14	1.89	-0.93	W	135	169	115	96	258
	5185.90	1.88	-1.51	W	101	107	99	55	146
	5336.81	1.58	-1.35	W	134	115	106	51	161
	5381.02	1.56	-2.12	W	115	80	64	59	121
	5418.80	1.57	-2.27	W	67	27	66	70	69
V II									
	4002.94	1.43	-1.28	W	30	32	57	22	117
	4005.71	1.82	-0.22	W	90	105	136	--	200
	4008.17	1.79	-1.61	W	8.5	8.5	26	17.4	66
	4023.39	1.80	-0.35	W	73	59	84	39	172
	4036.78	1.48	-1.42	W	21	15.6	44	18	73
	4039.57	1.82	-1.60	W	8.4	13.4	37	16.5	28
	4183.43	2.05	-0.77	W	30	26	45	--	128
Cr I									
	3919.16	1.03	-0.14	CB	92	72	135	67	136
	4254.35	0.00	-0.27	CB	185	136	168	110	273
	4274.80	0.00	-0.39	CB	159	135	145	96	195
	4511.90	3.07	+0.37	CB	--	6.0	--	9.6	57
	4616.13	0.98	-0.95	CB	30	24	55	28	41

	λ	χ(ev)	log gf	log gf source	HR 114	HR 906	HR 2085	HR 4825	HR 4685
Cr I									
	4626.19	0.96	-1.00	CB	15.0	17.0	56	25	40
	4646.17	1.03	-0.49	CB	46	--	71	52	70
	4652.16	1.00	-0.79	CB	19.0	--	47	33	42
	4664.20	3.11	+0.37	CB	7.0	10.6	46	8.7	35
	5345.81	1.00	-0.98	CB	64	55	63	60	101
	5348.32	1.00	-1.29	CB	36	14.0	43	45	56
Cr II									
	4252.62	3.86	-1.85	W	42	40	35	21	117
	4284.21	3.85	-1.64	W	50	49	51	23	139
	4555.02	4.07	-1.44	W	56	70	66	37	149
	4592.09	4.07	-1.37	W	84	77	82	31	139
	4616.64	4.07	-1.51	W	70	72	63	48	124
	4634.11	4.07	-1.19	W	83	99	89	50	143
	4848.24	3.85	-1.13	W	76	94	77	--	175
	4876.41	3.86	-1.94	W	127	118	66	47	171
	5308.44	4.05	-2.00	Pr	57	76	40	31	83
	5310.70	4.05	-2.39	Pr	40	38	22	13.0	51
	5313.59	4.06	-1.98	Pr	66	77	51	26	105
	5334.88	4.05	-1. 4	Pr	52	46	34	27	129
	5508.60	4.14	-1.87	Pr	14.4	20	27	36	55
Mn I									
	4030.77	0.00	-0.48	CB	231	191	281	234	258
	4033.07	0.00	-0.64	CB	185	155	241	164	211
	4034.49	0.00	-0.88	CB	118	86	157	94	129
	4035.73	2.11	+0.37	CB	119	92	163	108	192
	4048.76	2.13	+0.25	CB	92	90	138	75	174
	4083.62	2.13	+0.24	CB	38	42	104	68	83
	4502.22	2.91	+0.18	CB	--	8.7	--	14.0	18.0

	λ	χ(ev)	log gf	log gf source	HR 114	HR 906	HR 2085	HR 4825	HR 4685
Mn I									
	6016.64	3.16	0.00	CB	--	11.1	29	15.1	--
	6021.80	3.06	+0.16	CB	--	10.8	42	--	--
Fe I									
	3815.84	1.48	+0.60	CW	255	247	322	290	289
	3856.37	0.05	-1.13	CW	256	--	297	248	279
	3865.52	1.01	-0.56	CW	203	184	222	153	251
	3871.80	2.95	-0.15	CW	94	57	136	75	--
	3872.50	0.99	-0.54	CW	223	219	284	196	283
	3878.02	0.96	-0.50	CW	229	238	251	228	264
	3895.65	0.11	-1.47	CW	202	179	218	200	235
	3902.94	1.56	+0.12	CW	223	211	260	201	274
	3920.26	0.12	-1.49	CW	177	149	130	127	205
	3922.91	0.05	-1.41	CW	208	173	235	158	258
	3927.92	0.11	-1.29	CW	231	204	220	198	257
	3955.35	3.28	-0.41	CW	44	54	96	61	71
	3983.96	2.73	+0.06	CW	104	83	168	116	149
	3998.05	2.69	-0.04	CW	97	75	170	82	145
	4005.24	1.56	-0.07	CW	236	237	261	237	242
	4007.27	2.76	-0.45	CW	45	49	60	39	86
	4021.87	2.76	+0.12	CW	105	100	135	84	156
	4029.64	3.26	-0.42	CW	50	61	83	50	114
	4039.94	2.73	-1.54	CW	22	25	34	30	53
	4040.65	3.30	-0.30	CW	42	40	82	47	125
	4043.90	2.73	-0.56	CW	65	64	111	71	111
	4044.61	2.83	-0.17	CW	56	51	109	58	88
	4045.81	1.48	+0.68	CW	315	338	463	376	462
	4059.72	3.54	-0.52	CW	21	18.0	36	16	36
	4063.54	1.56	+0.43	CW	263	273	328	259	344
	4067.98	3.21	+0.29	CW	79	78	106	64	135

	λ	χ(ev)	log gf	log gf source	HR 114	HR 906	HR 2085	HR 4825	HR 4685
Fe I									
	4070.76	3.24	+0.01	CW	55	67	73	55	119
	4071.74	1.61	+0.40	CW	231	216	248	202	260
	4073.76	3.14	-0.14	CW	60	52	70	42	112
	4074.79	3.05	-0.14	CW	56	51	85	56	94
	4076.63	3.21	+0.24	CW	140	120	194	139	215
	4084.49	3.33	+0.13	CW	55	51	68	56	101
	4091.56	2.83	-1.28	CW	16.0	15.0	--	13.0	48
	4107.49	2.83	+0.06	CW	80	45	96	69	90
	4112.97	4.18	-0.02	CW	57	43	77	45	76
	4114.44	2.83	-0.47	CW	55	37	79	45	55
	4120.21	2.99	-0.43	CW	45	26	59	34	63
	4123.74	2.61	-1.13	CW	34	25	49	38	83
	4126.19	3.33	-0.35	CW	45	49	71	44	82
	4132.06	1.61	-0.16	CW	209	190	254	151	280
	4132.90	2.84	-0.02	CW	73	74	118	65	119
	4133.86	3.37	-0.48	CW	41	41	71	39	116
	4134.68	2.83	+0.18	CW	110	105	166	99	174
	4136.51	3.37	-0.82	CW	10.0	15.0	17.0	--	23
	4137.00	3.41	+0.12	CW	74	63	104	52	123
	4139.93	0.99	-2.86	CW	12.0	15.0	21	15.9	--
	4141.86	3.02	-1.04	CW	11.0	13.8	27	24	60
	4143.41	3.05	+0.61	CW	208	--	200	114	224
	4143.87	1.56	-0.07	CW	208	223	241	160	264
	4147.67	1.48	-1.47	CW	78	59	80	60	88
	4153.90	3.40	+0.33	CW	112	126	159	99	175
	4156.80	2.83	+0.13	CW	115	105	145	106	162
	4157.78	3.42	+0.17	CW	79	69	93	47	116
	4174.91	0.91	-2.34	CW	47	22	67	42	49
	4176.57	3.37	+0.04	CW	75	64	77	55	114
	4181.75	2.83	+0.46	CW	167	151	201	120	259

	λ	χ(ev)	log gf	log gf source	HR 114	HR 906	HR 2085	HR 4825	HR 4685
Fe I									
	4182.38	3.02	-0.37	CW	29	32	64	47	79
	4187.04	2.45	+0.17	CW	142	127	145	83	222
	4187.80	2.42	+0.13	CW	173	154	186	118	247
	4191.43	2.47	+0.06	CW	157	141	192	119	229
	4200.93	3.40	-0.22	CW	46	44	64	27	78
	4202.03	1.48	-0.25	CW	200	213	208	128	320
	4203.98	2.84	-0.21	CW	90	88	122	58	150
	4207.13	2.83	-0.69	CW	35	34	66	36	80
	4210.35	2.48	-0.19	CW	124	104	126	66	169
	4213.65	2.84	-0.55	CW	42	37	63	31	79
	4217.55	3.43	+0.12	CW	74	72	96	43	137
	4222.21	2.45	-0.35	CW	105	89	126	57	173
	4225.46	3.42	+0.13	CW	90	113	129	77	226
	4227.43	3.33	+0.90	CW	173	176	187	132	289
	4235.94	2.42	+0.31	CW	178	158	190	116	270
	4238.81	3.40	+0.47	CW	107	90	102	75	177
	4240.37	3.55	-0.59	CW	32	21	45	29	46
	4245.25	2.86	-0.44	CW	63	42	99	62	124
	4247.43	3.37	+0.45	CW	105	108	123	65	196
	4248.22	3.07	-0.53	CW	27	18.0	53	36	76
	4260.47	2.40	+0.63	CW	219	217	225	183	309
	4266.96	2.73	-0.87	CW	24	16.5	28	24	44
	4267.83	3.11	-0.34	CW	41	28	42	40	53
	4271.15	2.45	+0.25	CW	157	158	157	127	228
	4271.76	1.48	+0.20	CW	235	225	248	196	309
	4285.44	3.24	-0.42	CW	33	37	58	33	88
	4291.46	1.56	-1.99	CW	18.0	17.8	31	28	26
	4298.04	3.05	-0.56	CW	36	17.0	48	25	59
	4325.76	1.61	+0.36	CW	235	227	270	219	297
	4327.92	3.30	-0.90	CW	18.0	8.0	17.0	10.1	35

	λ	χ(ev)	log gf	log gf source	HR 114	HR 906	HR 2085	HR 4825	HR 4685
Fe I									
	4352.74	2.21	-0.56	CW	73	57	95	55	85
	4375.93	0.00	-2.59	CW	79	48	100	60	82
	4387.87	3.07	-0.62	CW	24	35	60	40	51
	4388.41	3.60	+0.02	CW	51	48	95	57	88
	4408.41	2.20	-0.95	CW	61	54	92	67	89
	4415.12	1.61	-0.13	CW	211	237	248	161	255
	4422.57	2.84	-0.22	CW	64	62	99	61	113
	4427.31	0.05	-2.51	CW	101	55	95	76	110
	4430.61	2.22	-1.02	CW	71	44	70	65	85
	4433.22	3.65	-0.14	CW	49	26	76	41	69
	4442.34	2.20	-0.50	CW	89	72	91	73	116
	4443.19	2.86	-0.22	CW	75	86	89	69	127
	4447.72	2.22	-0.58	CW	82	67	94	62	101
	4466.58	2.83	+0.18	CW	102	104	131	85	159
	4469.38	3.65	+0.19	CW	101	88	113	85	156
	4476.02	2.84	+0.14	CW	122	107	140	101	157
	4485.67	3.68	-0.40	CW	18.0	16.9	71	37	48
	4490.08	3.02	-0.74	CW	12.0	25	36	26	25
	4525.14	3.61	+0.03	CW	81	74	110	74	163
	4528.61	2.18	-0.20	CW	160	146	176	119	216
	4587.13	3.57	-0.91	CW	7.2	10.0	13.0	9.0	29
	4602.00	1.61	-2.50	CW	--	10.4	15.3	11.0	11.0
	4602.94	1.48	-1.46	CW	51	42	88	42	67
	4611.28	3.65	-0.13	CW	56	38	82	48	62
	4625.05	3.24	-0.63	CW	27	26	54	28	61
	4635.84	2.84	-1.46	CW	8	20	23	--	18.0
	4637.51	3.28	-0.60	CW	28	29	61	44	51
	4638.01	3.60	-0.35	CW	42	37	70	47	74
	4643.46	3.65	-0.59	CW	21	17.5	35	31	39
	4647.43	2.69	-0.47	CW	44	49	73	54	70

	λ	χ(ev)	log gf	log gf source	HR 114	HR 906	HR 2085	HR 4825	HR 4685
Fe I									
	4668.14	3.26	-0.30	CW	51	49	79	57	81
	4707.28	3.24	-0.23	CW	42	39	80	64	75
	4710.28	3.02	-0.74	CW	31	20	--	28	32
Fe II									
	4122.63	2.58	-2.73	LW c	115	96	140	72	181
	4128.73	2.58	-2.76	W	47	56	65	36	141
	4178.85	2.58	-2.00	W	172	188	157	83	299
	4233.16	2.58	-1.43	W	239	264	266	152	359
	4273.31	2.70	-2.27	W	87	71	70	33	208
	4296.56	2.70	-2.36	W	130	124	108	68	280
	4303.16	2.70	-2.00	W	163	161	120	79	275
	4351.76	2.70	-1.76	W	257	254	255	210	319
	4385.38	2.78	-2102	W	124	130	160	94	219
	4416.81	2.78	-2.09	W	126	141	125	65	187
	4472.92	2.84	-2.80	W	55	68	78	60	131
	4489.18	2.83	-2.23	W	100	120	120	76	185
	4491.40	2.85	-2.09	W	121	123	107	68	179
	4508.28	2.85	-1.76	W	148	161	141	84	219
	4515.33	2.84	-1.91	W	141	153	141	71	220
	4541.52	2.85	-2.29	W	94	99	81	45	165
	4555.89	2.83	-1.79	W	179	211	196	118	288
	4576.33	2.84	-2.22	W	95	96	87	49	153
	4582.83	2.84	-2.44	W	69	95	75	36	145
	4583.82	2.81	-1.25	W	207	252	203	127	312
	4620.51	2.83	-2.63	W	66	72	75	38	116
	4656.97	2.89	-2.53	W	86	60	85	61	164
	4666.75	2.83	-2.64	W	65	85	102	68	167
	4670.17	2.58	-2.87	W	73	76	95	56	99
	4923.92	2.88	-0.93	Sm	276	336	236	170	(406)

	λ	χ(ev)	log gf	log gf source	HR 114	HR 906	HR 2085	HR 4825	HR 4685
Fe II									
	5197.56	3.22	-1.77	Pr	145	(255)	171	114	277
	5264.80	3.22	-1.24	Pr	165	182	122	119	--
	5325.55	3.21	-2.59	Pr	103	86	52	32	157
	5414.08	3.21	-2.85	Pr	41	36	51	45	80
	5425.26	3.19	-2.67	Pr	53	67	52	48	94
	5534.86	3.23	-2.19	Sm	--	80	101	122	172
	6084.11	3.19	-2.79	Pr	11.0	31	--	--	38
	6149.23	3.87	-1.96	Pr	26	67	68	51	89
	6247.56	3.86	-1.55	Pr	77	90	99	93	144
Co I									
	4020.90	0.43	-1.58	CB	8.3	14.0	22	8.0	23
	4058.60	2.00	-0.67	CB	45	26	86	55	60
	4121.32	0.92	-0.03	CB	47	25	79	50	61
Ni I									
	3858.30	0.42	-0.62	CB	165	147	211	124	213
	4401.55	3.18	+0.83	CB	91	93	141	97	150
	4604.99	3.47	+0.77	CB	31	44	52	41	84
	4606.23	3.58	+0.30	CB	--	7.0	14.0	13.4	36
	4648.65	3.47	+0.78	CB	40	46	62	44	93
	4686.22	3.58	-0.39	CB	--	24	29	12.8	37
	4714.42	3.37	+0.84	CB	68	46	117	76	115
	4715.78	3.53	+0.26	CB	21.0	17.0	30	26	52
	4980.16	3.59	+0.56	CB	42	36	50	38	72
	5115.40	3.82	+0.32	CB	18.0	45	49	27	98
	5155.76	3.88	+0.54	CB	11.0	15.0	40	15.2	71

	λ	χ(ev)	log gf	log gf source	HR 114	HR 906	HR 2085	HR 4825	HR 4685
Ni II									
	4015.50	4.03	-1.25	W	45	65	71	45	152
	4067.05	4.03	-0.59	W	139	150	180	117	287
	4244.80	4.03	-2.03	W	7.0	--	--	--	48
	4362.10	4.03	-1.43	W	16.0	13.8	22	20	68
Cu I									
	5105.54	1.38	-1.70	CB	16.5	18.0	17.0	15.0	16.0
	5782.13	1.64	-1.56	CB	--	11.5	--	--	12.5
Zn I									
	4722.22	4.01	+0.69	CB	15.0	9.3	40	25	70
	4810.53	4.06	+0.86	CB	21	8.5	46	41	57
Sr II									
	4077.71	0.00	-0.78	CB	277	271	325	256	511
	4215.52	0.00	-0.99	CB	230	260	305	184	360
Y II									
	3950.35	0.10	-0.71	CB	75	79	(124)	46	167
	3982.59	0.13	-0.79	CB	76	57	85	52	151
	4177.54	0.41	-0.24	CB	199	190	205	130	322
	4309.62	0.18	-0.98	CB	114	92	134	99	239
	4358.73	0.10	-1.61	CB	37	22	54	46	75
	4374.94	0.41	-0.14	CB	176	176	173	122	259
	4398.02	0.13	-1.25	CB	52	45	65	28	115
Zr II									
	4149.22	0.80	-0.13	CB	142	121	155	99	246
	4150.97	0.80	-1.02	CB	25	19.0	24	11.0	75
	4156.24	0.71	-0.85	CB	78	70	121	--	181

	λ	χ(ev)	log gf	log gf source	HR 114	HR 906	HR 2085	HR 4825	HR 4685
Zr II									
	4208.99	0.71	-0.54	CB	52	33	72	31	132
	4211.88	0.52	-1.21	CB	24	25	43	14.5	88
	4317.32	0.71	-1.48	CB	13.0	10.0	8.0	9.5	27
	5112.38	1.66	-1.00	CB	22	20	23	17.0	--
Ba II									
	4554.03	0.00	+0.17	LW d	200	185	184	119	289
	4934.10	0.00	-0.14	LW d	232	224	204	149	290
	5853.67	0.60	-1.08	LW d	51	35	56	75	119
	6141.72	0.70	-0.16	LW d	104	96	164	136	221
La II									
	3988.51	0.40	-0.26	CB	15.3	7.5	35	12.2	127
	4086.72	0.00	-0.60	CB	17.6	25	36	18.0	124
	4123.23	0.32	-0.40	CB	24	17.8	40	--	147
	4263.59	1.95	+0.03	CB	11.0	18.0	15.0	8.0	41
	4322.51	0.17	-1.62	CB	--	7.0	13.0	--	40
	4333.76	0.17	-0.60	CB	22	20	36	32	52
	4662.51	0.00	-2.04	CB	--	16.9	19.0	--	--
	4748.73	0.92	-1.20	CB	20	9.0	22	--	33
Ce II									
	3882.45	0.32	-0.06	CB	64	60	122	--	135
	4120.83	0.32	-0.74	CB	8.2	--	--	6.5	34
	4137.65	0.04	+0.09	CB	18.0	23	--	20	101
	4142.40	0.22	-0.14	CB	24	41	54	36	107
	4193.09	0.74	-0.10	CB	--	5.5	14.0	7.0	36
	4202.94	0.56	-0.34	CB	13.5	25	18.0	14.5	60
	4418.78	0.38	+0.03	CB	8.0	11.0	15.0	--	50
	4486.91	0.29	-0.62	CB	--	10.3	8.0	11.7	31

	λ	χ(ev)	log gf	log gf source	HR 114	HR 906	HR 2085	HR 4825	HR 4685
Nd II									
	4061.09	0.47	+0.03	CB	19.3	22	25	17.0	54
	4462.98	0.56	-0.84	CB	--	5.8	8.8	6.1	28
Sm II									
	4424.34	0.48	-0.42	CB	6.7	8.0	17.0	12.0	35
	4467.34	0.66	-0.39	CB	6.0	--	--	10.0	28
Eu II									
	4129.73	0.00	-0.31	CB	20	12.5	23	20	95
	4205.05	0.00	-0.08	CB	42	--	72	35	194
Gd II									
	4251.73	0.38	-0.39	CB	8.5	10.5	5.0	5.4	53

	λ	HD 108486	HR 4750	HR 4751	HR 4780	HR 1368	HR 1376	HR 1389
C I								
	4771.72	50	43	44	55	67	62	45
	4775.87	--	16.0	27	--	--	11.0	8.0
	4932.00	19.0	41	--	18.0	17.0	13.9	19.0
	5052.12	91	55	104	65	112	151	60
	5380.24	--	32	35	61	29	21	23
Na I								
	5682.63	25	62	83	45	54	82	19.5
	5688.20	35	117	92	69	76	95	19.0
	5895.92	249	320	330	280	285	274	197
	6160.75	--	25	21	--	15.0	24	11.0
Mg I								
	4702.90	152	135	140	154	123	136	82
	5172.68	280	296	305	310	328	335	211
	5183.60	300	330	340	315	420	400	235
	5528.42	159	120	186	108	120	106	63
Al I								
	3944.01	225	271	250	173	253	273	180
	3961.52	202	224	188	142	215	221	128
Si I								
	5645.67	18.0	21	--	--	--	--	--
	5665.60	--	2-	--	--	--	--	--
	5690.47	--	--	34	--	13.0	--	--
	5708.43	53	23	49	--	29	36	16
	5772.25	23	20	--	20	--	28	--
	5793.12	19.0	--	27	18.0	--	--	--
	5948.58	--	42	64	28	--	62	24
	6254.25	--	33	57	13.0	47	76	20

	λ	HD 108486	HR 4750	HR 4751	HR 4780	HR 1368	HR 1376	HR 1389
Si II								
	4128.05	129	166	177	130	--	152	152
	4130.88	141	196	196	141	130	178	164
S I								
	4694.13	17.0	16.0	12.0	23	12.5	12.5	11.0
	4695.45	15.0	16.0	9.3	--	--	--	--
	4696.25	--	8.0	--	--	--	--	--
	6046.04	--	20	20	12.0	11.0	15.4	14.5
Ca I								
	4226.72	243	252	269	241	276	223	142
	4283.01	72	49	42	89	--	42	14.0
	4435.69	50	--	61	56	84	72	20
	4455.89	35	19	45	--	--	50	10.0
	5588.76	85	57	117	118	62	36	--
	5601.29	39	30	90	--	33	14.3	--
	5857.45	81	26	--	93	51	31	24
	6162.17	--	--	129	83	--	27	19.0
Sc II								
	4246.83	--	97	200	240	--	134	38
	4294.77	--	12.0	18.0	35	--	10.0	9.0
	4314.08	105	126	164	220	156	146	94
	4320.74	88	130	144	204	135	120	70
	4325.01	54	--	66	120	--	77	25
	4374.45	34	--	--	145	--	76	--
	5239.82	--	13.0	48	61	17.0	32	--
	5526.81	20	--	26	--	32	39	20
Ti I								
	3958.21	63	110	47	64	86	91	53

	λ	HD 108486	HR 4750	HR 4751	HR 4780	HR 1368	HR 1376	HR 1389
Ti I								
	4286.01	--	--	13.0	19.0	--	32	--
	4457.43	16.0	16.0	--	24	--	41	--
	4534.78	16.0	23	--	14.0	--	15.0	8.0
Ti II								
	3913.46	202	320	--	--	261	288	197
	4028.33	77	110	131	--	108	129	95
	4056.21	20	30	52	12.0	26	46	18.0
	4290.22	214	255	269	219	--	227	172
	4300.05	190	275	261	238	240	212	196
	4301.93	124	179	198	144	209	143	131
	4312.86	95	205	159	141	143	145	139
	4316.81	35	55	66	40	51	35	36
	4386.86	40	51	100	77	76	90	45
	4394.06	30	70	89	59	68	68	42
	4389.77	91	138	167	126	132	157	93
	4411.08	--	56	--	--	--	72	47
	4411.94	14.0	19.0	--	21	23	45	17.0
	4417.72	81	180	156	151	147	134	91
	4418.34	31	68	--	44	--	62	32
	4421.95	30	39	61	49	--	45	32
	4443.80	117	208	190	195	182	193	143
	4450.49	67	124	149	109	140	160	79
	4468.49	114	195	177	213	174	201	147
	4488.32	34	64	101	78	75	85	52
	4501.27	165	216	189	185	177	205	139
	4533.97	217	303	248	256	--	--	134
	4544.01	--	39	16.0	23	26	30	12.3
	4563.76	145	214	177	200	172	258	126
	4568.31	10.2	--	18.0	8.0	--	17.2	16.0
	4571.97	192	268	239	221	250	187	102

	λ	HD 108486	HR 4750	HR 4751	HR 4780	HR 1368	HR 1376	HR 1389
Ti II								
	4589.96	88	85	100	76	88	109	64
	4779.99	--	50	--	86	67	64	76
	4805.11	35	102	--	109	85	97	90
	5129.14	84	54	156	115	138	170	61
	5185.90	52	59	105	85	91	72	31
	5336.81	40	58	171	115	78	81	50
	5381.02	58	29	112	--	58	60	40
	5418.80	--	31	47	24	45	19.0	21
V II								
	4002.94	32	42	45	--	45	78	25
	4005.71	58	114	--	65	--	169	87
	4008.17	14.5	27	24	10.0	20	48	9.0
	4023.39	65	62	105	51	84	109	74
	4036.78	12.0	32	32	18.0	23	39	22
	4039.57	12.0	15.0	--	--	--	20	--
	4183.43	--	--	--	19.0	--	74	38
Cr I								
	3919.16	72	101	125	48	--	175	81
	4254.35	143	205	230	148	197	229	123
	4274.80	109	193	188	123	159	205	111
	4511.90	17.0	19.0	--	20	--	--	8.4
	4616.13	35	32	60	--	--	85	23
	4626.19	14.0	30	39	--	39	76	15.0
	4646.17	37	51	96	22	78	100	14.2
	4652.16	--	30	57	--	28	79	21
	4664.20	--	21	--	--	--	20	10.8
	5345.81	67	58	95	58	83	121	30
	5348.32	--	25	45	--	35	62	--

	λ	HD 108486	HR 4750	HR 4751	HR 4780	HR 1368	HR 1376	HR 1389
Cr II								
	4252.62	28	61	97	37	75	122	63
	4284.21	44	92	103	43	86	130	84
	4555.02	47	112	109	76	93	132	77
	4592.09	77	93	126	72	--	140	74
	4616.64	70	120	121	76	92	124	65
	4634.11	76	155	150	114	86	158	112
	4848.24	123	100	205	91	--	151	67
	4876.41	69	89	143	99	118	181	91
	5308.44	84	31	45	62	--	98	56
	5310.70	34	--	39	55	38	67	55
	5313.59	45	99	67	63	104	129	74
	5334.88	94	55	64	--	63	127	82
	5508.60	43	36	--	50	30	32	15.0
Mn I								
	4030.77	215	240	305	145	360	300	115
	4033.07	166	216	256	123	276	255	110
	4034.49	76	139	138	69	162	173	42
	4035.73	82	150	178	71	132	193	111
	4048.76	106	147	147	82	138	152	100
	4083.62	29	60	124	23	113	145	23
	4502.22	22	27	24	12.0	12.2	2.8	10.5
	6016.64	--	34	18.0	--	20	41	14.5
	6021.80	--	43	--	19.0	--	18.5	--
Fe I								
	3815.84	254	298	300	--	279	303	174
	3856.37	218	260	--	--	--	272	152
	3865.52	185	227	210	165	218	232	146
	3871.80	126	119	142	58	142	207	40
	3872.50	225	234	285	172	303	280	141

	λ	HD 108486	HR 4750	HR 4751	HR 4780	HR 1368	HR 1376	HR 1389
Fe I								
	3878.02	213	239	272	192	--	308	127
	3895.65	175	178	147	134	202	228	95
	3902.94	180	292	259	193	286	293	138
	3920.26	141	208	203	139	210	232	109
	3922.91	164	235	223	141	226	277	117
	3927.92	202	273	257	167	259	314	138
	3955.35	46	64	106	34	63	120	21
	3983.96	85	152	172	55	192	225	61
	3998.05	127	119	164	54	--	209	37
	4005.24	215	296	327	206	358	325	117
	4007.27	28	62	--	21	69	110	15.0
	4021.87	81	124	156	65	163	192	48
	4029.64	60	77	62	47	51	78	40
	4039.94	20	35	40	--	--	54	10.4
	4040.65	65	70	129	28	--	147	28
	4043.90	65	77	118	45	106	140	41
	4044.61	56	66	116	32	99	126	25
	4045.81	384	430	430	273	493	514	230
	4059.72	--	30	50	15.0	26	66	9.0
	4063.54	279	334	340	223	339	377	196
	4067.98	95	122	134	56	98	136	47
	4070.76	47	86	114	36	67	122	51
	4071.74	197	253	230	186	255	274	161
	4073.76	46	68	114	35	84	123	19.0
	4074.79	47	87	102	32	103	122	22
	4076.63	97	169	222	73	202	228	56
	4084.49	39	106	102	35	--	108	30
	4091.56	--	24	--	25	--	19.2	17.0
	4107.49	--	70	79	35	70	110	21
	4112.97	45	60	--	33	63	78	30
	4114.44	24	77	49	13.0	48	65	29

	λ	HD 108486	HR 4750	HR 4751	HR 4780	HR 1368	HR 1376	HR 1389
Fe I								
	4120.21	26	63	61	30	56	68	17.0
	4123.74	--	78	104	--	--	107	12.5
	4126.19	28	61	72	35	--	89	25
	4132.06	166	241	309	162	262	277	133
	4132.90	60	102	176	53	155	136	31
	4133.86	29	90	98	33	79	121	17.0
	4134.68	74	185	154	83	170	176	42
	4136.51	22	30	--	--	--	46	19.0
	4137.00	67	106	135	57	123	139	50
	4139.93	--	20	26	--	--	45	7.3
	4141.86	22	--	32	17.0	--	72	12.0
	4143.41	--	218	--	125	--	221	88
	4143.87	212	241	261	181	298	241	140
	4147.67	45	75	97	40	98	127	26
	4153.90	137	160	171	74	169	180	53
	4156.80	123	141	194	71	--	198	35
	4157.78	57	130	118	62	93	128	37
	4174.91	35	--	67	25	31	93	10.0
	4176.57	39	110	133	60	100	137	35
	4181.75	160	174	276	152	255	261	82
	4182.38	39	60	--	33	--	102	25
	4187.04	141	195	198	120	192	204	84
	4187.80	156	237	254	148	231	249	116
	4191.43	135	208	249	121	241	244	71
	4200.93	--	66	85	24	63	92	27
	4202.03	185	274	299	201	295	287	152
	4203.98	60	95	150	57	138	146	47
	4207.13	--	55	101	37	--	91	16.0
	4210.35	98	159	167	88	137	154	58
	4213.65	25	61	88	31	60	94	20
	4217.55	70	130	148	61	90	142	41

	λ	HD 108486	HR 4750	HR 4751	HR 4780	HR 1368	HR 1376	HR 1389
Fe I								
	4222.21	92	136	161	92	135	174	64
	4225.46	104	160	218	79	169	210	48
	4227.43	180	245	262	161	227	245	121
	4235.94	142	259	244	170	225	263	116
	4238.81	107	159	171	97	174	163	70
	4240.37	--	32	52	22	28	53	16.3
	4245.25	56	83	132	45	96	129	25
	4247.43	120	168	161	101	166	173	65
	4248.22	38	41	53	19.0	51	87	16.0
	4260.47	210	270	286	222	300	255	147
	4266.96	13.0	21	49	--	22	65	19.0
	4267.83	42	64	54	38	41	77	19.0
	4271.15	--	214	196	162	--	252	122
	4271.76	--	295	273	234	264	296	188
	4285.44	55	79	75	--	58	111	15.6
	4291.46	29	24	37	--	--	33	--
	4298.04	35	43	83	20	43	81	17.0
	4325.76	224	286	--	223	284	335	175
	4327.92	18.0	19.0	24	--	--	42	12.5
	4352.74	--	72	85	39	81	118	28
	4375.93	56	82	82	34	76	125	24
	4387.87	--	30	76	32	--	82	19.3
	4388.41	44	60	85	35	--	105	24
	4408.41	--	70	91	44	114	137	21
	4415.12	155	225	236	186	241	280	111
	4422.57	67	95	106	59	121	167	34
	4427.31	61	113	116	60	139	174	33
	4430.61	71	71	89	53	--	140	22
	4433.22	46	67	--	43	63	99	21
	4442.34	62	124	122	68	121	151	42
	4443.19	75	122	116	71	--	127	40

	λ	HD 108486	HR 4750	HR 4751	HR 4780	HR 1368	HR 1376	HR 1389
Fe I								
	4447.72	66	93	111	54	99	137	38
	4466.58	110	117	132	84	135	176	60
	4469.38	65	91	129	73	132	151	43
	4476.02	113	163	142	92	124	193	69
	4485.67	20	42	--	30	30	61	13.5
	4490.08	28	34	--	--	41	62	38
	4525.14	86	130	146	--	110	190	38
	4528.61	146	200	189	136	164	246	94
	4587.13	14.5	--	--	--	11.0	25	8.3
	4602.00	--	--	--	--	--	21	--
	4602.94	35	62	53	42	92	105	16.1
	4611.28	47	64	73	44	73	120	24
	4625.05	49	32	--	--	50	96	12.1
	4635.84	28	--	16.0	--	--	20	--
	4637.51	40	50	63	--	--	82	17.0
	4638.01	45	56	62	36	--	87	23
	4643.46	--	31	--	--	40	53	16.4
	4647.43	41	81	106	42	82	110	10.0
	4668.14	35	43	91	52	--	92	12.0
	4707.28	--	78	67	57	66	81	30
	4710.28	--	--	40	39	31	65	--
Fe II								
	4122.63	66	158	163	85	124	160	106
	4128.73	38	93	91	52	--	105	44
	4178.85	150	258	254	197	--	218	155
	4233.16	235	338	324	277	332	290	223
	4273.31	--	176	119	103	81	138	105
	4296.56	--	219	230	131	170	213	144
	4303.16	144	230	223	189	177	196	168
	4351.76	199	278	248	234	274	309	177

	λ	HD 108486	HR 4750	HR 4751	HR 4780	HR 1368	HR 1376	HR 1389
Fe II								
	4385.38	115	199	179	136	174	235	115
	4416.81	92	191	158	131	166	185	116
	4472.92	--	103	111	62	96	135	53
	4489.18	90	149	144	78	139	189	96
	4491.40	90	174	144	--	132	172	100
	4508.28	121	218	165	164	137	213	136
	4515.33	134	216	171	137	142	207	125
	4541.52	100	159	134	90	100	245	80
	4555.89	184	241	237	202	219	290	147
	4576.33	79	145	112	106	120	145	85
	4582.83	77	123	131	100	117	155	65
	4583.82	195	272	244	276	235	267	207
	4620.51	61	96	84	75	69	121	62
	4656.97	84	78	124	94	88	95	60
	4666.75	110	153	130	90	--	135	66
	4670.17	35	67	92	59	--	55	37
	4923.92	254	244	355	325	300	285	280
	5197.56	(222)	177	189	177	229	246	87
	5264.80	174	92	193	136	165	196	--
	5325.55	92	94	165	75	111	135	96
	5414.08	--	52	124	--	44	51	28
	5425.26	--	79	106	92	--	87	52
	5534.86	128	131	189	90	121	118	80
	6084.11	39	38	41	--	--	43	--
	6149.23	--	59	67	33	68	92	48
	6247.56	73	70	(214)	97	89	147	75
Co I								
	4020.90	12.0	14.0	16.0	15.0	15.8	44	11.5
	4058.60	45	51	77	38	78	119	20.0
	4121.32	20	58	66	26	78	98	18.0

	λ	HD 108486	HR 4750	HR 4751	HR 4780	HR 1368	HR 1376	HR 1389
Ni I								
	3858.30	141	212	196	119	187	232	129
	4401.55	97	190	179	65	144	214	50
	4604.99	38	74	50	41	93	112	24
	4606.23	15.5	16.0	25	--	--	71	23
	4648.65	57	116	106	51	85	122	36
	4686.22	30	35	30	49	--	63	19.5
	4714.42	76	135	120	81	91	188	51
	4715.78	30	50	30	28	40	100	23
	4980.16	78	64	87	41	88	170	35
	5115.40	60	42	--	41	97	163	--
	5155.76	55	42	51	35	78	141	28
Ni II								
	4015.50	59	122	133	53	100	174	69
	4067.05	164	249	255	129	262	226	152
	4244.80	25	33	--	--	10.4	52	24
	4362.10	36	50	59	31	34	80	43
Cu I								
	5105.54	27.0	36	38	42	55	82	16.8
	5782.13	26.0	36	31	28	--	36	--
Zn I								
	4722.22	63	64	75	46	35	95	27
	4810.53	78	62	74	53	48	96	27
Sr II								
	4077.71	350	450	438	276	482	533	230
	4215.52	315	403	357	265	392	398	219

	λ	HD 108486	HR 4750	HR 4751	HR 4780	HR 1368	HR 1376	HR 1389
Y II								
	3950.35	153	150	143	80	194	167	61
	3982.59	86	152	98	61	107	183	49
	4177.54	242	300	287	202	302	325	145
	4309.62	142	179	198	118	221	229	78
	4358.73	31	--	74	31	91	127	25
	4374.94	146	263	203	171	258	244	121
	4398.02	70	114	82	50	73	125	34
Zr II								
	4149.22	174	205	133	128	155	163	108
	4150.97	33	58	25	35	27	46	17.0
	4156.24	121	127	--	78	--	139	31
	4208.99	57	93	43	64	--	49	41
	4211.88	43	89	35	37	--	40	31
	4317.32	--	24	13.0	--	--	10.0	14.0
	5112.38	--	29	--	--	17.4	25	--
Ba II								
	4554.03	181	264	227	189	234	322	144
	4934.10	239	242	296	152	305	322	164
	5853.67	--	64	155	35	96	122	27
	6141.72	153	140	243	121	145	241	72
La II								
	3988.51	30	81	88	--	--	154	20
	4086.72	37	58	94	--	88	116	17.0
	4123.23	35	82	81	--	97	122	15.6
	4263.59	16.0	23	36	15.0	24	52	14.4
	4322.51	16.5	28	16.0	9.0	11.9	34	--
	4333.76	28	73	48	11.0	47	105	--
	4662.51	--	18.0	--	--	--	17.0	--

	λ	HD 108486	HR 4750	HR 4751	HR 4780	HR 1368	HR 1376	HR 1389
La II								
	4748.73	--	18.0	19.0	35	24	47	12.0
Ce II								
	3882.45	38	62	62	20	94	97	38
	4120.83	9.0	26	33	--	--	22	12.5
	4137.65	37	79	93	--	145	116	20
	4142.40	45	60	110	30	103	136	23
	4193.09	14.0	12.5	27	11.0	15.8	44	11.5
	4202.94	24	24	54	--	--	60	10.5
	4418.78	18.0	30	52	34	--	60	11.0
	4486.91	14.6	22	--	--	15.7	47	14.5
Nd II								
	4061.09	31	51	64	23	46	87	10.7
	4462.98	16.0	15.0	16.5	11.5	19.2	40	--
Sm II								
	4424.34	17.0	23	19.0	22	41	68	14.0
	4467.34	11.5	23	22	15.0	--	44	10.5
Eu II								
	4129.73	27	82	79	22	82	171	15.0
	4205.05	76	115	134	53	169	223	54
Gd II								
	4251.73	23	29	29	18.0	23	50	20

λ	HR 1428	HR 1458	HR 1519	HR 1672	HR 2291	HR 5055	HR 7850	HR 8410
C I								
4771.72	45	37	29	77	46	29	55	59
4775.87	--	--	--	18.0	--	--	--	23
4932.00	22	21	12.5	23	17.5	11.0	35	40
5052.12	120	91	95	84	124	45	95	110
5380.24	20	49	38	33	21	18.3	57	40
Na I								
5682.63	75	--	48	113	34	--	34	78
5688.20	74	60	40	131	60	24	45	101
5895.92	274	225	267	334	260	211	261	400
6160.75	--	--	21	23	25	--	--	--
Mg I								
4702.90	95	69	87	176	140	124	100	147
5172.68	307	230	340	300	350	328	340	318
5183.60	333	256	350	320	370	348	360	385
5528.42	115	116	103	113	115	86	51	153
Al I								
3944.01	186	159	260	272	275	154	199	299
3961.52	168	160	210	243	183	151	182	212
Si I								
5645.67	10.0	--	--	23	12.0	--	--	26
5665.60	--	--	--	24	--	--	--	21
5690.47	--	--	--	39	19.0	--	--	--
5708.43	--	24	--	49	29	--	19.0	62
5772.25	14.2	--	21	32	14.3	--	17.0	46
5793.12	--	--	13.6	--	--	--	--	19.0
5948.58	31	39	39	46	35	--	25	39
6254.25	34	25	--	40	23	--	22	50

λ	HR 1428	HR 1458	HR 1519	HR 1672	HR 2291	HR 5055	HR 7850	HR 8410
Si II								
4128.05	--	110	--	170	161	--	110	210
4130.88	139	114	158	223	193	101	106	241
S I								
4694.13	(8.4)	--	7.7	40	12.8	6.9	16.7	37
4695.45	--	--	--	34	10.0	--	--	14.7
4696.25	--	--	--	18.0	5.0	--	--	--
6046.04	--	--	16.6	32	14.0	15.0	--	--
Ca I								
4226.72	209	179	218	241	285	--	268	325
4283.01	85	59	--	31	66	--	--	89
4435.69	70	--	36	94	69	18.0	93	32
4455.89	--	34	35	58	21	--	27	--
5588.76	75	79	43	52	55	21	36	80
5601.29	49	--	--	34	39	--	18.0	32
5857.45	63	88	46	47	60	19.2	51	85
6162.17	58	--	54	45	94	33	104	68
Sc II								
4246.83	128	--	--	79	95	--	--	134
4294.77	10.0	30	--	12.0	12.1	--	--	22
4314.08	129	134	--	140	121	42	145	176
4320.74	121	130	93	134	110	64	139	165
4325.01	--	51	--	46	55	--	55	58
4374.45	--	54	--	48	40	14.5	111	99
5239.82	28	--	13.3	24	19.0	17.0	55	--
5526.81	27	--	26	--	23	11.6	20	33
Ti I								
3958.21	67	--	91	130	138	58	67	167

λ	HR 1428	HR 1458	HR 1519	HR 1672	HR 2291	HR 5055	HR 7850	HR 8410
Ti I								
4286.01	--	--	--	21	17.5	12.0	7.9	26
4457.43	--	--	82	56	25	5.0	--	55
4534.78	12.0	--	--	24	12.5	--	--	--
Ti II								
3913.46	199	180	250	315	277	157	195	330
4028.33	93	42	84	112	121	40	80	185
4056.21	27	30	28	46	25	--	--	32
4290.22	--	242	323	225	273	--	250	311
4300.05	175	222	--	257	272	188	202	328
4301.93	130	158	--	214	192	--	172	222
4312.86	106	115	110	195	163	87	115	255
4316.81	39	--	39	97	32	--	19.0	64
4386.86	64	33	34	116	60	23	40	97
4394.06	49	27	30	93	66	18.0	61	84
4399.77	97	51	84	154	158	--	173	187
4411.08	43	25	52	45	49	21	--	72
4411.94	21	18.0	--	--	14.0	--	--	37
4417.72	100	75	--	144	140	74	139	182
4418.34	56	20	--	51	46	11.4	--	80
4421.95	40	28	--	55	39	31	--	42
4443.80	156	104	240	200	221	169	194	282
4450.49	117	70	95	159	133	57	125	173
4468.49	160	79	188	199	224	111	195	284
4488.32	56	30	42	109	58	15.0	46	81
4501.27	171	96	143	198	194	119	171	212
4533.97	220	180	--	266	272	215	254	348
4544.01	23	85	10.3	40	23	7.5	--	39
4563.76	160	--	178	181	208	157	172	206
4568.31	--	--	--	--	11.3	--	--	--
4571.97	197	130	198	258	260	192	214	301

λ	HR 1428	HR 1458	HR 1519	HR 1672	HR 2291	HR 5055	HR 7850	HR 8410
Ti II								
4589.96	77	--	43	94	--	33	85	96
4779.99	43	--	40	51	72	28	57	90
4805.11	78	53	59	104	80	39	81	138
5129.14	123	81	135	154	129	82	115	187
5185.90	36	56	58	77	72	--	75	123
5336.81	55	46	55	76	79	36	79	125
5381.02	59	27	26	--	37	21	43	40
5418.80	22	--	12.6	29	32	--	--	45
V II								
4002.94	53	36	--	79	56	--	29	101
4005.71	--	--	--	136	140	--	--	190
4008.17	--	--	--	31	17.2	--	--	43
4023.39	80	35	85	105	94	37	73	139
4036.78	19.2	29	--	32	44	--	24	35
4039.57	--	12	--	--	15.4	--	--	25
4183.43	--	--	--	84	56	15.7	28	85
Cr I								
3919.16	111	62	--	138	103	41	--	149
4254.35	140	90	176	197	217	98	115	268
4274.80	129	86	186	181	198	81	131	264
4511.90	--	--	--	--	--	--	--	10.3
4616.13	--	23	27	49	37	--	--	48
4626.19	35	--	--	44	26	--	--	44
4646.17	62	--	48	124	53	16.8	--	54
4652.16	29	--	20	60	26	--	--	44
4664.20	--	--	--	39	17.5	--	--	--
5345.81	41	--	37	132	45	--	34	105
5348.32	17.0	--	10.2	45	19.7	--	23	55

λ	HR 1428	HR 1458	HR 1519	HR 1672	HR 2291	HR 5055	HR 7850	HR 8410
Cr II								
4252.62	69	43	64	102	72	17.2	42	117
4284.21	75	75	--	125	77	40	--	131
4555.02	71	53	--	123	85	--	--	119
4592.09	94	--	--	168	90	--	--	118
4616.64	84	--	78	136	96	75	75	114
4634.11	90	--	88	152	122	102	100	127
4848.24	--	73	--	183	99	103	131	176
4876.41	104	62	139	145	165	115	69	187
5308.44	--	55	38	59	48	34	--	81
5310.70	47	38	14.0	45	--	12.5	--	91
5313.59	80	42	90	94	78	43	52	143
5334.88	74	70	31	75	70	--	45	122
5508.60	--	44	--	75	25	--	22	31
Mn I								
4030.77	245	115	295	310	292	139	253	376
4033.07	178	110	236	244	246	122	161	292
4034.49	109	40	88	137	146	40	80	190
4035.73	115	78	106	145	152	62	79	203
4048.76	119	65	150	184	169	54	130	212
4083.62	69	33	64	122	73	22	36	119
4502.22	23	15.0	14.0	26	--	--	--	14.9
6016.64	15.5	--	--	38	19.8	--	--	30
6021.80	--	38	26	26	14.5	--	--	--
Fe I								
3815.84	208	210	249	250	257	212	248	286
3856.37	--	--	--	223	255	--	--	286
3865.52	178	130	148	219	227	149	149	281
3871.80	123	52	--	141	136	61	--	207
3872.50	208	180	--	275	230	212	232	316

λ	HR 1428	HR 1458	HR 1519	HR 1672	HR 2291	HR 5055	HR 7850	HR 8410
Fe I								
3878.02	--	240	--	275	271	--	--	307
3895.65	179	180	181	231	185	145	134	274
3902.94	217	188	254	311	247	212	224	314
3920.26	134	148	220	210	205	139	121	268
3922.91	178	150	189	240	245	124	154	300
3927.92	200	140	220	265	288	159	167	298
3955.35	52	29	41	103	49	11.3	42	104
3983.96	123	75	110	221	128	65	85	220
3998.05	112	77	--	155	120	--	134	198
4005.24	245	160	295	320	272	250	246	356
4007.27	53	44	--	84	53	--	--	106
4021.87	117	41	113	155	130	67	75	199
4029.64	57	43	--	81	120	--	54	158
4039.94	--	27	40	41	38	--	--	61
4040.65	92	41	--	124	102	--	--	173
4043.90	74	28	37	120	93	--	34	121
4044.61	61	27	64	95	84	--	71	114
4045.81	380	265	440	371	430	258	364	557
4059.72	30	19.0	20	50	36	--	16.5	52
4063.54	269	194	290	341	320	213	267	429
4067.98	85	60	83	97	120	35	54	167
4070.76	66	38	71	99	86	14.7	31	146
4071.74	188	--	206	231	247	132	166	305
4073.76	74	33	58	96	92	25	--	140
4074.79	66	39	--	91	68	--	40	119
4076.63	134	50	215	203	156	69	92	231
4084.49	44	48	--	85	68	28	--	108
4091.56	--	--	16.0	31	40	--	22	71
4107.49	66	48	--	117	65	--	31	134
4112.97	49	23	--	71	47	11.5	--	76
4114.44	43	18.0	--	84	35	14.3	--	70

λ	HR 1428	HR 1458	HR 1519	HR 1672	HR 2291	HR 5055	HR 7850	HR 8410
Fe I								
4120.21	49	--	37	--	53	15.0	--	118
4123.74	--	27	--	120	84	--	32	129
4126.19	54	37	--	66	49	10.2	16.0	96
4132.06	182	109	263	288	268	149	177	352
4132.90	95	55	129	122	107	--	71	133
4133.86	71	23	--	115	96	32	53	154
4134.68	96	50	83	162	146	--	55	200
4136.51	--	--	--	26	22	--	18.0	49
4137.00	72	--	107	130	95	--	60	143
4139.93	20	--	--	21	10.0	--	--	30
4141.86	40	18.0	50	55	32	15.0	27	70
4143.41	192	180	--	215	218	--	--	253
4143.87	--	--	--	235	265	225	247	335
4147.67	69	26	39	96	77	--	27	118
4153.90	118	49	--	159	167	--	--	201
4156.80	--	--	96	164	161	--	106	216
4157.78	80	40	60	93	117	--	--	142
4174.91	56	--	--	42	45	10.0	--	81
4176.57	74	39	--	106	104	26	--	145
4181.75	155	76	198	202	225	107	141	260
4182.38	56	--	--	80	66	--	--	102
4187.04	138	80	--	198	200	148	--	266
4187.80	153	88	--	235	230	--	214	288
4191.43	152	96	192	234	223	89	144	272
4200.93	59	22	37	79	46	10.0	25	91
4202.03	179	125	--	291	265	157	197	358
4203.98	91	33	69	141	117	55	57	168
4207.13	106	--	--	99	47	13.7	29	67
4210.35	--	51	79	138	156	56	86	204
4213.65	53	31	16.0	77	56	14.5	--	93
4217.55	87	37	58	127	125	63	60	153

λ	HR 1428	HR 1458	HR 1519	HR 1672	HR 2291	HR 5055	HR 7850	HR 8410
Fe I								
4222.21	109	50	102	162	155	50	81	202
4225.46	126	--	167	189	149	63	--	202
4227.43	153	136	--	231	235	--	--	292
4235.94	165	110	216	229	261	125	170	353
4238.81	123	50	141	143	155	--	--	210
4240.37	33	--	--	43	24	--	21	53
4245.25	74	33	--	118	87	--	--	131
4247.43	110	--	100	141	150	--	--	216
4248.22	55	25	--	69	49	--	--	91
4260.47	195	150	260	289	276	189	186	342
4266.96	31	27	--	45	33	--	--	72
4267.83	49	29	--	68	52	--	--	87
4271.15	136	--	--	222	209	--	--	270
4271.76	187	190	320	282	286	--	254	348
4285.44	58	51	27	81	58	--	20	96
4291.46	28	--	--	21	13.5	--	--	31
4298.04	--	30	--	61	45	--	15.7	76
4325.76	207	243	260	278	307	233	252	372
4327.92	--	29	--	--	16.1	--	--	46
4352.74	67	27	--	107	73	25	30	100
4375.93	69	24	39	98	86	37	51	118
4387.87	36	--	--	47	37	--	--	47
4388.41	67	--	50	106	56	41	--	79
4408.41	58	22	64	121	69	--	--	84
4415.12	197	95	143	238	240	154	254	308
4422.57	89	36	98	146	120	43	56	170
4427.31	91	34	57	149	120	41	79	147
4430.61	78	35	86	122	115	23	--	99
4433.22	56	--	43	82	57	18.5	--	78
4442.34	85	42	96	150	119	70	--	143
4443.19	100	47	140	163	105	--	--	180

λ	HR 1428	HR 1458	HR 1519	HR 1672	HR 2291	HR 5055	HR 7850	HR 8410
Fe I								
4447.72	84	34	50	122	122	--	82	115
4466.58	106	--	79	171	93	57	104	170
4469.38	103	36	--	170	127	125	60	132
4476.02	108	47	66	172	111	74	94	165
4485.67	27	--	--	69	26	--	--	51
4490.08	--	--	47	96	18.9	16.5	30	35
4525.14	82	38	74	178	106	26	78	138
4528.61	173	67	176	219	206	103	152	246
4587.13	--	--	--	37	12.7	--	--	--
4602.00	15.6	--	--	--	--	--	--	11.0
4602.94	54	--	25	100	60	15.1	--	80
4611.28	60	--	30	104	71	15.7	--	92
4625.05	60	--	46	78	53	28	--	69
4635.84	--	--	--	13.0	--	--	--	--
4637.51	--	--	34	69	45	--	--	40
4638.01	--	--	30	78	39	--	--	42
4643.46	--	--	41	63	23	--	--	49
4647.43	60	--	60	140	64	22	--	62
4668.14	--	--	64	129	64	--	--	47
4707.28	41	--	33	98	59	--	--	69
4710.28	--	--	--	25	23	--	--	35
Fe II								
4122.63	98	84	--	154	147	61	69	210
4128.73	57	44	87	97	88	20	59	134
4178.85	148	150	--	231	235	--	--	318
4233.16	223	220	354	296	305	276	254	376
4273.31	79	84	90	128	161	41	76	208
4296.56	136	126	199	214	221	133	119	315
4303.16	131	167	--	197	220	153	--	292
4351.76	264	135	200	289	284	192	255	293

λ	HR 1428	HR 1458	HR 1519	HR 1672	HR 2291	HR 5055	HR 7850	HR 8410
Fe II								
4385.38	146	80	213	234	191	152	190	245
4416.81	111	71	--	170	179	132	180	240
4472.92	83	44	60	141	94	61	60	141
4489.18	114	68	130	197	144	97	160	180
4491.40	104	74	124	164	159	105	126	230
4508.28	144	85	131	198	205	133	140	247
4515.33	132	99	140	198	183	122	140	220
4541.52	85	75	107	144	119	84	98	173
4555.89	206	122	245	268	245	182	230	296
4576.33	100	71	76	141	133	78	84	146
4582.83	89	79	66	177	118	53	79	165
4583.82	240	151	206	283	285	231	255	319
4620.51	57	--	57	--	103	49	78	119
4656.97	74	--	81	169	96	61	--	95
4666.75	89	61	98	234	94	--	--	113
4670.17	--	--	--	72	63	--	--	53
4923.92	250	243	330	332	348	231	275	472
5197.56	197	134	267	136	254	159	219	330
5264.80	--	55	240	129	187	123	169	156
5325.55	96	72	80	130	104	--	57	148
5414.08	69	78	47	--	38	29	--	65
5425.26	73	72	--	127	59	25	37	135
5534.86	122	138	182	155	130	--	83	181
6084.11	23	75	21	--	62	--	34	49
6149.23	43	100	--	109	83	--	96	99
6247.56	109	130	139	149	124	124	--	99
Co I								
4020.90	22	16.0	9.7	27	11.7	--	19.0	41
4058.60	55	21	24	86	60	14.5	30	76
4121.32	66	28	38	84	69	29	35	117

λ	HR 1428	HR 1458	HR 1519	HR 1672	HR 2291	HR 5055	HR 7850	HR 8410
Ni I								
3858.30	165	100	159	212	202	123	181	242
4401.55	135	56	92	195	147	74	102	168
4604.99	50	--	48	127	62	14.9	--	93
4606.23	33	--	28	49	28	7.5	--	43
4648.65	85	--	67	159	82	44	--	85
4686.22	28	--	--	62	34	--	--	42
4714.42	81	82	66	171	116	57	90	142
4715.78	27	24	28	109	45	17.0	--	57
4980.16	83	33	72	137	95	22	83	132
5115.40	--	61	73	72	78	16.0	79	120
5155.76	85	66	--	67	55	--	38	105
Ni II								
4015.50	97	35	72	134	113	26	42	166
4067.05	170	123	268	264	240	126	179	286
4244.80	--	--	--	64	28	--	--	70
4362.10	39	26	56	86	39	21	54	71
Cu I								
5105.54	33	18.0	16.7	63	31	24	33	61
5782.13	11.0	33	17.7	55	20	13.5	18.5	46
Zn I								
4722.22	38	12.0	28	89	60	17.3	42	64
4810.53	58	18.0	32	100	70	14.5	47	76
Sr II								
4077.71	371	275	475	510	434	311	372	605
4215.52	306	220	340	334	363	246	275	426

λ	HR 1428	HR 1458	HR 1519	HR 1672	HR 2291	HR 5055	HR 7850	HR 8410
Y II								
3950.35	112	60	--	152	162	82	109	241
3982.59	93	117	185	155	155	97	78	228
4177.54	215	180	270	271	317	159	224	397
4309.62	147	116	210	228	226	113	144	275
4358.73	72	25	66	121	86	22	78	118
4374.94	210	124	--	228	241	157	279	311
4398.02	71	32	68	119	110	25	70	140
Zr II								
4149.22	128	82	180	179	232	120	125	317
4150.97	31	28	--	51	71	11.6	32	120
4156.24	--	--	172	206	185	82	71	241
4208.99	48	49	--	82	146	54	78	183
4211.88	--	38	32	76	113	--	--	136
4317.32	--	--	--	48	32	--	21	51
5112.38	16.3	--	13.5	19.0	30	--	22	--
Ba II								
4554.03	244	126	230	259	269	173	215	378
4934.10	256	148	284	281	329	234	295	350
5853.67	112	61	117	129	119	33	94	189
6141.72	185	151	230	211	240	157	188	290
La II								
3988.51	71	--	58	120	93	26	33	178
4086.72	70	31	75	114	83	18.0	26	129
4123.23	87	35	--	119	88	22	--	168
4263.59	28	20	23	46	25	11.0	--	57
4322.51	21	10.0	12.0	34	26	12.0	12.5	53
4333.76	77	--	61	80	58	--	29	99
4662.51	--	--	--	31	11.2	--	--	--

λ	HR 1428	HR 1458	HR 1519	HR 1672	HR 2291	HR 5055	HR 7850	HR 8410
La II								
4748.73	28	--	--	46	21	--	--	46
Ce II								
3882.45	70	--	32	95	58	26	33	95
4120.83	--	--	--	--	10.0	--	--	35
4137.65	61	32	75	97	64	--	--	135
4142.40	81	22	82	145	84	17.0	40	136
4193.09	28	--	12.0	45	27	--	14.5	60
4202.94	39	17.3	--	65	44	11.0	36	91
4418.78	--	--	32	69	41	12.0	--	57
4486.91	20	16.0	13.9	44	20.0	--	22	35
Nd II								
4061.09	48	11.0	15.2	63	55	8.2	23	80
4462.98	25	8.0	11.0	43	20.0	5.0	9.0	27
Sm II								
4424.34	35	14.5	15.0	57	29	6.2	18.0	47
4467.34	29	14.8	--	56	22	--	--	35
Eu II								
4129.73	82	27	78	163	97	9.0	31	161
4205.05	142	43	183	192	165	44	162	269
Gd II								
4251.73	30	22	27	49	40	8.0	--	69

REFERENCES

Abt, H. A. 1961, Ap. J. Suppl., 6, 37.

Abt, H. A. 1965, Ap. J. Suppl., 11, 429.

Abt, H. A. 1966, Vistas in Astronomy, 8, 75.

Abt, H. A. 1967, The Magnetic and Related Stars, ed. R. C. Cameron (Baltimore: Mono Book Corp.), 173.

Abt, H. A. 1969, Private Communication.

Abt, H. A., Barnes, R. C., Biggs, E. S., and Osmer, P. S. 1965, Ap. J., 142, 1604.

Abt, H. A., and Bidelman, W. P. 1969, Ap. J., 158, 1091.

Abt, H. A., and Chaffee, F. H. Jr. 1967, Ap. J., 148, 459.

Abt, H. A., Geary, J., Hudson, K., Rydgren, A., and Wilcox, R. n.d., Kitt Peak Natl. Obs., Tucson, unpublished.

Abt, H. A., and Hunter, J. H. Jr. 1962, Ap. J., 136, 381.

Abt, H. A., Meinel, A. B., Morgan, W. W., and Tapscott, J. W. 1968, An Atlas of Low-Dispersion Grating Stellar Spectra.

Abt, H. A., and Snowden, M. S. 1964, Ap. J., 139, 1139.

Alexander, J. B. 1967, M. N., 137, 41.

Allen, C. W. 1963, Astrophysical Quantities (London: Anthelone Press).

Aller, L. H. 1947, Ap. J., 106, 76.

Aller, L. H. 1967, The Magnetic and Related Stars, ed. R. C. Cameron (Baltimore: Mono Book Corp.), 327.

Aller, L. H., and Chapman, S. 1960, Ap. J., 132, 461.

Anderson, C. M., Stoeckley, R., and Kraft, R. P. 1965, Ap. J., 143, 299.

Arnett, W. D., Hansen, C. J., Truran, J. W., and Cameron, A. G. W. 1968, Nucleosynthesis (New York: Gordon and Breach, Science Publishers, Inc.), 1.

Athay, R. G., and Skumanich, A. 1968, Ap. J., 152, 211.

Auer, L. H., and Mihalas, D. 1970, Ap. J., 160, 233.

Babcock, H. W. 1958, Ap. J., 128, 228.

Barry, D. C. 1967, Ph. D. Dissertation: University of Arizona.

Barry, D. C. 1970, Ap. J. Suppl., 19, 281.

Baschek, B., and Oke, J. B. 1965, Ap. J., 141, 1404.

Baschek, B., and Reimers, D. 1969, Astron. and Astrophys., 2, 240.

Batten, A. H. 1967a, Ann. Rev. of Astron. and Astrophys., 5, 25.

Batten, A. H. 1967b, Pub. Dom. Ap. Obs. Victoria, 13, 119.

Berger, J., and Fringant, A. M. 1951, Comptes Rendues, 232, 2185.

Berger, J., Fringant, A. M., and Menneret, C. 1956, Ann. d'Astr., 19, 294.

Bessell, M. S. 1969, Ap. J. Suppl., 18, 167.

Bidelman, W. P. 1956, P.A.S.P., 68, 318.

Bidelman, W. P. 1960, I.A.U. Trans., 10, 677.

Bidelman, W. P., and Victor, R. C. 1966, P.A.S.P., 78, 550.

Bohm-Vitense, E. 1960, Zs. f. Ap., 49, 243.

Bond, H. E. 1970, P.A.S.P., 82, 321.

Boyarchuk, A. A. 1963, Pub. Crim. Ap. Obs., 29, 219.

Breger, M. 1969, Ap. J. Suppl., 19, 79.

Breger, M. 1970a, Astrophys. L., 3, 67.

Breger, M. 1970b, preliminary report on pulsation in Am stars, to be published.

Brown, R. H., Davis, J., Allen, L. R., and Rome, J. M. 1967, M. N., 137, 393.

Brunck, W. E. 1963, M. S. Thesis: Case Institute of Technology.

Burbidge, E. M., and Burbidge, G. R. 1957, Ap. J., 126, 357.

Byard, P. B. 1967, J. Quant. Spectrosc. and Rad. Transf., 7, 559.

Byard, P. B. 1968, J. Quant. Spectrosc. and Rad. Transf., 8, 1543.

Chaffee, F. H. Jr. 1968, Ph. D. Dissertation: University of Arizona.

Chaffee, F. H. Jr. 1970, Astron. and Astrophys., 3, 291.

Chromey, F. R., Faber, S. M., Wood, A., and Danziger, I. J. 1969, Ap. J., 158, 599.

Conti, P. S. 1965a, Ap. J. Suppl., 11, 47.

Conti, P. S. 1965b, Ap. J., 142, 1594.

Conti, P. S. 1967, The Magnetic and Related Stars, ed. R. C. Cameron (Baltimore: Mono Book Corp.), 321.

Conti, P. S. 1969a, Ap. J., 156, 661.

Conti, P. S. 1969b, Ap. J., 158, 1085.

Conti, P. S. 1970, P.A.S.P., 82, 781.

Conti, P. S., and Deutsch, A. J. 1966, Ap. J. 145, 742.

Conti P. S., and Deutsch, A. J. 1967, Ap. J., 147, 368.

Conti, P. S., and Strom, S. E. 1968a, Ap. J., 152, 483.

Conti, P. S., and Strom, S. E. 1968b, Ap. J., 154, 975.

Conti, P. S., and van den Heuvel, E. P. J. 1970, Astron. and Astrophys., in press.

Conti, P. S., Wallerstein, G., and Wing, R. 1965, Ap. J., 142, 999.

Corliss, C. H., and Bozman, W. R. 1962, N.B.S. Monograph No. 53.

Corliss, C. H., and Tech, J. L. 1968, N.B.S. Monograph No. 108.

Corliss, C. H., and Warner, B. 1964, Ap. J. Suppl., 8, 395.

Cowley, C. R., and Warner, B. 1967, Observatory, 87, 117.

Cowley, A., Cowley, C., Jaschek, M., and Jaschek, C. 1969, A. J., 74, 375.

Cox, J. P., and Giuli, R. T. 1968, Stellar Structure, Vol. 2 (New York: Gordon and Breach, Science Publishers, Inc.), 626.

Crawford, D. L. 1966, Trans. I.A.U. Symp. No. 24, 170.

Crawford, D. L., and Barnes, J. V. 1969a, A. J., 74, 407.

Crawford, D. L., and Barnes, J. V. 1969b, A. J., 74, 818.

Crawford, D. L., Barnes, J. V., Faure, B. Q., Golson, J. C., and Perry, C. L. 1966, A. J., 71, 709.

Crawford, D. L., and Stromgren, B. 1966, Vistas in Astronomy, 8, 149.

de Loore, C. 1970, Astrophys. and Sp. Sci., 6, 60.

Deutsch, A. J. 1967, The Magnetic and Related Stars, ed. R. C. Cameron (Baltimore: Mono Book Corp.), 181.

Deutsch, A. J. 1969, Private Communication.

Eggen, O. J. 1955, A. J., 60, 407.

Eggen, O. J. 1957, A. J., 62, 45.

Eggen, O. J. 1958, M. N., 113, 65.

Eggen, O. J. 1959, Observatory, 79, 197.

Elste, G. H. 1969, paper presented to the 130th Meeting of the A.A.S., Albany, New York, August 11-14th.

Ferrar, O., Jaschek, M., and Jaschek, C. 1970, Astron. and Astrophys., 5, 318.

Fowler, W. A., Burbidge, E. M., Burbidge, G. R., and Hoyle, F. 1965, Ap. J., 142, 423.

Garrison, R. F. 1967, Ap. J., 147, 1003.

Garz, T., Holweger, H., Kock, M., and Richter, J. 1969, Astron. and Astrophys., 2, 446.

Garz, T., and Kock, M. 1969, Astron. and Astrophys., 2, 274.

Glaspey, J. W., Doctoral Dissertation in preparation, University of Arizona, Tucson.

Golay, M. 1964, Pub. Obs. de Geneve, Series A, No. 68, 64.

Grasdalen, G. L., Huber, M., and Parkinson, W. H. 1969, Ap. J., 156, 1153.

Greenstein, J. L. 1948, Ap. J., 107, 151.

Greenstein, J. L. 1949, Ap. J., 109, 121.

Hack, M. 1955a, Contr. Milano-Merate Obs., No. 60.

Hack, M. 1955b, Contr. Milano-Merate Obs., No. 65.

Hack, M. 1955c, Mem. Soc. Astr. Ital., 26, 499.

Hack, M. 1956a, Mem. Soc. Astr. Ital., 27, 201.

Hack, M. 1956b, Mem. Soc. Astr. Ital., 27, 439.

Hack, M. 1956c, Mem. Soc. Astr. Ital., 27, 469.

Hack, M. 1965, Vistas in Astronomy, 7, 107.

Harlan, E. A. 1969, A. J., 74, 916.

Hayes, D. S. 1970, Ap. J., 159, 165.

Heard, J. F., and Petrie, R. M. 1966, Proc. I.A.U. Symp. No. 30.

Henry, R. C. 1969, Ap. J. Suppl., 18, 47.

Hertzsprung, E. 1911, Potsdam Publ., 22, 1.

Hoffleit, D. 1964, Catalogue of Bright Stars (New Haven: Yale University Observatory).

Honeycutt, R. K., and McCuskey, S. W. 1966, P.A.S.P., 78, 289.

Huber, M., and Tobey, F. L. Jr. 1968, Ap. J., 152, 609.

Inglis, D. R., and Teller, E. 1939, Ap. J., 90, 439.

Jaschek, M., and Jaschek, C. 1959, Zs. f. Ap., 47, 29.

Jaschek, M., and Jaschek, C. 1960, Zs. f. Ap., 50, 155.

Jaschek, M., and Jaschek, C. 1962, La Plata Symposium on Stellar Evolution (La Plata: National University of La Plata Press), 137.

Jaschek, M., and Jaschek, C. 1967, The Magnetic and Related Stars, ed. R. C. Cameron (Baltimore: Mono Book Corp.), 381.

Jaschek-Corvalon, M., and Jaschek, C. 1957, A. J., 62, 343.

Jefferies, J. T. 1966, Abundance Determinations in Stellar Spectra, I.A.U. Symp. No. 26 (New York: Academic Press), 207.

Johnson, H. L., and Mitchell, R. I. 1962, Comm. Lunar and Planet. Lab., 1, 73.

Johnson, H. L., Mitchell, R. I., Iriate, B., and Wisziewski, W. 1966, Comm. Lunar and Planet. Lab., 4, 99.

Kohl, K. 1964, Zs. f. Ap., 60, 115.

Komarov, N. S. 1965, Contr. Crimean Ap. Obs., 33, 273.

Kopylov, I. M., Belyakina, T. S., and Vitrichenko, E. A. 1963, Pub. Crimean Ap. Obs., 29, 181.

Kraft, R. P. 1965, Ap. J., 142, 681.

Kraft, R. P. 1967, Ap. J., 148, 129.

Kurucz, R. 1969, Ap. J., 156, 235.

Lambert, D. L., and Warner, B. 1968a, M. N., 138, 183.

Lambert, D. L., and Warner, B. 1968b, M. N., 138, 213.

Lambert, D. L., and Warner, B. 1968c, M. N., 138, 229.

Lambert, D. L., and Warner, B. 1968d, M. N., 140, 197

Larimer, J. W., and Anders, E. 1970, Geochim. and Cosmochim. Acta, 34, 367.

Linnell, A. P. 1966, A. J., 71, 458.

Livingston, W. and Smith, M. A. 1970, Kitt Peak Natl. Obs., Tucson, unpublished.

Loeb, L. B. 1934, The Kinetic Theory of Gases (New York: McGraw-Hill).

Matsushima, S. 1969, Ap. J., 158, 1137.

Maury, A. C. 1897, Harv. Ann., 28, 1.

Michaud, G. 1970, Ap. J., 160, 641.

Miczaika, G. R., Franklin, F. A., Deutsch, A. J., and Greenstein, J. L. 1956, Ap. J., 124, 134.

Miller, M. H., and Bengston, R. D. 1969, Ap. J., 156, 393.

Milton, R. L., and Conti, P. S. 1968, Ap. J., 154, 1147.

Moore, C. 1945, A Multiplet Table of Astrophysical Interest (Princeton: Princeton University Press).

Morgan, W. W. 1935, Observatory, 57, 118.

Morgan, W. W. 1970, private communication.

Morgan, W. W., and Bidelman, W. P. 1946, Ap. J., 104, 245.

Morgan, W. W., Keenan, P. C., and Kellman, E. 1943, An Atlas of Stellar Spectra (Chicago: University of Chicago Press).

Morton, D. and Adams, T. 1968, Ap. J., 151, 611.

Nissen, P. E. 1970, Astron. and Astrophys., 6, 138.

Oke, J. B., and Conti, J. B. 1966, Ap. J., 143, 134.

Olson, E. C. 1969, P.A.S.P., 81, 97.

Pecker-Wimel, C. 1953, Ann. d'Astr., 16, 321.

Pesch, P. 1967, Ap. J., 148, 781.

Powell, A. L. T. 1969, Astrophys. L., 2, 11.

Praderie, F. 1967, Ann. d'Astr., 30, 773.

Praderie, F. 1968, Ann. d'Astr., 31, 15.

Prbzylski, A. 1954, M. N., 114, 406.

Preston, G. W. 1961, Ap. J., 132, 797.

Renson, P. 1967, Ann. d'Astr., 30, 697.

Rogerson, J. B. 1969, Ap. J., 158, 797.

Roman, N. G. 1949, Ap. J., 110, 205.

Roman, N. G., Morgan, W. W., and Eggen, O. J. 1948, Ap. J., 107, 107.

Rozis-Saulgeot, R. M. 1962, Comptes Rendues, 255, 258.

Rudkjøbing, M. 1950, Ann. d'Astr., 13, 69.

Sanders, R. H. 1967, Ap. J., 150, 971.

Sargent, W. L. W. 1964, Ann. Review of Astron. and Astrophys., 2, 297.

Sargent, W. L. W. 1968, Ap. J., 152, 885.

Schatzman, E. 1969, Astron. and Astrophys., 3, 331.

Slettebak, A. 1949, Ap. J., 109, 547.

Slettebak, A. 1954, Ap. J., 119, 146.

Slettebak, A. 1955, Ap. J., 121, 653.

Slettebak, A. 1970, Private Communication.

Slettebak, A., Bahner, K., and Stock, J. 1961, Ap. J., 134, 195.

Smith, M. A. 1970, Ap. J., 161, 1181.

Smith, R. C. 1966, Zs. f. Ap., 63, 166.

Strittmatter, P. A., and Sargent, W. L. W. 1966, Ap. J., 145, 130.

Strom, S. E., and Avrett, E. H. 1965, Ap. J. Suppl., 12, 1.

Strom, S. E., Gingerich, O., and Strom, K. M. 1966, Ap. J., 146, 880.

Strom, S. E., Gingerich, O., and Strom, K. M. 1968, Observatory, 88, 160.

Stromgren, B. 1956, Vistas in Astronomy, 2, 1336.

Stromgren, B. 1963, Q.J.R.A.S., 4, 8.

Stromgren, B. 1966, Basic Astronomical Data, ed. K. Aa. Strand (Chicago: University of Chicago Press), 123.

Stromgren, B., and Perry, C. 1965, Photoelectric uvby Photometry for 1217 Stars Brighter than V = $6^m.5$, unpublished.

Struve, O. 1950, Stellar Evolution (Princeton: Princeton University Press), 56.

Struve, O., and Elvey, C. T. 1934, Ap. J., 79, 409.

Struve, O., and Swings, P. 1942, Observatory, 64, 291.

Takens, R. J. 1970, Astron. and Astrophys., 5, 244.

Titus, J., and Morgan, W. W. 1940, Ap. J., 92, 256.

Uesugi, A., and Fukuda, I. 1969, Univ. of Kyoto, unpublished.

Underhill, A. 1969, Univ. of Leiden, unpublished.

Unsold, A. 1955, Physik der Sternatmospharen (Berlin: Springer-Verlag).

van den Heuvel, E. P. J. 1968a, B.A.N., 19, 309.

van den Heuvel, E. P. J. 1968b, B.A.N., 19, 422.

van den Heuvel, E. P. J. 1969, P.A.S.P., 81, 815.

van't Veer-Menneret, C. 1963, Ann. d'Astr., 26, 289.

Varsovsky, C. M., 1962, La Plata Symposium on Stellar Evolution (La Plata: National University of La Plata Press), 137..

Wallerstein, G., and Conti, P. S. 1969, Ann. Rev. of Astron. and Astrophys., 7, 99.

Wallerstein, G., and Helfer, H. L. 1960, Ap. J., 132, 553.

Wallerstein, G., and Hunziker, W. 1964, Ap. J., 140, 214.

Warner, B. 1965, M. N., 129, 263.

Warner, B. 1966, M. N., 133, 389.

Warner, B. 1967, Memoirs R.A.S., 70, 165.

Warner, B. 1968, M. N., 138, 229.

Warner, B., and Cowley, C. R. 1967, J. Quant. Spectrosc. and Rad. Transf., 7, 751.

Watson, W. D. 1970, Ap. J., in press.

Weaver, H. L. 1946, P.A.S.P., 58, 246.

Weaver, H. L. 1950, A. J., 55, 82.

Weaver, H. L. 1952, Ap. J., 116, 612.

Whaling, W., Martinez-Garcia, M., Mickey, D. L., and Lawrence, G. H. 1970, paper presented at the Second International Conference on Beam Foil Spectroscopy, Lysekil, Sweden, June 7-12th.

Wolff, S. C., Kuhi, L. V., and Hayes, D. S. 1968, Ap. J., 152, 871.

Wright, K. O. 1955, I.A.U. Trans., 9, 739.

Wright, K. O. 1967, The Magnetic and Related Stars, ed. R. C. Cameron (Baltimore: Mono Book Corp.), 399.

Wright, K. O., Lee, E. K., Jacobson, T. V., and Greenstein, J. L. 1964, Pub. Dom. Ap. Obs. Victoria, 12, 113.

Young, A. 1970, P.A.S.P., in press.